ENGINEERING ASPECTS OF ROCKFALL
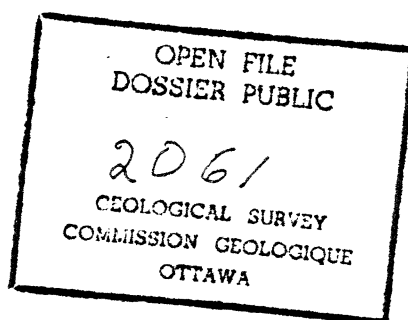# HAZARDS IN CANADA

Report
to
The Geological Survey of Canada and Transport Canada
(Research Project UP-T6-004-1)

Prepared by
O. Hungr, Ph.D., P. Eng.
Project Engineer, Thurber Consultants
and -
S.G. Evans, Ph.D.
Research Scientist, Geological Survey of Canada

Thurber Consultants Ltd.
Vancouver, B.C.

G.C. Morgan, P. Eng.
Review Consultant

File No. 16-11-4
January 24, 1989

SUMMARY

This report documents research into the engineering aspects of rockfall carried out jointly by the Geological Survey of Canada (Terrain Sciences Division) and Thurber Consultants Ltd. The study achieved the following results:

— The economic significance of rockfall hazards in Canada in terms of probability of occurrence and magnitude of resulting losses was evaluated. In general, it was found that losses due to rockfall damage in settlements have so far been very small in Canada, probably due to the low population density. Losses suffered by transportation routes have been much more significant and can be measured in millions of dollars per year. Losses sustained by the Pacific Salmon Fishery have been estimated in the billions of dollars (Chapter 2).

— A review of the basic mechanisms (initiation and dynamics) of fragmental (small scale) rockfall was carried out and the frequency and distribution of rockfall was investigated (Chapters 3, 4 and 5).

— Three alternative methods of predicting the behaviour of rockfall have been described, based on geological evidence, empirical correlation and direct analysis. New methods and rockfall hazard criteria have been derived (Chapter 6).

— A microcomputer program (ROCKFALL) suitable for analysis of rockfall trajectories was developed, incorporating advanced modelling features. Its application to a number of actual case histories was described and its use in simulating rockfall behaviour was demonstrated (Chapter 7 and 8).

A more detailed summary of the main findings is given in Chapter 9.

THURBER

ACKNOWLEDGEMENTS

THURBER

TABLE OF CONTENTS

THURBER

1. INTRODUCTION

1.1 Definition

Rockfall is a slope process involving the detachment of rock fragments and their fall, and subsequent rolling, sliding, bouncing and deposition near the foot of the slope (Varnes, 1978; Hutchinson, 1988). Rockfall occurs on natural cliffs, excavated rock faces, or steep exposures of coarse-grained soils. Sizes of fragments vary from small pebbles through boulders to large blocks containing several thousands of cubic metres of rock. Classifications of rockfall by size or volume have been proposed by Rapp (1960), Whalley (1984) and others.

A rockfall event may involve the displacement of a single fragment or several pieces. It may also begin by the detachment of a more or less coherent block, followed by its disintegration in the course of movement. The largest rockfalls ($>10^6 m^3$) invariably disintegrate and proceed by flow-like motion of unsorted masses of fragments called a "stürzstrom" (Heim, 1932), "rock avalanche" (McConnell and Brock, 1904), or "rockfall avalanche" (Varnes, 1978) where inclusion of the term "rockfall" implies an episode of free fall within the avalanche path.

This study is concerned with events near the lower end of the magnitude spectrum, up to approximately 100,000 m^3, involving rocks of at least moderate strength. Such events are dominated by free, independent movement of individual fragments and could thus be called "fragmental rockfall" (Hungr and Evans, 1988) They are distinguished from large rockfalls, or those involving weak materials, which move primarily by the mass flow of fragmental rock and are consequently different both in behaviour and effects.

1.2 Purpose of the Study

The present study has the following objectives:

a. Assess the cost of rockfall damage in Canada in terms of life loss and material losses.

b. Review the physical aspects of rockfall detachment, motion and deposition.

c. Evaluate and develop alternative methods of engineering and geological analysis available for prediction and mitigation of rockfall hazards particularly with respect to settlements and transportation routes.

d. Present several detailed case histories of rockfall accidents, in order to describe their typical circumstances.

Rockfall problems associated with the instability of man-made mining excavation slopes have not been considered in this study.

THURBER

2. COSTS OF ROCKFALL DAMAGE IN CANADA

2.1 The Nature of Rockfall Damage

Moving rockfall fragments may impact directly on buildings, motor vehicles or trains, and physical facilities related to energy transmission or the primary resource base. Stationary rockfall fragments which have come to rest on roads or railways may cause indirect damage by causing road accidents or derailments. In addition, rockfall fragments may partially dam rivers (Wetmiller et al., 1988) or may cause significant displacement waves if they enter enclosed bodies of water (e.g. Brock, 1904).

2.2 Buildings and Settlements

Rockfall damage to buildings is rare in Canada, possibly due to the low population densities which so far do not exert much pressure towards the development of marginal land. This is to be compared with the impact of rockslides and rock avalanches at Quebec City (1889), Frank, Alberta (1903) and Jane Camp, British Columbia (1915) which destroyed many buildings and resulted in a total of 177 deaths (see Table 2.1).

As seen in Table 2.1* the destruction of buildings by fragmental rockfall is responsible for only 4 known deaths in Canada over this period!

There may be a relatively large number of accidents which do not involve casualties or personal injuries and remain unrecorded. For example, houses were damaged by rockfall in Springdale, Newfoundland in 1976 and in Barnhartvale, B.C. in 1974. Even more frequent are cases of rockfall that impact upon developed land which cause no significant damage although they have the potential to do so.

Indirect costs of rockfall are perhaps of greater economic importance at present than direct damage. Use of marginally suitable land is increasing at a rapid rate. Since the mid-seventies, some provincial governments have required professional geotechnical inspections and approvals of development proposals on such land (e.g. Lister, 1980). Areas considered subject to rockfall hazard may be covered by restrictive covenants bound with the property title, prohibiting or regulating their development. Similar procedures are used in other countries, for example Switzerland, Austria and parts of the United States (e.g. Aulitzky, 1974).

The amount of land subject to alienation due to perceived rockfall hazards is quite substantial in mountainous parts of Canada. Unfortunately, no systematic record of land use restrictions has been kept by provincial authorities. As an estimate, based on cases known to the authors, approximately 300 ha of land have been subjected to rockfall-related restrictions in British Columbia over the last ten years. The market value of this land is about 15 million dollars.

2.3 Transportation Routes

Recorded fatal rockfall accidents on roads and railroads in Canada are listed in Table 2.1 and involve a total of 9 fatalities. Again, there probably is a large number of lesser accidents, the records of which could not be separated from general accident statistics. Also, a very large number of traffic accidents probably occur which are directly caused by the presence of rockfall debris on roads. Court registry records indicate a total of $260,000 in two recent rockfall injury settlements connected with road accidents in B.C.

Material costs of rockfall hazards include prevention/maintenance costs and the costs of traffic delays and repairs to the damaged roadway.

---

* Tables in this report are found at the end of each Chapter

THURBER

The British Columbia Ministry of Transportation and Highways yearly budget for rockfall prevention activities such as scaling and rock cut stabilization work is $3 to $3.5 million. Canadian National Railway's yearly budget for rockfall prevention in British Columbia has been approximately $1 to $2 million since 1971, most of which has been spent in the Fraser and Thompson Canyons (Theodore, 1986). On average, this amounts to approximately $400 to 800 per km of track per year. The above figures represent the level of effort required to maintain traffic lines in the Cordillera. A certain lesser amount of expenditure is also required to reduce rockfall activity from road cuts in other parts of the country (e.g. Magni, 1984; Carter et al, 1984), but no separate figures are available.

An illustration of the direct costs associated with rockfall accidents on railways is provided by records maintained since 1980 by the B.C. Rail in North Vancouver, British Columbia.* The company operates a railway system consisting of approximately 2,000 km of track, much of which extends through the mountainous coastal and interior regions of B.C. A total of 327 rockfall incidents have been recorded over the 7 year period from January 1980 to December 1987. These ranged from small rocks on track stopping trains briefly, to major track blockages and derailments.

Only 9 of the incidents (3%) involved direct "hits" of the train by falling rocks, all of these being of minor scale and causing little damage. The bulk of the recorded damage resulted from rock depositing on and blocking or damaging the track. One fatality and 9 injuries were recorded during this period, most of which resulted from derailments.

The costs recorded were only the "direct" expenditures, usually labour, connected with clearing and repair of the track. Indirect costs such as train delays, schedule changes and lost business were not recorded. The total direct costs amount to $3,903,200 over the 7 year period, or an approximate average of $280 per km of track per year.

The distribution of the recorded accidents according to the direct costs is shown in Figure 2.1.** Of the total cost 68% was incurred in 2 major derailments, averaging $1.3 M each. Only 8% of the total cost is attributed to 308 small scale accidents, averaging a little over $1,000 each, i.e. 94% of the total number of accidents account for only 8% of the total cost.

This would lead to the conclusion that the most cost-effective remedial measures are those concentrating on the major potential problem locations. However, such a conclusion should be used with caution since indirect costs (e.g. delays) could add substantially to the losses associated with minor accidents. On busy rail lines, train delays may account for as much as $50,000 per hour.

It must be stressed that the above costs were incurred in spite of a systematic and intensive effort at rock cut stabilization by the railway. In the absence of such effort, the damage costs would undoubtedly rise dramatically.

2.4 The Pacific Salmon Fishery

Rockfalls may impact on the health of the Pacific Salmon Fishery when rockfall fragments constrict or block river channels that are used by migrating salmon. The best documented event of this kind involved a relatively small rockfall into the constrained channel of the Fraser River at Hell's Gate in the Fraser Canyon during the construction of the CNR in 1914. The rockfall had a catastrophic effect on the Fraser River salmon fishery from which it still has not yet recovered.

---

* These records have been released to the authors by the courtesy of Messrs. V.W. Shtenko, P. Eng. and J.C. Leighton, P. Eng. of B.C. Rail.

**Figures in this report are found at the end of each Chapter.

THURBER

The debris constricted the channel thus creating an obstacle for migrating salmon in their cyclic return to their spawning grounds. It is probably the most costly landslide in the Nation's history because of the long term loss in yield of salmon from the Fraser. In 1978 dollars, the total loss to both the sockeye and the pink salmon fishery amounted to $2.6BN for the period 1951 to 1978 (International Pacific Salmon Fisheries Commission, 1980), a loss directly attributable to the effect of the 1914 blockage. Fishways were constructed at Hell's Gate between 1944 and 1966 at a cost of $1.36M to provide passage for the salmon past the obstruction.

2.5   Discussion

Rockfall has so far caused surprisingly little life loss and injury in Canada. Even allowing for imperfect records, it is clear that total casualties within this century due to small scale (fragmental) rockfall, exclusive of mining and construction accidents, do not exceed a few tens of cases. As shown in Table 2.2, the annual probability of a Canadian being killed by small scale rockfall, calculated based on these records, lies in the order of 10^{-8}. This is lower then the probability of deaths due to lightning (Morgan, 1986). The probability of demise due to large scale rock avalanches appears an order of magnitude higher, although the temporal and spatial distribution of such disasters is naturally highly erratic.

In comparison, Norway has recorded on average one or two small scale rockfall deaths per year between 1870 and 1940 (Bjerrum and Jorstad, 1968) leading to a probability of 5×10^{-7}. Many of these cases may involve persons in the open such as mountain climbers. In Japan, 78 persons per year on average perish due to landslides other than debris flows, of which some proportion must be due to small scale rockfall (Schuster and Flemming, 1986). The corresponding upper bound annual per capita probability is 7.6×10^{-7}, and this could be considered as a representative figure for a densely populated country.

In summary, life loss due to rockfall in a sparsely populated country such as Canada is very minor. In contrast, indirect economic losses due to land alienation in response to potential rockfall hazards are quite considerable. At the same time, however, land alienation may be kept to a minimum by accurate definition of the areas affected using methods discussed in this report.

Economic losses due to rockfall accidents on transportation routes are inevitable, but are being reduced by systematic application of stabilization and protective measures (e.g. Piteau and Peckover, 1978; Theodore, 1986). Here again, the ability to accurately predict rockfall behaviour will lead to major financial savings.

Rockfalls into constrained river channels draining into the Pacific may also impact on the Pacific Salmon Fishery. The 1914 Hell's Gate rockfall, which partially blocked the migration of salmon to their spawning grounds is probably the most expensive landslide in Canada's history.

THURBER

Table 2.1

FATAL CANADIAN ACCIDENTS CAUSED BY THE IMPACT OF ROCK SLOPE MOVEMENTS

A. Buildings

Locality	Province	Year	Fatalities	Buildings damaged or destroyed	Magnitude (m³)	Source
Quebec City	Quebec	1889	51	13	53,000 m³	Baillairgé, 1893, contemporary newspapers
Frank	Alberta	1903	70	~20	30,000,000	McConnell & Brock, 1904
Jane Camp	B.C.	1915	56	?	100,000 m³	—
Hedley	B.C.	1939	2	4	100	—
Sunnybrae	B.C.	1983	2	1	70	Miller, 1983

B. Highways and Railways

Locality	Province	Year	Fatalities	Magnitude (m³)	Source
Thompson Canyon	B.C.	1971	2	?	—
Porteau	B.C.	1962	2	?	—
Hope	B.C.	1965	4	$47 \times 10^6 m^3$	Matthews & McTaggart, 1978
Squamish	B.C.	1983	1	2	—
Fraser Canyon	B.C.	1986	1	?	—
B.C. Rail, Seton Lake	B.C.	1965	1	1	—
B.C. Rail, Seton Lake	B.C.	1980	1	?	—

Table 2.2

PROBABILITY OF ACCIDENTAL LIFE LOSS IN CANADA

Cause	Basis	Annual Probability per Capita	Source
small scale rockfall	13 in 87 years	1×10^{-8}	this study
large rockslide-avalanche	190 in 87 years	1.4×10^{-7}	this study
lightning strike	?	2.0×10^{-7}	Morgan (1986)
snow avalanche	7/year	3.5×10^{-7}	Stethem and Schaerer, 1979, 1980
car travel (B.C., 1984)		3.0×10^{-4}	Morgan (1986)

THURBER
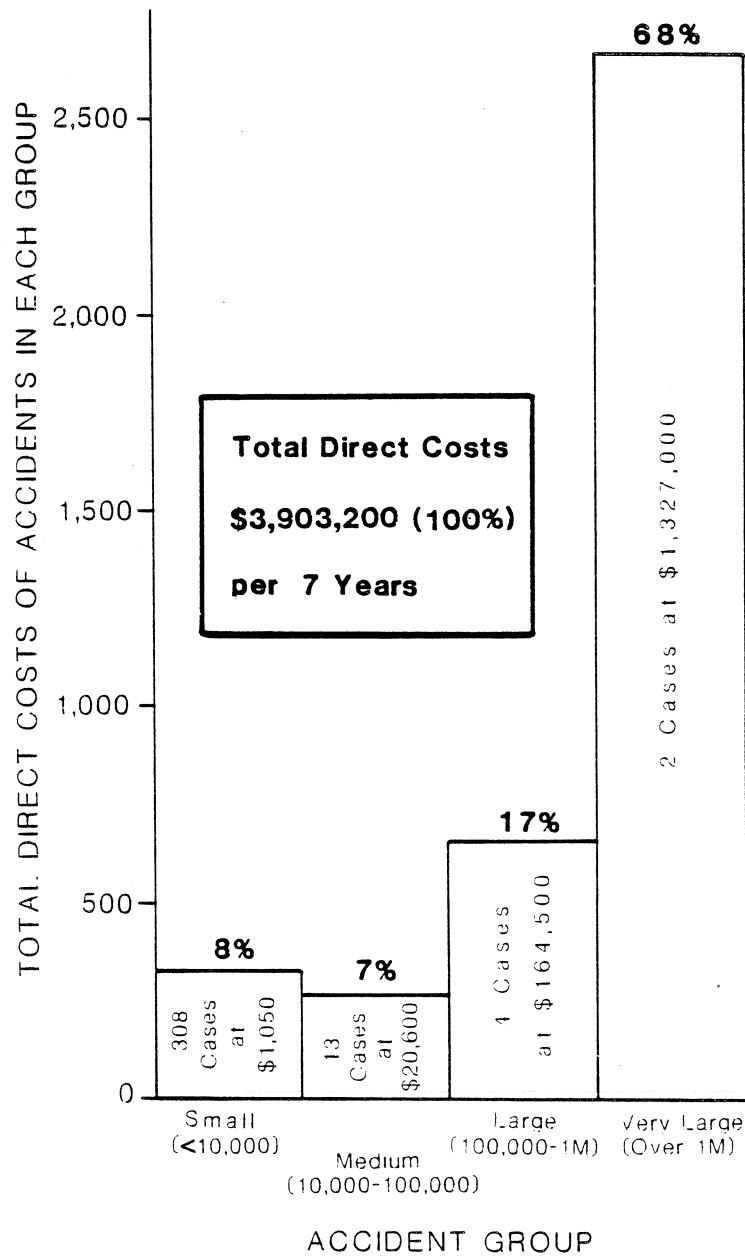
Figure 2.1. Distribution of rockfall-related accident costs, B.C. Rail System, 1980-1987 (direct repair costs only).

3. THE ROCKFALL PROCESS-INITIATION

3.1 Rock Weathering Processes

Small scale fragments detach themselves from cliffs along existing discontinuities such as joints, bedding planes, faults and cleavage surfaces. To a minor extent, development of new discontinuities (cracks) aids the process of detachment.

There are several processes which cause rock fractures to open or propagate (e.g. Embleton and Thornes, 1979; Whalley, 1984). Some practical results of geomorphological research into the mechanics of these processes are reviewed in the following:

(a) Frost Action: Frost wedging is the effect of ice crystallization pressures in cracks. Large ice pressures will only form in a closed freezing system. Consequently, for the maximum wedging effect, the crack must contain water close to the rock surface and freezing must proceed from the surface inward into the rock (Battle, 1960). Increased quantity of water available within the crack system appears to promote the wedging action (Washburn, 1973). Thus, poorly drained areas of a rock slope will be subject to more rapid deterioration and produce more frequent rockfall than dry areas, other things being equal. Near-surface drainage of rock faces by means of diversion of surface flows and sealing of fractures using shotcrete will reduce the frost wedging activity.

Frost wedging produces fragments whose size is limited to the scale order of the frost penetration depth, typically 0.5 to 1.5 m.

(b) Water Pressure: Water pressure generated in rock slopes (Harper, 1975) can cause rockfalls (e.g., Hutchinson, 1972). Freezing of joint water may block the outlets of a saturated joint system, which may cause a temporary rise of pore pressures within the slope.

Under normal circumstances, freezing obstruction of discharge outlets should be offset by a simultaneous reduction of infiltration due to the same cause. An abnormal increase of groundwater pressure results when rapid infiltration occurs during thaw through open joints while the outlets are still frozen. This condition probably occurs most often in cases of incipient failure masses characterized by deformations and tension cracks. The probability of incipient failures accelerating therefore increases during thaw conditions.

(c) Other Types of Physical Weathering: Crystal growth and hydration of minerals operate to cause general disintegration of the rock mass but will rarely be identified as trigger mechanisms for any but the smallest fragment falls. The same is probably true with respect to repeated strong warming and cooling of the rock surface (Tamburi, 1974). Nevertheless, it is safe to conclude that rockfall involving fragment sizes measured only in centimetres will be somewhat more frequent in time periods and areas exposed to strong warming and cooling, other things being equal.

3.2 Rockfall and Earthquakes

Earthquakes are an important trigger for both small and large scale rockfall. Keefer (1984) in reviewing landslides triggered by 40 historical earthquakes notes that rockfalls are the most abundant landslides caused by earthquakes. Govi (1977), for example, studied rockfalls triggered by the 1976 earthquakes in the Friuli region of Northern Italy where two separate shocks occurred, with Magnitudes of 6.4 and 6.1. Govi (1977) documented approximately 150 rockfalls

triggered by these earthquakes within a 25 square kilometre region surrounding the epicentres. Many of these rockfalls involved blocks tens of tons in weight, travelling down paths longer than 500 m. The density of rockfall occurrence reduced rapidly with distance from the epicentres.

In the western United States many earthquake triggered rockfalls were reported by Witkind et al. (1962) and Hadley (1964) as a result of the 1959 Hebgen Lake Earthquake (M = 7.1). Similar effects were reported by Harp et al. (1984) for the 1980 Mammoth Lakes, California, earthquake sequence (M = 6.1) and Keefer et al. (1985) for the 1983 Borah Peak, Idaho Earthquake (M = 7.3). The longer term effect on rockfall frequency is illustrated by Clark et al. (1972) who report a significant increase in rockfall activity at a site in the Chugach Mountains, Alaska during the years following the 1964 Alaska Earthquake (M = 8.4).

In the Canadian Cordillera the 1946 Vancouver Island earthquake (M = 7.2) triggered numerous rockfalls (Hodgson 1946; Mathews, 1979) as did the 1985 Nahanni earthquakes (M = 6.6 and 6.9) (Evans et al., 1987; Wetmiller et al., 1988). A large rockfall triggered by the second Nahanni earthquake partially blocked the Canyon of the North Nahanni River (Fig. 3.1). It is also noted that Indian tradition identifies the origins of certain large boulders in the Similkameen Valley, B.C. with the earthquake of 1872. However, no factual records exist.

The potential of a megaearthquake (M ≥ 8.5) occurring on the Cascadia subduction zone has been discussed by Rogers (1988). Should such an event take place it is probable that widespread damaging rockfall activity would occur throughout southwestern British Columbia and could strongly alter the probability estimates discussed in section 2.4.

3.3   Detachment Mechanisms

Rockfall may initiate by means of tensile or bending failure, buckling, planar or wedge sliding or toppling, as illustrated in Figure 3.2. The statics of these processes are relatively well understood (e.g. Hoek and Bray, 1977; Piteau and Martin, 1982), although there is very rarely enough quantitative data available for a complete mechanical analysis of a given incipient failure and prediction of its detachment.

(a)   Tensile or bending failure: This is a failure of a cliff protrusion, exploiting the existence of an incipient, non-persistent joint or other plane of weakness. As shown schematically in Figures 3.2a and 3.2b, the protruding fragment will be attached to the rock mass by a connection consisting of a bridge of intact or nearly intact rock material, partly severed by the incipient discontinuity (e.g. Schindler, 1987). Being subject to a permanent stress due to the weight of the block as well as to cyclic stresses due to groundwater pressures, ice or mineral volume change pressures or vibrations, the bridge will ultimately fail, leading to a sudden detachment. Overhangs in rock cuts and steep cliffs can be secured by means of rock bolts, designed so as to reinforce the connection between the overhanging fragment and the rock surface. Alternatively, threatening protrusions can be removed by bar scaling or light blasting charges (e.g. Fookes and Sweeney, 1976; Peckover and Kerr, 1977; Piteau and Peckover, 1978). Such work is generally carried out on the basis of experienced judgment.

(b)   Buckling Failure: Cliff walls are areas of stress concentration as well as high stress anisotropy. Major stresses parallel with the fall line of the cliff combined with poor confinement in the perpendicular direction often produce buckling failure of thin sheets of rock separated by joints.

Buckling failure may occur in massive igneous and metamorphic rocks along sheeting joints on steeply inclined bedding (Figure 3.2c). Such failures have been observed to occur in freshly exposed mine slopes and are undoubtedly one of the important mechanisms of deterioration of slopes in massive strong rocks.

A related process also occurs in sedimentary sequences, as illustrated in Figure 3.2d, based on Williams and Davies (1984). In this case, creep and swelling of shale partings gradually increase the eccentricity of a column of rock to facilitate eventual buckling failure. Each of the buckling mechanisms involves rapid failure. The volumes of detached rock are usually small.

(c) <u>Planar and Wedge Sliding</u>: Sliding is a common detachment process which may take many forms. Figure 3.3a illustrates the simplest configuration, that of a block resting on an inclined discontinuity plane. The mechanics of this model have been understood at least since the mid-eighteenth century. The driving force, being the downslope component of the weight of the block, is resisted by friction on its base. The frictional strength is a function of the effective normal stress on the base, calculated as the normal component of weight reduced by any groundwater pressure which may be present and divided by the base area. The friction behaviour of natural rock discontinuity surfaces is often strongly non-linear, especially in the case of high roughness (Barton and Choubey, 1977).

A block may exist in the configuration shown in Figure 3.3a, for a considerably long period of time before failing suddenly and becoming a source of rockfall. Some of the following factors are responsible for such ultimate loss of strength:

— Weathering and weakening of the contact rock at the base of the block.

— Creep displacements due to volume changes, frost action and delayed asperity deformations (Balk, 1939). Often, a block may gradually creep downslope over a period of many years until a point is reached where the slope is sufficiently steep or the discontinuity sufficiently smooth for sudden failure to occur. Such displacements have been measured by Dodds (1966).

— Fatigue or creep failure of the discontinuity.

— Earthquake or other vibrations. A simple theory of block displacements due to earthquake vibrations was developed by Newmark (1966). A more advanced method of calculating the seismic stability of blocks has been proposed by Li and Whitman (1986).

A sliding surface may also extend through weathered intact rock, as shown in Figure 3.2b. A block slide may be combined with the tensile failure of a rock bridge on the uphill side of the block, as shown in Figure 3.3c.

Wedge slides occur along two or several connecting discontinuities (Figure 3.4a). Their mechanism is similar to that of block slides, except that the lateral inclination of the discontinuities increases stability to some extent (Hoek and Bray, 1977). It is often the case that one of the discontinuities forming a wedge is incipient or non-persistent. Under such circumstances, the detachment of the wedge is conditional on the fracturing of intact rock bridges by a long term crack propagation process. As a result of this, wedge slides often behave retrogressively as illustrated in Figure 3.4b. Although a large part of a wedge may have failed in the past, another failure may issue from the same location in the future. In fact, multiple retrogressions of wedge masses are commonly seen in natural rock slopes (cf. the Hedley case, Section 8.3). The individual failure episodes may be separated by hundreds of years.

THURBER

(d) <u>Toppling failure</u>: Steep, medium to closely spaced discontinuities in the rock mass give rise to toppling failure (e.g. Wyllie, 1980) (Figures 3.5 a and b). Single block toppling (Figure 3.5a) may be triggered by a long term creep deformation of the highly stressed rock beneath the toe of the block. Gradual tilting may then occur, until the equilibrium is lost. The entire process was observed and recorded by Schumm and Chorley (1964) who monitored a sandstone tower for 6 years, observing an exponentially increasing tilt due to the creep of the shale foundation, leading eventually to a catastrophic collapse of the tower.

Multiple block toppling (Figure 3.5b) is a more subtle process, often occurring in combination with sliding displacements. For example, in the example illustrated, sliding failure of the frontal key block would trigger toppling of the entire assembly.

Mechanical analysis of toppling has been discussed by Goodman and Bray (1976), and Goodman (1980) and others, but it is often difficult to obtain the precise geometrical data required for such analysis.

Groundwater pressure, if present, constitutes a very important element in the equilibrium of rock masses subject to toppling and often acts as a trigger for toppling failure. Slope surface drainage will therefore reduce the probability of failure. Design of stabilization measures such as rockbolts can be based on the premise of increasing resisting moments in proportion to the increase of driving moments resulting from the rise of water pressure in cracks.

Effects of earthquake shocks upon toppling stability have not so far been studied.

3.4 Prediction of Rockfall Occurrence

The detachment of rock fragments is preceded by displacements, the observation of which often provides an advance notice of a fall. The observations may be qualitative or quantitative.

Qualitative observations related to rockfall occurrence include symptoms listed in Table 3.1. It appears from literature that those rock slopes that are frequently visited and observed, generally give ample warning of impending failure, provided that the failure mass exceeds several thousands of m^3. Many examples exist as a result, especially from European literature, of natural rock failures being recognized in advance, facilitating timely evacuation of residents or other measures. The following series of quotations from Schneider (1942) describes a typical sequence of events from the Swiss Alps:

"The name Gspaltenberg (literally Cracked Mountain) which designates the peak to the west of the head of our slide, is apt. We find there vertical cracks that run towards the interior of the mountain. In 1889 and 1897 there were also rock detachments which had no connection with the latest slide....."

"Last spring, in the grassy hollow at the highest point of the slide, it was established that there were fissures 5 cm in width and sags of the same size. By the beginning of June these had expanded to 20 cm maximum. At the beginning of July, the formation of fissures increased and spread westward as far as the course of the Hagerbach. Labourers working at that altitude observed daily movements of up to 2 cm."

"The event began on June 6 with two preliminary slides which released approximately 20,000 m^3. It was clear that a very large complex would drop to the valley along a steep slip plane. Inspections were subsequently carried out by the cantonal planning department and by army

THURBER

geologists. Within a few days, rapid changes took place in the unstable zone. The number of falling rocks also increased."

"The first main slide occurred on July 23, with a volume of approximately 300,000 m³. A second large failure at the same site was preceded by increased loosening of rocks at the foot of the moving mass, tearing of tree roots accompanied by explosive sounds audible 3 km away and rumbling noises from the interior of the mountain, which may have been the sounds of rocks falling into cracks."

Evacuation of residents was effected based on these observations.

Rockfalls of smaller magnitude are manifested by precursory signs less conspicuous then those described above, but nevertheless visible by a sufficiently detailed observation.

Where potential movements are recognized, systematic displacement monitoring can provide a more quantitative basis for failure prediction. A collection of pre-failure observations reported in the literature is presented in Table 3.2. In each of the reported cases, either the maximum displacement magnitude or rate are within a perceptible range and there is no question that the imminent failure potential can be recognized from such data. Prediction of the actual time of failure is based on an assessment of displacement accelerations and is quite subjective (Voight and Kennedy, 1978).

The prominence of all the precursory symptoms increases with the volume of rock involved in the failure. The value of the observation techniques in predicting seismically triggered rockfall has not yet been assessed.

Table 3.1

A CHECKLIST OF SYMPTOMS INDICATIVE OF POTENTIAL DETACHMENT
OF A ROCK FRAGMENT

A. <u>General Configuration</u>
— Fragment separated by through-going discontinuities.
— Potentially unstable position with respect to one or several detachment mechanisms, see Figs. 3.2 through 3.5.

B. <u>Evidence of Deteriorating Stability</u>
— Adjacent recent falls.
— Signs of water presence, or movement, in fractures.
— Active erosion, including slaking and swelling breakdown of weak zones, frost wedging, water flow erosion and root penetration.

C. <u>Evidence of Movement</u>
— Open tension cracks and other fractures.
— Abnormal minor spalls and fracturing.
— Block displacement inconsistent with rock structure.
— Signs of shear displacements along discontinuities.
— Tilted trees.

D. <u>Evidence of On-going or Recent Movement</u>
— Freshly opened tension cracks and fractures (disturbed soil, moss, lichen and other vegetation).
— Recently altered water flow patterns.
— Increased frequency of minor falls.
— Visibly altered geometry.

THURBER

Table 3.2

PRE-FAILURE DISPLACEMENT OBSERVATIONS OF SMALL TO MEDIUM ROCKFALLS

Location	Volume (m³)	Mechanism	Months prior to failure when movements first observed	Max. displacement prior to failure (mm)	Max. displacement rate prior to failure (mm/day)	Source
Iran	10	slide	–	–	2	Dodds, 1966
Decin Czechoslovakia	2,700	topple	42	350	–	Zvelebil, 1985
Steep Rock Mine, Ontario	10,000	topple	10	3,000	300	Brawner, 1987
Bristen, Switzerland	10,000	–	10	–	30	Ecole Polytechnique Federale de Lausanne, 1985
Linthal, Switzerland	20,000	slide	72	–	200	Eisbacher and Clague, 1984
Libby Dam, Montana	33,000	wedge	48	50	–	Banks and Strohm, 1974
Tarbella, Pakistan	300,000	slide	4	300	2	Khaliq and Haq, 1985
Threatening Rock, New Mexico	?	topple	72	–	–	Schumm and Chorley, 1964

Figure 3.1. Oblique view of rockfall (estimated volume = 0.1 million m³) triggered by the December 1985 Nahanni Earthquake (M = 6.9). View is to the west, up river into the gorge of the North Nahanni River. The rockfall debris consisted of Paleozoic dolomites which formed a dam across the river. Ponding of the river behind the debris dam is still visible at the time this photograph was taken (9 January 1986). For scale, trees on the right-hand side of the photograph vary in height from 3 to 5 m.

THURBER
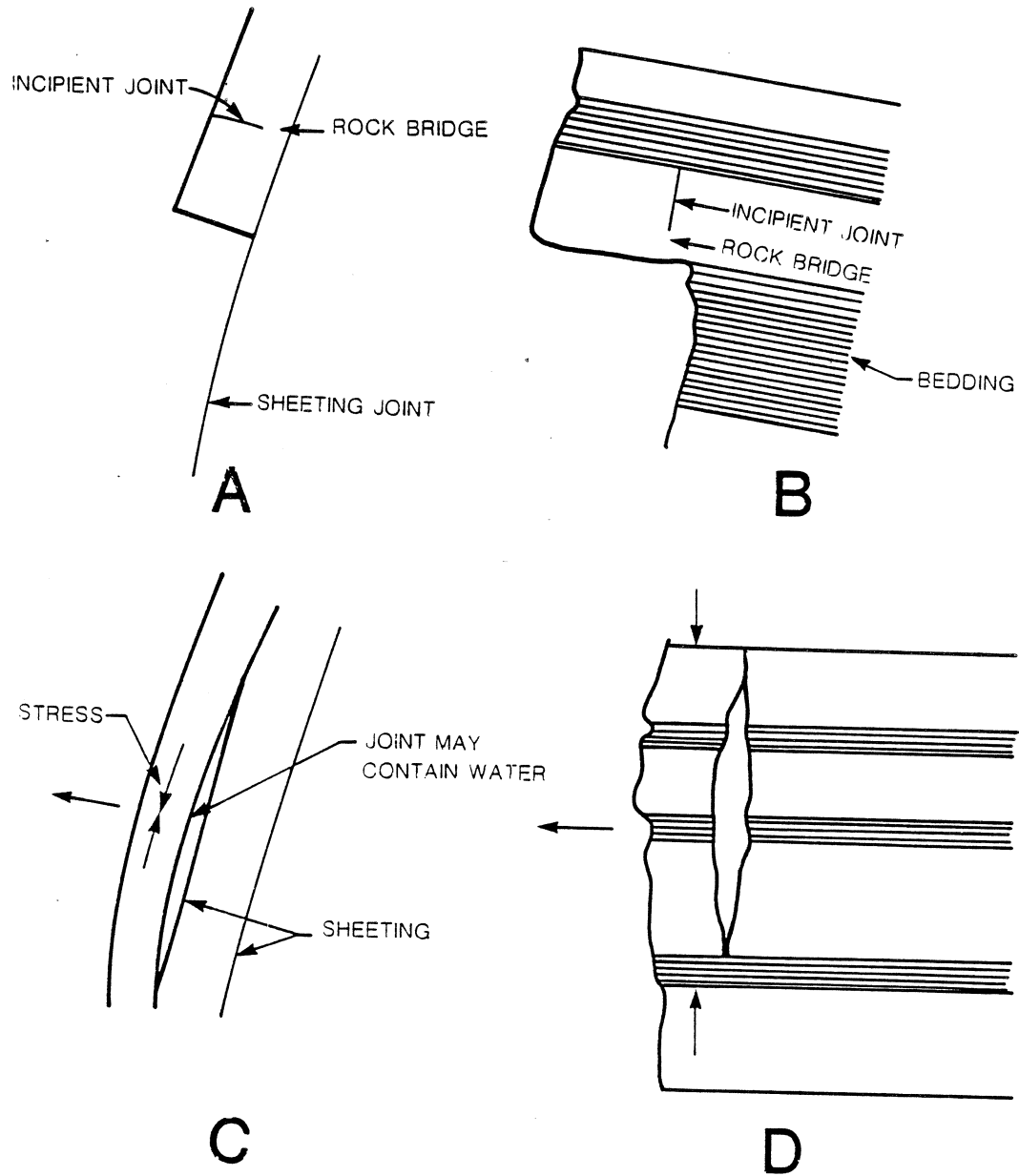
Figure 3.2. Detachment mechanisms I: A — Tensile failure; B— Bending failure; C — Buckling failure in massive rock; D — Buckling failure in stratified rock.

THURBER
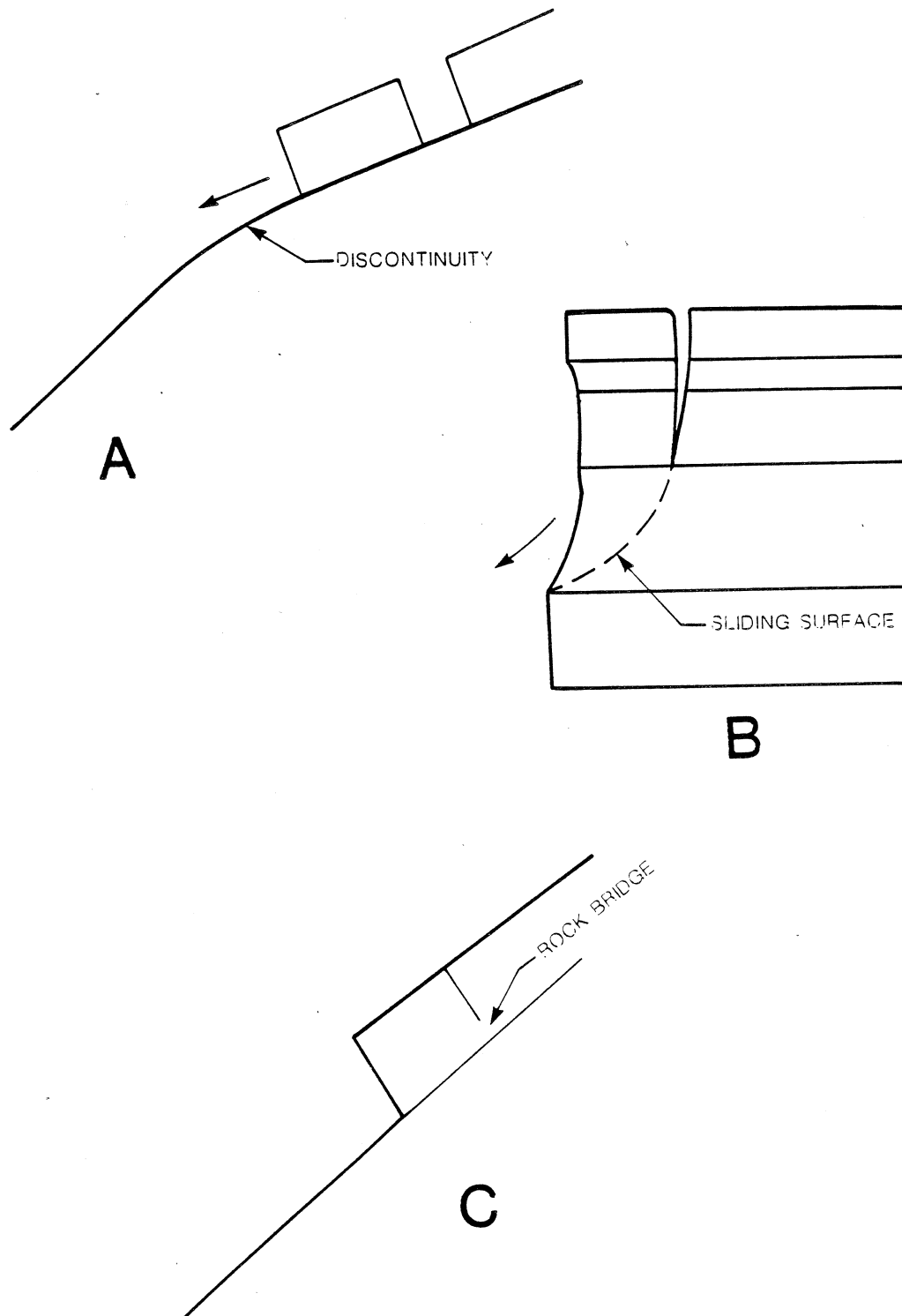
Figure 3.3. Detachment mechanisms II: A — Simple block sliding; B — Sliding through intact rock; C — Sliding combined with tensile failures.
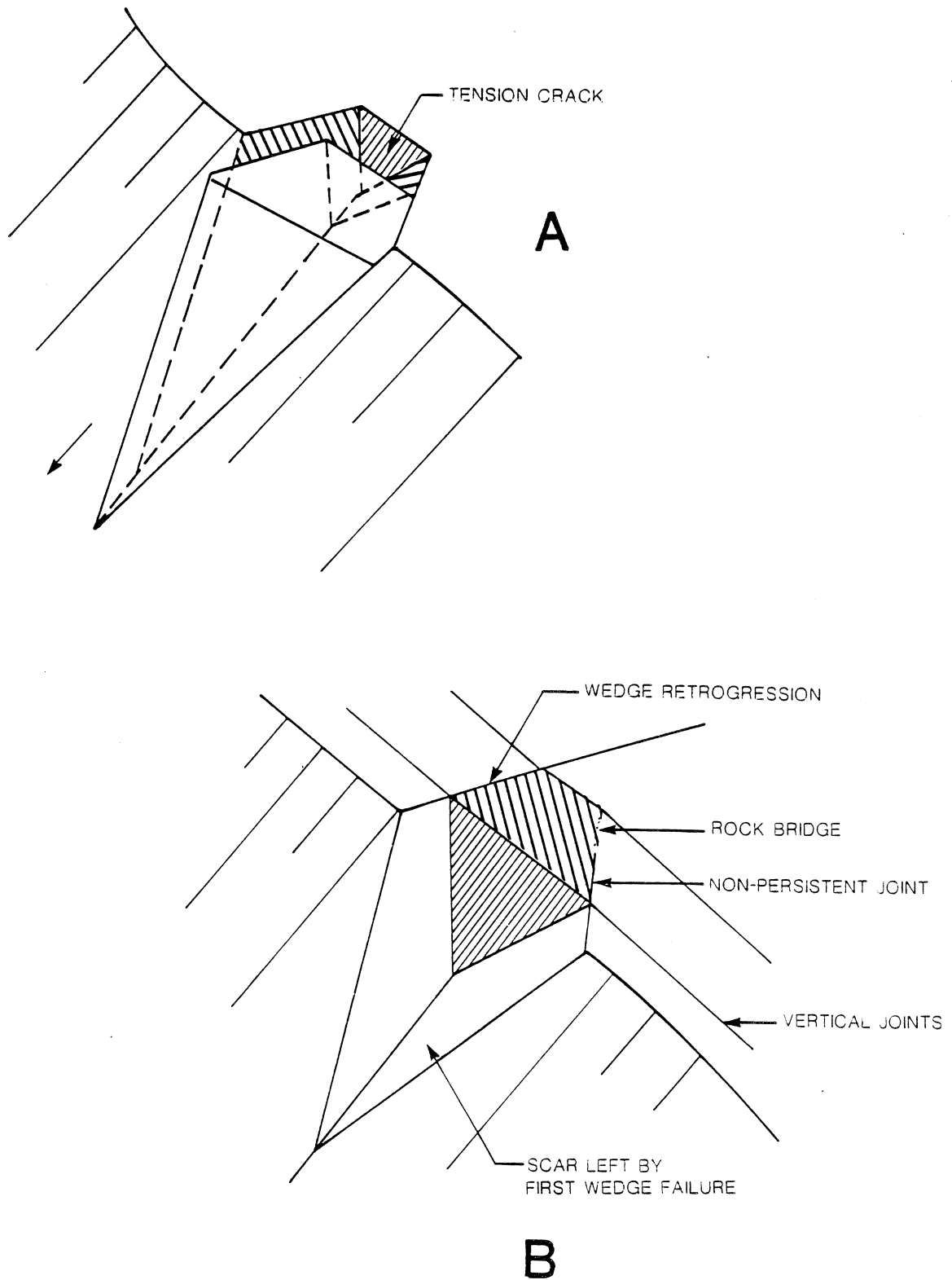
Figure 3.4. Detachment mechanisms III: A — Simple wedge; B — Retrogressive wedge.
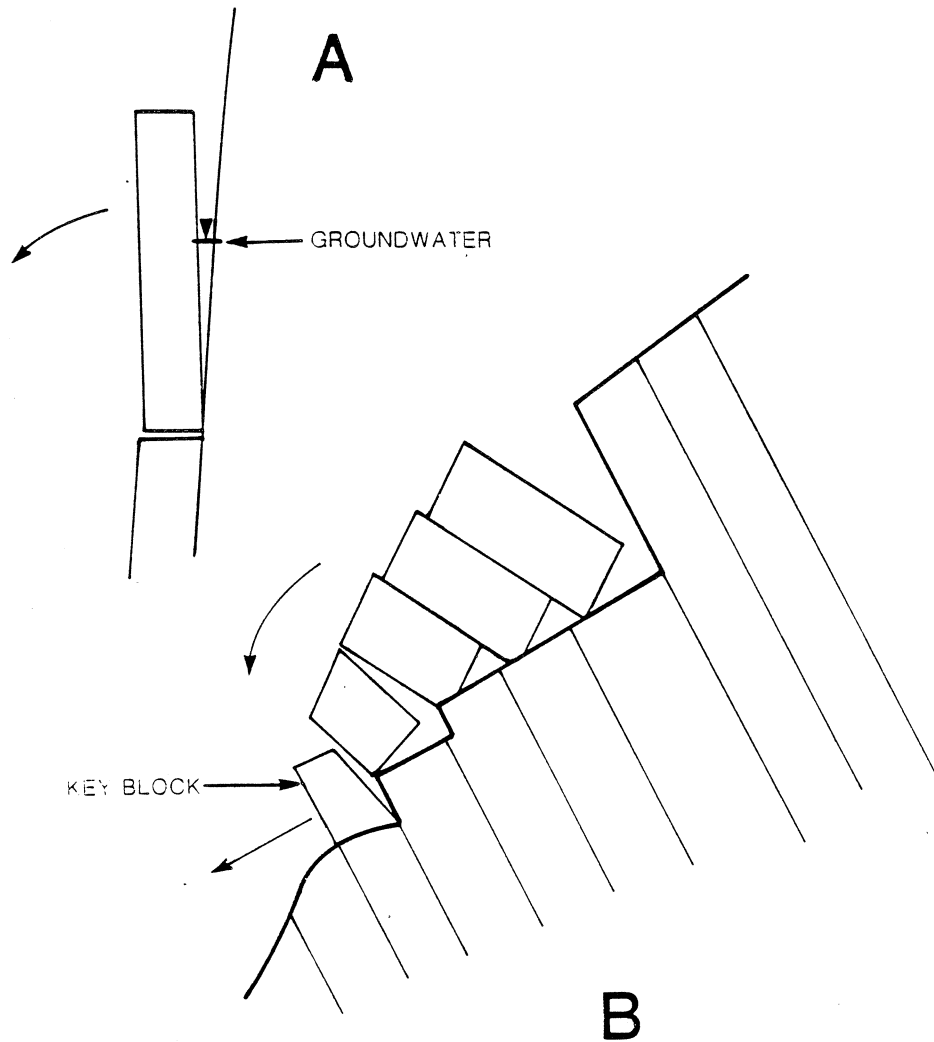
Figure 3.5. Detachment mechanisms IV: A — Single block toppling; B — Multiple block toppling.

4. THE ROCKFALL PROCESS-DYNAMICS

4.1 Rockfall Movement

A rock fragment begins moving after detachment by rolling or sliding. On slopes flatter than about 38°, the rolling or sliding movement mode may prevail throughout the displacement path. On steeper slopes, the fragment will accelerate and eventually transfer into free flight by either passing over a convex crest in the path (Figure 4.1a) or bouncing at a concave change in slope (Figure 4.1b).

The free flight occurs on a ballistic trajectory. The fragment may or may not rotate during flight and loses a small amount of energy by air resistance.

A collision occurs on contact with the ground surface, resulting in a complex exchange and reduction of momenta (Hungr, 1981), as discussed in Section 6.5. As a result, the fragment may rebound into another trajectory, begin rolling or sliding or stop abruptly, depending on the precise geometrical configuration of the impact, the amount of losses due to plastic deformation or breakage of the contact surfaces and the amount of rotation of the particle prior to contact.

Some general empirical observations regarding the behavior of rock fragments have been suggested based on observation of rockfalls and can be summarized as follows:

The response of a rock fragment to its contacts with the slope depends greatly on the roughness of the slope surface. When impacting a surface made up of particles of similar size to its own, the moving fragment often collides with faces nearly perpendicular to the direction of flight and stops abruptly (Ritchie, 1963, Statham, 1976). As a result of this, talus slopes develop distinct sorting from the finest fractions depositing near the apex of the deposit to the coarsest near the toe. The largest fragments will occasionally roll past the toe of the talus deposit (see Section 4.2).

On impact, rocks seldom rebound very high but rather change their linear momentum into angular momentum and begin to rotate or roll. For example, Ritchie (1963) observed rocks falling from cliffs 27 to 40 m high, inclined at 76 degrees and ending in a horizontal fallout area. Nearly all the rocks made their initial impact with the fallout area within less than 7 m distance from the cliff toe. However, many then rolled as much as 24 to 27 m farther.

The larger the volume of blocks, the lower their trajectories (Ritchie, 1963). The transition from bouncing to rolling movement mode will occur much sooner in case of large blocks than small ones. Blocks exceeding 10 m³ in volume begin rolling almost instantly after an initial impact on talus (Broili, 1974, Figure 4).

Total energy losses in high angle, high velocity impacts on talus surfaces derive primarily from breakage of the fragment and are typically as great as 75-85 percent (Broili, 1974). Thus, much of the energy accumulated in a long free fall is lost in the first impact on the talus.

"The shape of a rock fragment has little importance for its falling or rolling characteristics, unless it is long, like a pencil, which retards its roll and give eccentric action. Flat or angular shaped rocks made little difference" (Ritchie, 1963). A similar conclusion was derived by Statham (1976), who found little evidence for shape sorting in talus deposits (cf. Evans, 1976).

These observations have been used as guidance in the development of the dynamic model of rockfall, described in Chapter 7.

4.2 Rockfall Path Profile

The long term operation of rockfall processes produces talus slopes made up of rock fragments beneath the source slope. The depositional pattern exhibited in talus slopes reflects certain regularities. An important aspect is the natural "gravity" sorting by size mentioned above and observed by many authors (e.g. Gardner, 1970; Kotarba and Stromquist, 1984; Statham &

THURBER

Francis, 1986). Size sorting contributes an important roughness component to the talus slope surface which becomes the characteristic path profile for successive falls.

A typical example of talus sorting is shown in Fig. 4.2, derived from data collected on a talus cone in the Similkameen Valley, southern British Columbia by Worobey (1972). The mean particle size is seen in this instance to increase gradually from about 5 cm to 10 cm over approximately 300 m of slope length. Approximately the lowermost 40 m of the cone surface are built up of boulders with characteristic sizes of one metre or greater. The slope angle reduces to as little as 15° in the coarse basal accumulation.

The relatively low variation of grain size in the upper part of the cone is probably the result of redeposition by surficial talus flows, which are common in the area. Talus in other regions often shows more gradual sorting.

A rockfall dominated talus slope exhibits a typical profile as seen in Figure 4.3. Finer talus fragments accumulate below the apex (Point A) at an angle of approximately 38°. Lower down, the talus angle ranges from approximately 32° to 38°. The lowermost part of the talus deposit contains the largest fragment sizes and the talus slope angle sometimes falls to 10° or 20° as shown between Points B and C. Point C is the base of the talus deposit. Beyond this point the slope is no longer completely covered by talus particles.

The average talus angle is marked as β_1. In this paper, the surface to the right of Point C is termed the "substrate surface", consisting of material and landforms pre-dating the talus deposits. That part of the substrate surface covered discontinuously by scattered large boulders which have rolled or bounced beyond the base of the talus (C-D in Figure 4.3) is referred to here as the rockfall "shadow". We define the "shadow angle" as the angle between the outer margin of the shadow and the apex of the talus slope (β_2 in Figure 4.3).

A characteristic example of a rockfall shadow located on a river terrace in southwestern British Columbia is shown as Figure 4.4. The distal part of the shadow often contains only very few boulders which are sparsely distributed on the surface as shown in a vertical aerial view of a typical rockfall path in the Thompson River Valley, interior British Columbia reproduced as Figure 4.5.

THURBER
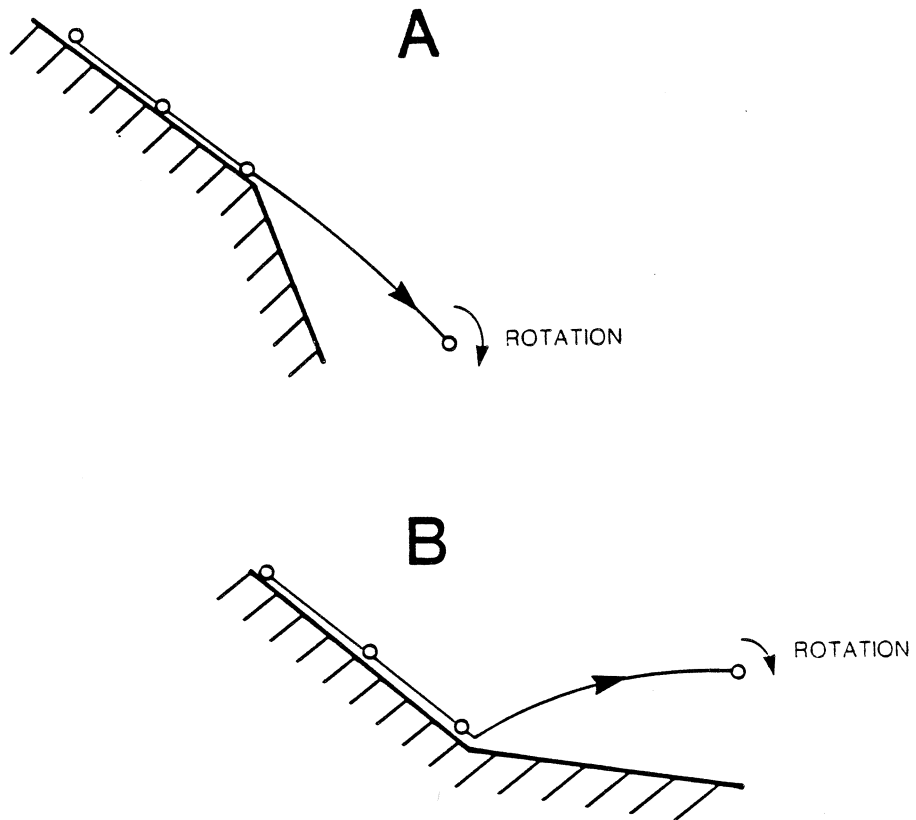
Figure 4.1. Two ways of transfer from rolling or sliding movement mode into free-flight trajectory.
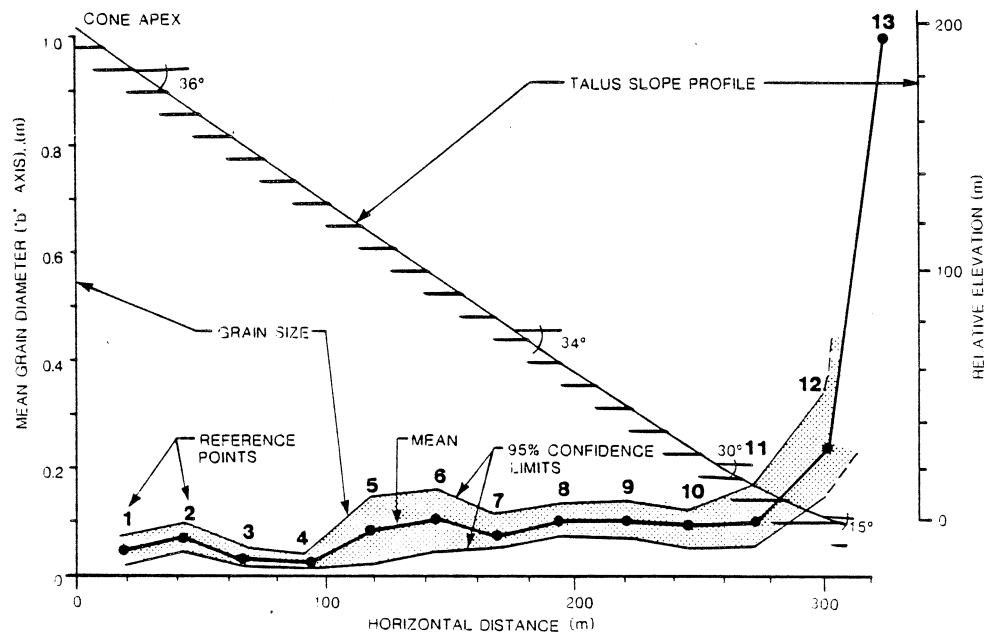
Figure 4.2. Typical downslope distribution of mean grain sizes in a talus deposit (data from Worobey, 1972).
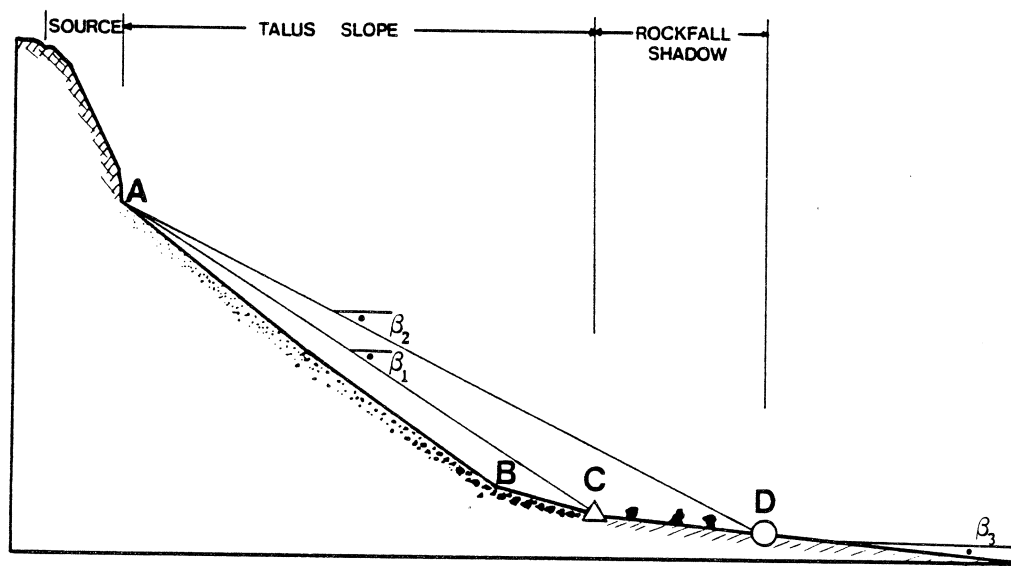
Figure 4.3. Schematic diagram of the characteristic rockfall path profile. A-C is the talus alope with mean angle β_1 and C-D is the rockfall show with a shadow angle β_2. β_3 is the substrate angle.

THURBER

Figure 4.4. An example of a typical rockfall shadow associated with talus slopes in the Similkameen Valley, British Columbia. Large rock fragments reached the terrace surface from rock slopes to the right of the field of view.

THURBER
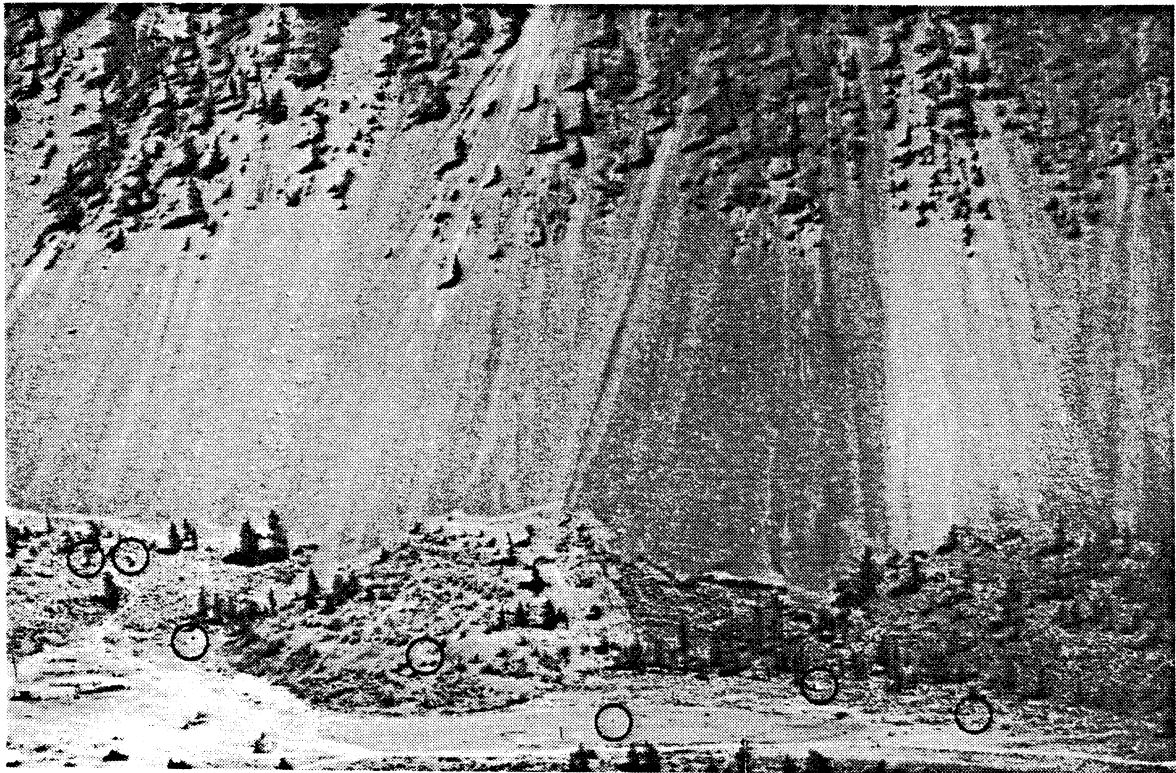
Figure 4.5. Aerial view of a rockfall shadow area at the base of talus slopes, Pukaist, Thompson River Valley, B.C. Some larger boulders in the rockfall shadow are circled. Farm buildings and small church are seen at lower left.

THURBER

5. FREQUENCY AND DISTRIBUTION OF ROCKFALL

5.1 Magnitude-Frequency Relationships

Each of the detachment mechanisms described in Section 3.2 contains a time element capable of producing delayed failure either due to a gradual decay of resistance or a temporary increase in the driving forces. Consequently, any rock slope contains a number of fragments which are only temporarily stable and will eventually fall. The frequency and magnitude of detachments depends upon the propensity of the rock to form the required mechanisms and upon trigger factors such as frost wedging, pore-water pressure rise, or seismic loading to initiate failure.

The magnitude-frequency relationship for rockfall has only been estimated in a few instances. Figure 5.1 reproduces that assembled by Gardner (1980) in the Highwood Pass, Alberta, an area characterized by carbonate sediments. The study area included a combined length of approximately 40 km of rock faces. Thus, a frequency-magnitude relationship per 100 m of rock face length can be derived approximately as indicated by the dotted area in Figure 5.1. These frequencies are very small. For example, an average 100 m long cliff sector could be expected to experience boulder falls exceeding 1 m^3 in magnitude only once in several centuries (cf. Douglas, 1980).

Similar low frequencies have been noted at several sites during the present study, as described in Section 6.2.

Some indication of failure incidence on cut slopes in bedrock can be obtained from records of track blockages in the Fraser Canyon kept by the CNR between the years 1948 and 1968 (Bell, 1980). The average frequency of failure from rock slopes (predominantly cut slopes) over this period was 0.09 per year per 100 m sector, as calculated from 36 observed events. The magnitudes of these rockfalls have not been recorded.

Undoubtedly, in every region there are certain cliff locations with greater than average propensity to generate rockfall, where the frequency is several orders of magnitude higher than average.

Some very detailed records of rockfall incidence from rock cuts have been kept by B.C. Rail in British Columbia in the late sixties. These indicate that the rockfall frequency is highly variable with location, as would be expected. The maximum frequencies observed during peak periods were of the order of 30 events per year per 100 m length of cuts.

5.2 Temporal Variation

It follows from the discussion in Section 3.1 that higher incidence of rockfall will coincide with the periods of freeze-thaw activity, high precipitation and snowmelt (e.g. Rapp, 1960; Luckman, 1976; Church et al., 1979; Gardner, 1980, 1983; Åkerman, 1984) in addition to earthquake events. This is borne out by examples of long term observations of rockfall frequency shown in Figure 5.2a and b. The Norwegian record (Figure 5.2a) indicates two peaks of frequency, a minor one in the late fall and a major one in early spring. The Fraser Canyon record (Figure 5.2b), is presumably affected by the high winter precipitation and frequent freezing level rises of southwestern British Columbia. It consequently shows a single peak in mid-winter. An almost identical trend has been recorded in 7 years of rockfall incident observations on the B.C. Rail system, shown in Fig. 5.3.

Daily fluctuations of rockfall activity have been reported by Gardner (1980, 1983) from the Highwood Pass study area, indicating a well-defined peak in the early afternoon during the time of highest temperature (Figure 5.4). Similar observations were reported by Luckman (1976), Church et al. (1979) and Åkerman (1984).

THURBER

5.3 Spatial Distribution of Rockfall Impact

Talus cone slope angles remain fairly constant during their gradual formation. As a result, it can be assumed that a relatively uniform thickness of material is added to the entire cone surface over any long period of time, as indicated in Figure 5.5. The probability of a unit volume of rock fragments landing at any particular location on the cone surface must then be approximately constant.

In some cases, the rate of growth of the cone surface can be estimated from geological evidence. In British Columbia, volcanic ash layers left by dated prehistoric volcano eruptions often provide the means of doing so.

In the Similkameen Valley talus cones, exposures of the Mazama ash deposited 6,600 years before present, can be found at a typical vertical depth of 3 m (Worobey, 1972). The corresponding mean vertical growth rate of the talus surface is 3/6,600 = 0.00045 m/year. The rate of growth in the direction normal to the cone surface is approximately (cos 34°) times the above, i.e. 0.00037 m/year (cf. Luckman, 1988).

The probability of fragments landing on a given square metre plot of the surface is a function of the mean particle diameter. To achieve the above growth rate with particles each of which is large enough to occupy 1 m³ of volume on deposition, for example, their frequency needs to equal 0.00037 landings/year/m². Particles with a tenth of that volume would require ten times the frequency. Gravel-sized particles with a characteristic dimension of 3 cm occupy a volume of 0.000027 m³ each and require a frequency of 14 landings/year/m². This relationship can be expressed as:

$$f_l = R_n / D_c^3 \qquad \text{Eqn. (5.1)}$$

where f_l is the frequency of landings per year per square metre of cone surface, R_n is the surface growth rate in the normal direction in m/year and D_c is the characteristic dimension of the mean rock fragment, defined as the side of a cube with the same volume as that occupied by the fragment in the deposit.

The mean landing frequency is therefore a function of the third power of the mean characteristic fragment size and consequently reduces slightly downhill as the fragment size increases (cf. Luckman, 1988). This is shown by the dashed line curve in Fig. 5.6, derived from the mean grain size distribution of Fig. 4.2. An approximate assumption is made here that the mean grain diameter is equal to the characteristic dimension.

The landing probability curve constructed on the premise of Eqn. 5.1 extends only to the toe of talus. In order to extend it beyond the toe into the rockfall shadow area, additional information is required.

This is provided by Fig. 5.7, showing the distribution of rockfall fragments with distance from the talus toe, measured at another site in the Similkameen Valley. The measurements were made on a plot of land 200 m wide, extending from the toe of the talus cone to the distal margin of the shadow. The distribution of boulder frequency versus distance from the toe is shown in the form of a histogram with a spacing of 20 m.

The absolute probability of landing within the shadow is obtained by assuming that the surface of the river terrace upon which the boulders rest is at least 5,000 years old (J. Ryder, pers. comm., 1988). The landing probabilities are then calculated by dividing the boulder landing counts given in Fig. 5.7 by 5,000 and by the area of 20 x 200 m. The resulting values are shown as triangular marks in Fig. 5.6. The two segments of the landing probability curve show continuity of slope, although they originate from two different sites.

THURBER

Impact hazard affecting a structure situated on or near the talus cone derives not only from fragments landing at that location but also from those crossing the location and destined to land further down the slope. This impact frequency, f_m can be estimated by integrating the landing probabilities over an influence area sketched in Fig. 5.8.

$$f_m = \int_{r_1}^{r_2} f_l \; r|r_1 \; dr \qquad \text{Eqn. (5.2)}$$

The equation must be integrated numerically, because f_l is an empirical function:

$$f_m = \sum_{r_1}^{r_2} f_l \; r_i|r_1 \; d \qquad \text{Eqn. (5.3)}$$

where i is a counter of sampling points regularly spaced at slope interval, d, downslope from the point in consideration. The point considered is located halfway between a pair of sampling points, as shown in Fig. 5.8.

The calculation results are given by the full line in Fig. 5.6 in terms of events per metre width.

Return period (T) of impact events at various locations can be estimated as:

$$T = 1 \Big/ f_m W \qquad \text{Eqn. (5.4)}$$

where W is the width of the area considered. The resulting return periods for a 10 m wide house site are indicated in Fig. 5.9. At 50 m from the talus margin, the impact probability is 0.00005 events/m and the corresponding return period for a 10 m house site is 1,900 years. A housing subdivision located at the same distance and covering an area 200 m wide would face a probability of being struck by a single boulder of 1 in 95 years.

Short term probabilities can vary considerably from the long term average.
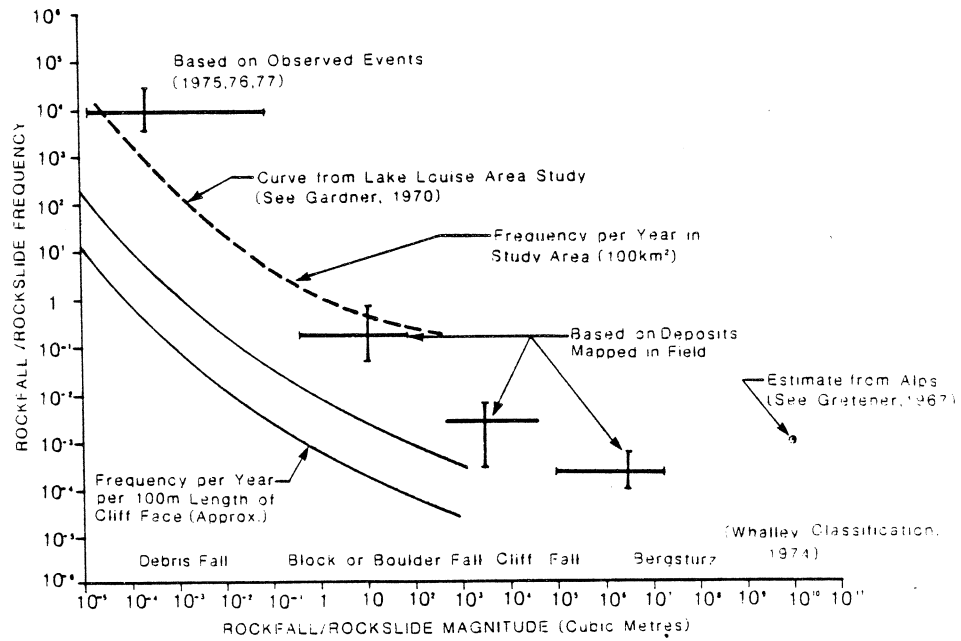
Figure 5.1. Approximate relationship between rockfall/rockslide frequency and magnitude for an area in the Rocky Mountains Front Ranges (after Gardner, 1980).
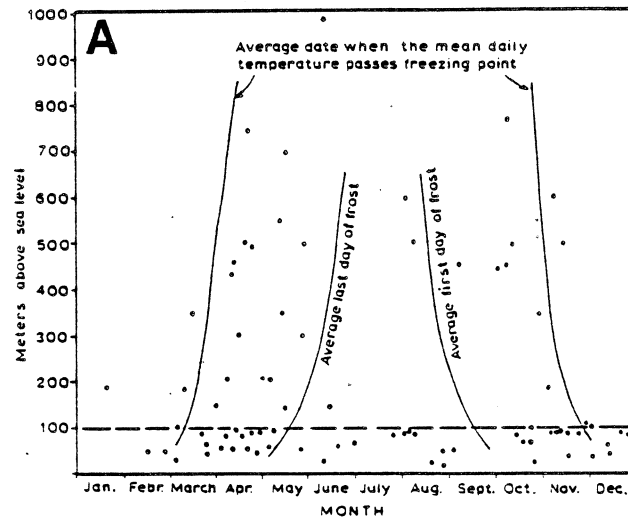
Rock falls in Eastern Norway in relation to altitude.
time of fall, and temperature. Dots indicate rock falls
occurring during the different seasons below and
above elevation 100 metres.
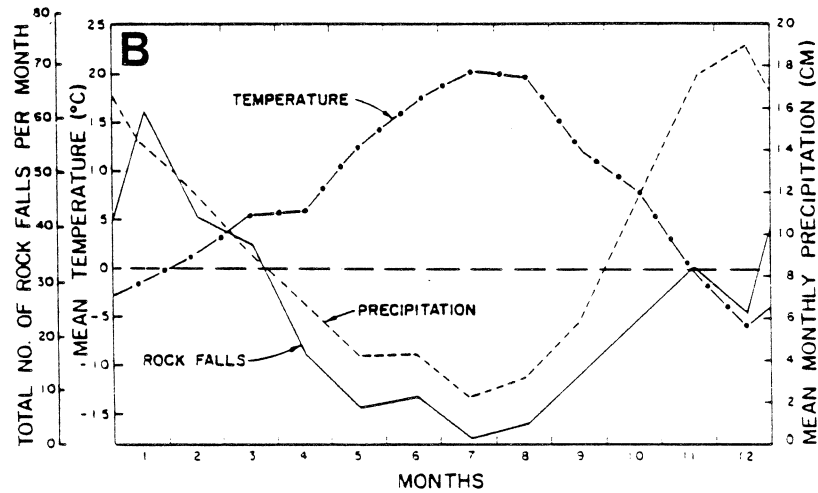
Figure 5.2. Rockfall frequency variation with seasons. A: Norway (Bjerrum and
Jorstad, 1968). B: Fraser Canyon, B.C. (Peckover and Kerr, 1977).
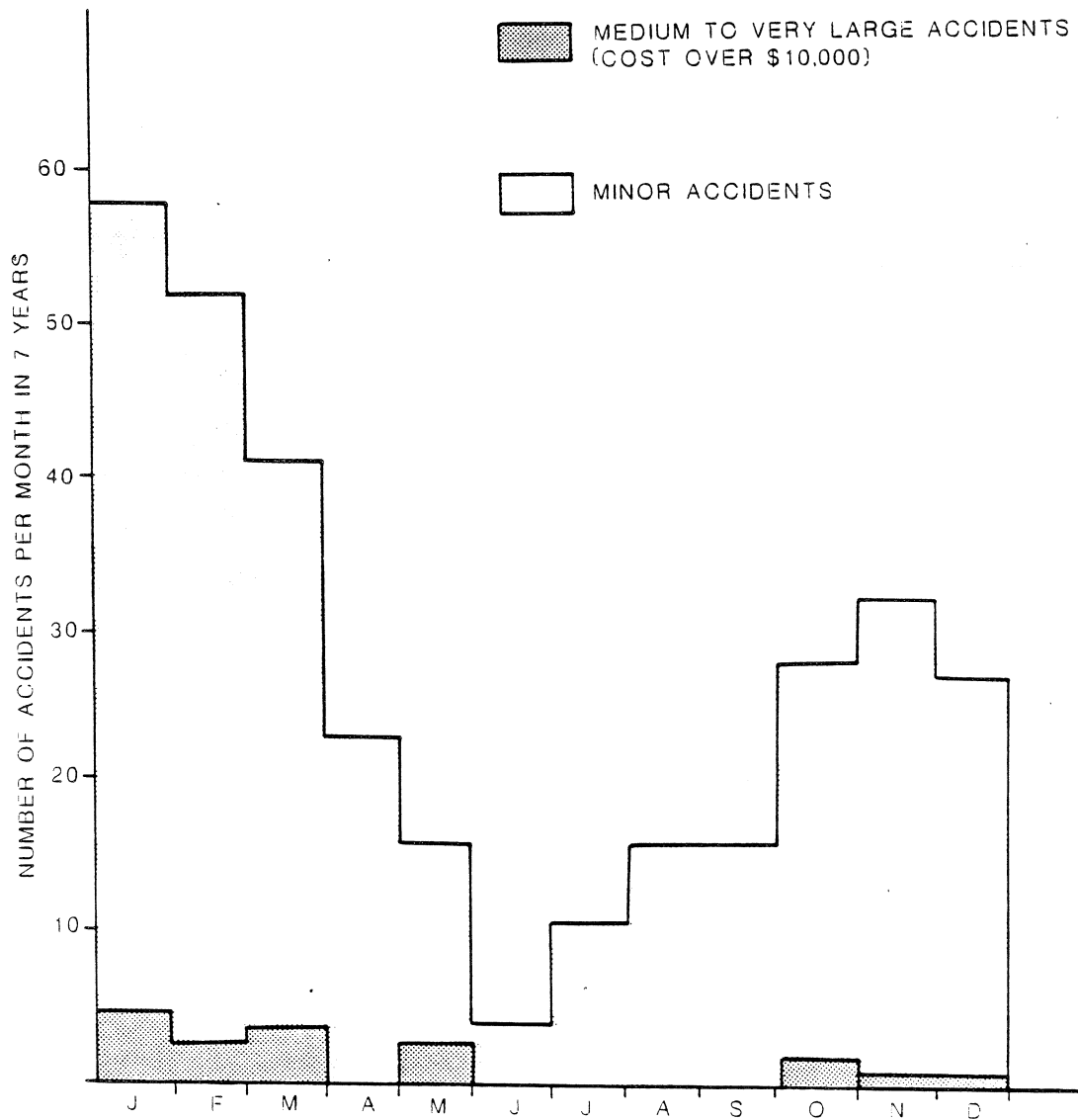
Figure 5.3. Seasonal rockfall incident distribution, B.C. Rail System, 1980 to 1987.

THURBER
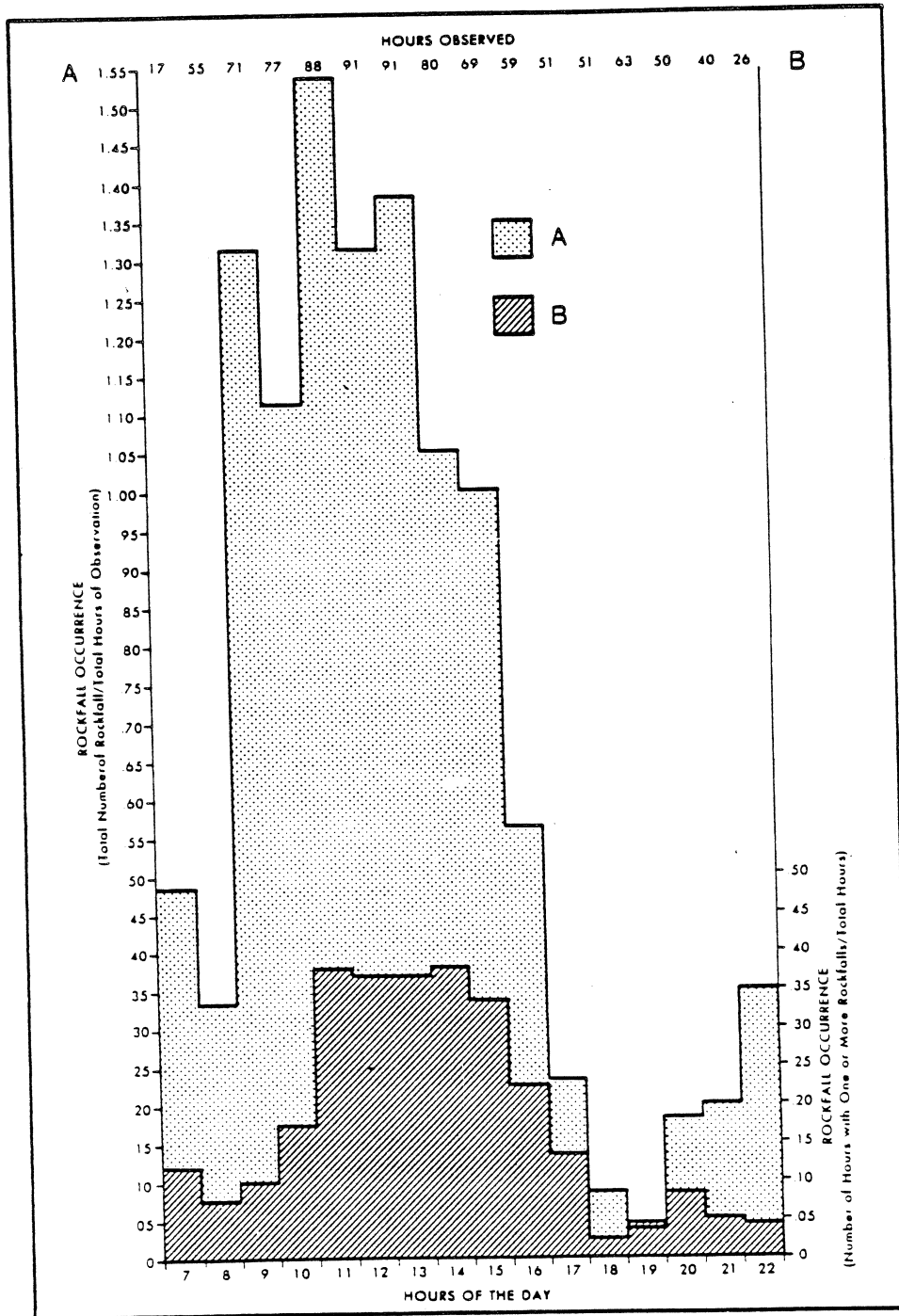
Observed rockfall/rockslide occurrence on the "average day," using data from 1975, 1976, and 1977. A shows the frequency of rockfalls for each hour. B shows the probability of observing one or more rockfalls/rockslides for each hour.

Figure 5.4.   Daily variation of rockfall frequency in the Highwood Pass study area, Alberta during summer months (Gardner, 1980).

THURBER
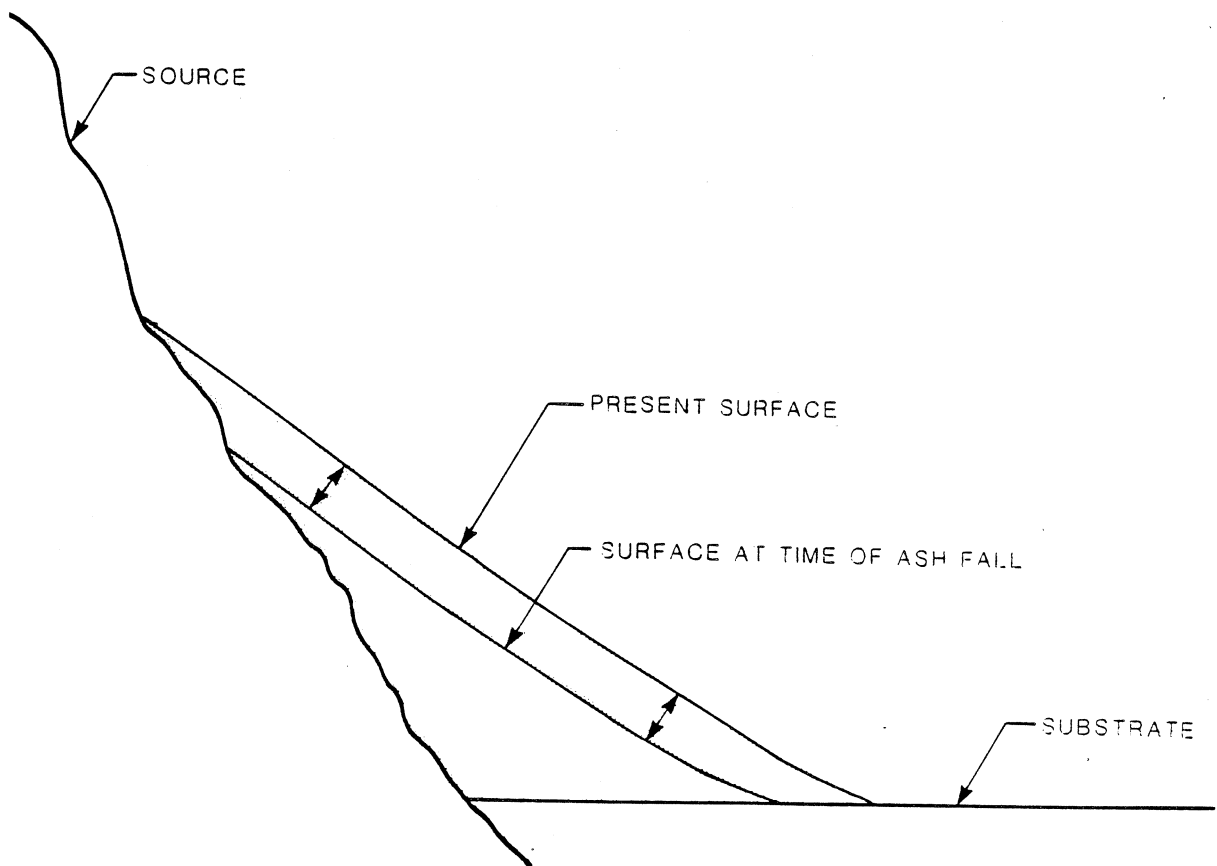
Figure 5.5. Schematic illustration of the concept of uniform talus surface growth rate.

THURBER
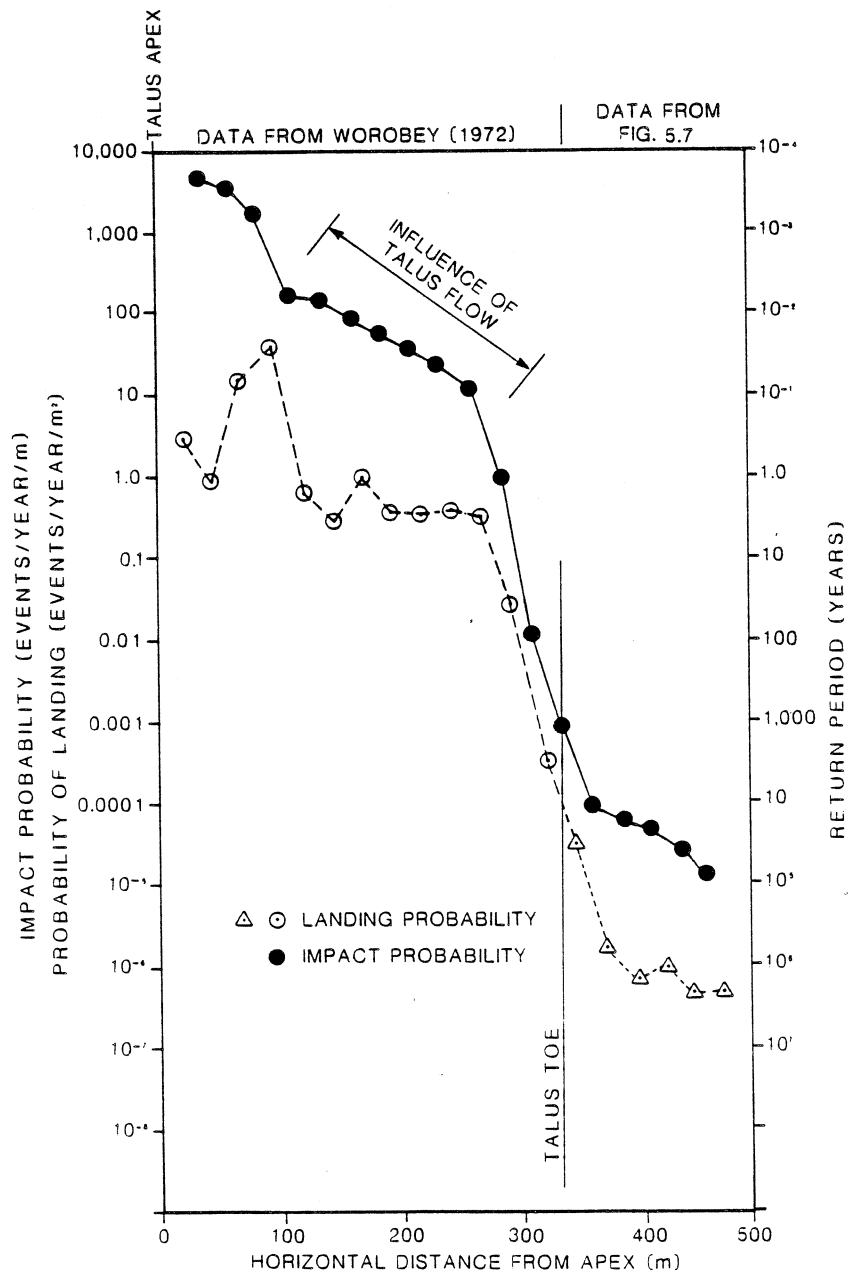
Figure 5.6. Landing and impact probability distributions calculated for the talus slope shown in Fig. 4.2.
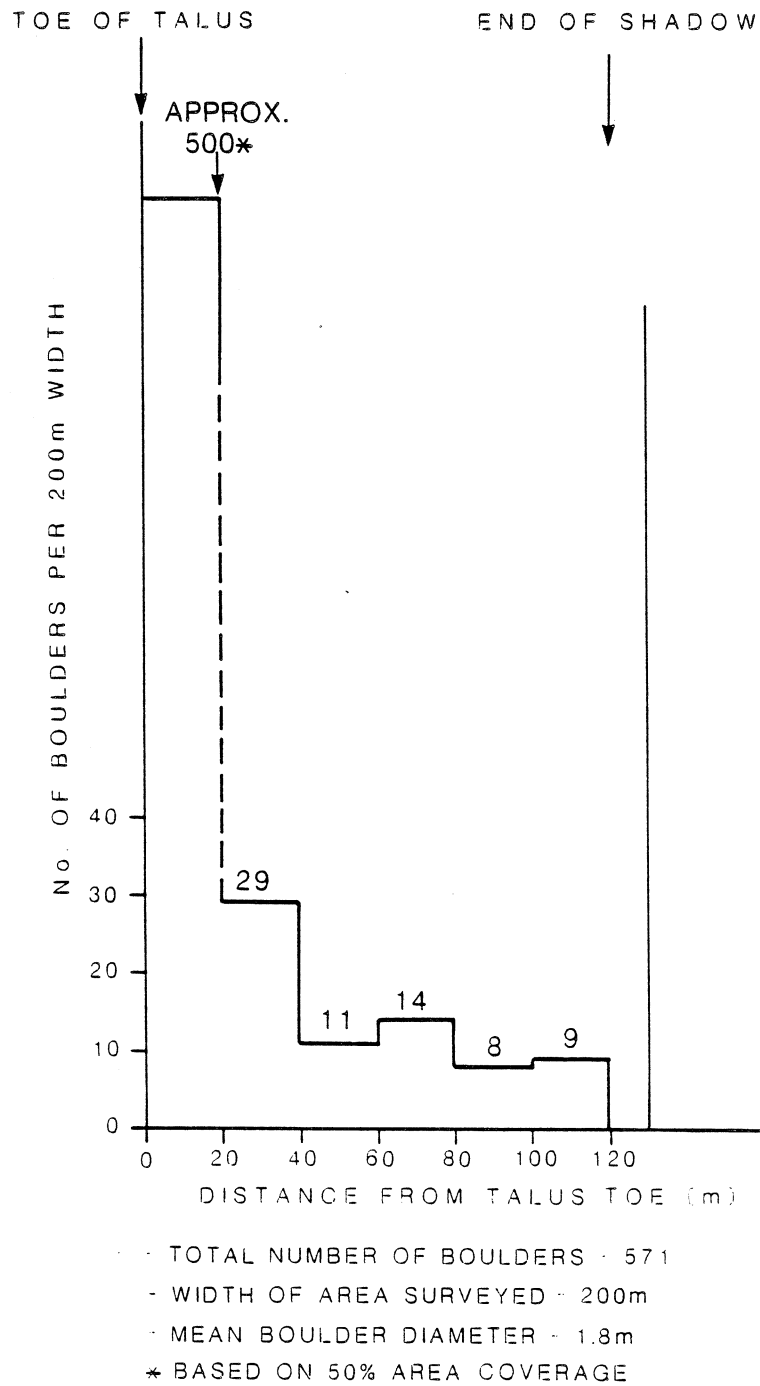
Figure 5.7. Distribution of boulders in the distal part of a rockfall shadow area surveyed in the Similkameen Valley, British Columbia.

THURBER
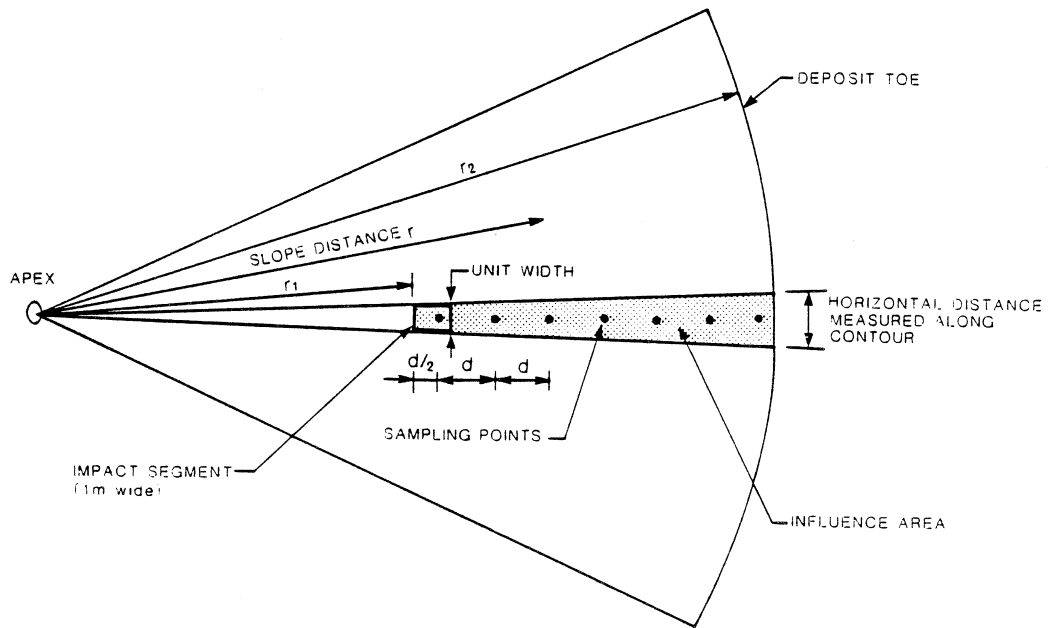
Figure 5.8. Unfolded plan of the cone surface, showing influence area used in calculations of impact frequency.
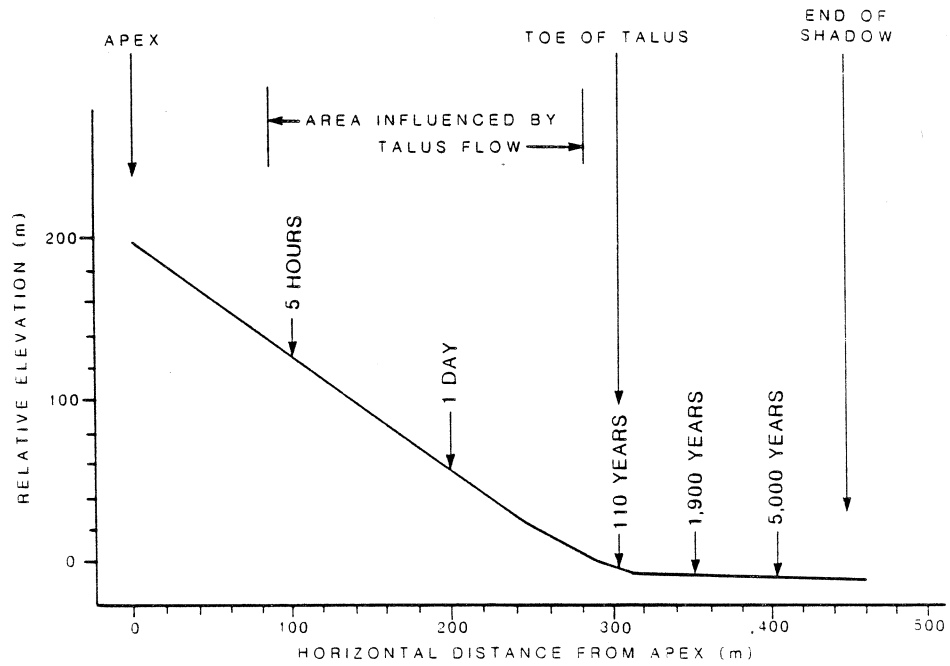
Figure 5.9. Approximate return periods for impact damage to a 10 x 10 m house site.

THURBER

6. PREDICTION OF ROCKFALL BEHAVIOUR

6.1 Parameters Required for Rockfall Hazard Assessment

The rockfall shadow area (see Chapter 4) surrounding the toe of talus deposits represents the true danger zone of the rockfall path. While the rockfall hazard is usually obvious on the talus surface itself, in the shadow area it sometimes may not be apparent.

For the purposes of protection of structures by means of hazard zoning, it is necessary to outline the length and width of the shadow area by estimating the length of maximum runout and the probability of fresh fragments reaching into the various parts of the hazard zone.

For design of protection measures such as catch fences or ditches, design velocities and sizes of fragments are required, or a direct assessment of the behaviour of the design rockfall event in the presence of the protective measures.

The techniques of rockfall behaviour prediction available for these purposes are reviewed in this chapter.

6.2 Analysis of Geological Evidence

In some cases, it is possible to ascertain the past behaviour of a rock slope over a long period on the basis of geological evidence. Such information can then be extrapolated so as to predict the reach of future rockfall within a given return period.

An example is provided by the evaluation of rockfall hazard at the community of Silverhope in southwestern British Columbia, located on an alluvial fan in front of a deltaic terrace. Immediately beyond the terrace, cliffs composed of massive Eocene quartz diorite and hornfels rise to a height of 600 m. Extensive talus deposits and fields of large boulders which have rolled behind the talus margins testify to rockfall activity, although the slopes are heavily forested and no accidents involving rockfall have been reported. The site has only been settled since the 1950's however, and no extensive historic record is available.

Figure 6.1 is a view from the crest of the source cliff (arrow) towards the community. The white dashed line marks a distinct, well defined limit of the boulder deposits (i.e. the edge of the rockfall shadow). No rockfall related boulders have been found outside this line. The terrace surface outside the rockfall shadow is underlain by a deposit of cross-bedded sand containing no gravel or boulders, which is exposed in a small quarry on the left side of the photo. The sand is of deltaic origin, deposited in standing water. However, no lake has existed at the site in the Holocene. Therefore, the surface of the terrace must be at least 11,000 years old, dating back to the last stages of glacial ice retreat from the valley (J.J. Clague, personal communication, 1986). The area outside the well defined boulder deposit limits therefore has a probability of less than 1:11,000 of being reached by rockfall from the cliff in a given year.

The general frequency of rockfall in this area was indicated by a detailed inspection of talus deposits beneath cliff fronts totalling approximately 2,700 m in length. The talus deposits are partly forested and heavily moss covered. Only 6 fragments were found whose appearance indicated that they have been deposited within the last year, their sizes varying from 0.01 to 0.1 m^3. The average frequency of fragments in this size range falling onto the talus apron therefore works out to 0.04 per year per 100 m length of cliffs, which is within the range of the frequency-magnitude curve described by Gardner (1980), shown in Figure 5.1. No fresh fragments or tree damage associated with rockfall were identified within the rockfall shadow area.

Not all sites provide sufficient evidence to allow such reasoning. If it were not possible to reliably date the substrate surface, if weathering conditions change (e.g. due to deforestation or a recent major instability), or if there were boulders of glacial or debris flow origin impossible to distinguish from rockfall deposits, then this method may not provide satisfactory answers.

6.3 Empirical Evaluation

It has been suggested that the minimum value for the shadow angle (β_2) defined in Figure 4.3 should be in the range of 28° to 30° (Lied, 1977). The authors have compiled 15 profiles of rockfall paths surveyed from two areas of southwestern British Columbia (Figure 6.2 and Table 6.1). The profiles have been plotted so as to join at the talus apex (Point A) as a common fulcrum.

The points representing the limit of the shadow plot consistently just below a line inclined at 27.5, irrespective of the height of the source cliff, length of path, or the substrate angle β_3. The data points represent locations both in the sparsely forested arid interior of British Columbia and in the Coast Mountains where the climate is humid and where there is dense forest cover outside the most active talus areas. It is noted that profiles 11 and 12 were measured in the area photographed in Figure 6.1.

The use of an empirical minimum shadow angle of 27.5° would appear to be a useful method for the preliminary estimation of maximum rockfall reach.

The authors have observed that the same angle applies at many other sites in British Columbia. Flatter angles sometimes result where the runout surface is exceptionally smooth. For example, a shadow angle of 24° has been measured for a single 4 m diameter boulder rolling or sliding over the smooth surface of a glacier near Whistler, B.C.

A theoretical explanation of the minimum shadow angle concept is given in Section 7.6.

6.4 Physical Modelling

Physical models of the rockfall process have been used on several occasions, both to investigate the nature of the process itself and to evaluate the design of specific remedial measures.

The principles of model similitude for rockfall have been reviewed by Camponuovo (1977). They include, among other considerations, similarity in block shape and surface roughness and the ability of the test fragments to break on impact as they do in full scale motion.

An acceptable degree of similitude has apparently been achieved by the ISMES Institute of Bergamo, Italy, on a 1:160 scale model of a part of Mt. S. Martino, a site of a major rockfall accident (Camponuovo, 1977). To achieve the required impact breakage, each of the model fragments was made up of an aggregate of smaller particles, held together by weak cement.

The model was used to evaluate the effectiveness of protective ditches and walls intended to safeguard buildings and roads in the area.

Less elaborate models have been used by Kirkby and Statham (1975), Azimi and Desvarreux (1977), Broili (1977), and others to study the behaviour and deposition patterns of rock fragments.

Full scale modelling programs have been described both by Ritchie (1963) and Broili (1974). Both have filmed fragments of various sizes released over cliffs. A number of useful general traits of rockfall behaviour have been found from these experiments. Some are reviewed in Section 4.1 and used to establish criteria for the mathematical model developed by the authors (in Chapter 7).

6.5 Analytical Approach

In recent years, several investigators turned their attention towards computer-based analytical models, simulating the actual progress of a rock fragment down its path (Piteau and Clayton, 1977; Azimi and Desvarreaux, 1977; Azimi et al., 1982; Aste et al., 1984, 1987; Wu 1985;

THURBER

Falcetta, 1985; Rochet, 1987a, b; Kobayashi and Kagawa, 1987; Descoeudres and Zimmerman, 1987; Spang, 1987; Spang and Rautenstrauch, 1988; Bozzolo et al., 1988). The models have to be capable of tracing the several different modes of movement by which rockfall travels:

a. Rolling and Sliding The motion of a fragment after detachment usually begins by sliding or rolling (Ritchie, 1963) and the same movement mode prevails prior to deposition. Both types of motion are amenable to analysis using a dynamic friction model:

$$a = g \left(\sin \alpha - \cos \alpha \, \tan \phi_d \right)$$
<div align="right">Eqn. (6.1)</div>

where a is the acceleration of the moving block, g the acceleration of gravity, α the path inclination angle and ϕ_d the dynamic friction angle, or rolling friction angle.

Statham (1976) back-calculated the dynamic friction angle by means of field experiments, rolling rocks of various sizes on talus surfaces. His results showed substantial scatter, but for particle sizes between one and four times smaller than the mean particle size of the talus, the friction angle ranged from 30° to 52°. There was a distinct trend for reduction of the angle with increasing relative size of the moving fragment.

b. Free Flight While in the air, the fragment moves along a ballistic trajectory described by the equation of the parabola shown in Figure 6.3a.

$$z = z_0 - \frac{v_z (x - x_0)}{v_x} - \frac{g}{2} \frac{(x - x_0)^2}{v_x^2}$$
<div align="right">Eqn. (6.2)</div>

Where x and z are the coordinates of the trajectory, and V_x and V_z are the horizontal and vertical components of velocity at the origin, whose coordinates are x_0 and z_0. Most of the existing models neglect air resistance.

c. Collision On contact with the ground surface, momentum transfer occurs between the particle and the ground. The moving particle has three components of linear momentum and three of rotational momentum. Upon collision, some of the momentum is consumed in generating impact and frictional forces. Also, a proportion of the linear momentum is transferred into angular momentum and vice versa. As a result, the angle of reflection is not generally equal to the angle of incidence and both the linear and angular velocities change in an impact.

The collision effects can be described mathematically under ideal circumstances. For example, the velocity components of a spherical particle impacting onto a planar surface (Figure 6.3b) are given by the following equations (Goldsmith, 1960):

Tangential component of rebound velocity:

$$V_t = \frac{5}{7} V_i \sin \theta - \frac{2}{7} R \omega_i$$
<div align="right">Eqn. (6.3)</div>

Normal component of rebound velocity:

$$V_n = -k V_i \cos \theta$$
<div align="right">Eqn. (6.4)</div>

Angular rebound velocity:

$$\omega_r = \frac{2}{7}\omega_i - \frac{5}{7}\frac{V_i \sin\theta}{R} \qquad \text{Eqn. (6.5)}$$

Where V_i is the incident velocity and θ its angle with the normal to the surface, ω_i is the incident angular velocity and R the sphere radius. The constant k is the normal restitution coefficient of the impact. The equations apply to the case where no slip occurs at the contact. Similar relationships can be derived for the case where the tangential impulse is limited to the frictional resistance at the contact.

Equations 6.3 to 6.5 imply the following:

— The normal momentum change is controlled only by the normal restitution coefficient and does not depend on rotation.

— Rotational momentum changes into tangential and vice versa.

— A particle which has no rotation prior to impact undergoes a reduction in its tangential momentum by a factor of 5/7 (71%) and begins rotating after impact with a peripheral velocity of 71% of the incident tangential velocity.

— A particle rotating with a peripheral velocity equal to the incident tangential velocity loses no tangential momentum.

The basic nature of these conclusions parallels some of the observations of Ritchie (1963) who noticed that falling rocks rapidly gather rotational momentum and move in long flat trajectories which gradually change into rolling.

While the mathematical concepts are interesting to consider, the actual impact conditions are much more complex. Eccentric impacts of an irregular particle against a rough surface give rise to highly complex changes in movements even if considered only in two dimensions. For example, Figure 6.4 compares two hypothetical impacts of a triangular fragment. In both cases, the particle shape is the same, as are the incident linear and angular velocities and direction angles. The only difference between A and B is a slight delay in the particle rotation, which causes B to contact the surface in a somewhat different manner. The resulting difference in the collision behaviour is dramatic. Particle A undergoes two contacts, followed by a backward rebound with slow rotations. Particle B rolls forward and probably loses little of either rotational or translational momentum. Subtle effects such as air resistance could account for the millisecond difference in timing represented by the two cases.

Further complications would result if sliding, crushing or breakage phenomena were considered and if the analysis was carried out in three dimensions. Notwithstanding these difficulties, attempts at developing a rigorous mathematical model describing the movement of a bounding rock fragment can be found in the literature.

6.6   Rigorous Models

Rigorous models consider the rock fragment a two or three-dimensional object with specific shape. When in flight, the object moves on a ballistic parabola and maintains the rotational momentum incurred in the latest impact. On approaching the path surface, the exact point of contact must be determined and all the reaction forces in it. Application of these forces in combination with a prescribed energy loss formula (e.g. a restitution coefficient) results in a change of flight direction, velocity and rotation, leading into another air trajectory.

THURBER

The analysis is relatively simple when rotational particles such as spheres or cylinders are used. The form of the contact is then constant and the collision formulas given earlier in Equations 6.3 to 6.5 may be applied. This forms the basis of computer models described by Benitez et al. (1977) and Kobayashi and Kagawa (1987).

The spherical impact model, while capable of a reasonable simulation of the bouncing of a ball upon a billiard table, cannot possibly account for the behaviour of an irregular rock fragment such as illustrated in Fig. 6.4. The assumption of regular symmetrical contact geometry imposes a set relationship between energy losses in the tangential and normal directions which does not apply for particles which are even slightly irregular. To correct this situation, the authors of the models discussed have chosen to perturb the slope surface angle by a random number. The resulting normal and tangential energy losses are then simply random functions of the approach velocities.

More complex models exist describing the rock fragment as a geometric body with a rectangular or polygonal cross section. The calculations are then substantially more complex, as it is necessary to consider the rotation angle of the particle, and the exact nature of the contact depending on this angle.

The first detailed application of the dynamic equilibrium equations to such a case is represented by the Discrete Element Model (e.g. Cundall, 1971). This deals only with moderate displacements and is therefore suitable only for simulating the initial stages of rockfall. Extensions of the model to the case of rockfall where contact episodes are separated by trajectory flight, have been described by Falcetta (1985) and, in three dimensions, by Descoudres and Zimmerman (1987).

As discussed in Section 6.5, it is considered impossible to provide an exact mathematical model of detailed surface irregularities, fragment shape, and contact deformation conditions for actual rockfall. The use of idealized parameters, while correct both physically and mathematically, can at best result in obtaining a random relationship between movement quantities before and after impact.

The chance element involved in collisions of actual particles on an uneven travel path is of such overwhelming importance, that these authors consider the development of rigorous models counterproductive. The simplified models described in the following section have fewer parameters and are thus better suited to both empirical calibration and stochastic treatment.

6.7 Simplified Models

In the simplified or "lumped mass" approach, the fragment is considered as a single point with mass m and velocity $\underline{v}$ (where the underlining signifies a vector quantity). The point moves along a ballistic trajectory while in the air. Upon contact with the slope, the velocity vector components, normal and tangential to the slope surface, are reduced as follows:

$$v_n' = v_n k_n \qquad \text{Eqn. (6.6)}$$

$$v_t' = v_t k_t \qquad \text{Eqn. (6.7)}$$

where the apostrophe marks the velocity components applicable after the impact. The coefficients k_n and k_t are referred to as the normal and tangential restitution coefficients.

No attempt is made to keep track of the rotational momentum. The two coefficients are taken as bulk measures of all the impact characteristics, incorporating deformation work, contact sliding and transfers of rotational to translational momentum and vice versa. As a result, the coefficients must depend on fragment shape, slope surface roughness, momentum and

deformational properties and, to a large extent, on the chance of certain conditions prevailing in a given impact.

In general, the restitution coefficients are random variables, whose range is controlled by a number of factors, some of which are described below.

The first published account of a lumped-mass rockfall dynamics model is that by Bhandari and Sharma (1976), concerned with the air trajectory only. Piteau and Clayton (1977) used a model described by a single constant restitution coefficient (i.e. $k_n = k_t$), perturbing the path inclination randomly to account for the variability of impact conditions. A similar model was used by Spang (1987).

The use of two separate restitution coefficients according to Equations 6.6 and 6.7 is reported by Azimi and Desvarreux (1977), Azimi et al. (1982) and Wu (1985). All of these considered the restitution coefficients as variables depending on certain impact parameters.

6.8   Variation of the Restitution Coefficients

As stated above, the restitution coefficients are random variables. Numerous empirical observations indicate, however, that their range of variation must be a function of impact momentum, in consequence of the work expenditure required by contact crushing and deformation. It is a common observation, for example, that a small stone dropped onto a rock surface can rebound as much as 50 to 70% of its original height. A large block dropped from a considerable height will fracture on impact and rebound negligibly.

Some computer models therefore introduce variation of the restitution coefficients as functions of the normal velocity (e.g. Azimi et al. 1982, Wu 1985, Kobayashi and Kagawa 1987).

The rigorous rockfall models require that the work expenditure by contact deformation be explicitly specified. A simple formula derived for this purpose by Falcetta (1985) and forming a part of the TRAJEC model (Aste et al., 1987) is described below.

The normal deformation at the contact is assumed to be described by a bi-linear force/displacement diagram illustrated in Figure 6.5. The initial stiffness of the contact is characterized by the coefficient C_1, applicable up to a "yield" force F_0. Above the yield, the contact stiffness reduces to C_2. The parameter C_2 can also be represented by a stiffness ratio R, equal to C_2/C_1. After the maximum contact force F_m is reached, the contact rebounds elastically with a rebound stiffness C_3.

If a light impact occurs, in which the yield force is not exceeded, then the normal restitution coefficient can be calculated as:

$$K_n^e = -\sqrt{\frac{C_1}{C_3}}$$

Eqn. (6.8)

In a strong impact, yielding occurs with expenditure of additional work and the resulting normal restitution coefficient becomes a function of the maximum constant force, F_m as follows:

$$K_n = K_n^e \sqrt{\frac{C_2}{\left[C_1 + \left(\frac{F_0}{F_m}\right)^2 (C_2 - C_1)\right]}}$$

Eqn. (6.9)

The maximum contact force can be derived from energy balance as a function of the approach normal velocity and particle mass, or:

$$F_m = \sqrt{C_2 \, v_n \, M + F_o^2 \, \frac{(C_1 - C_2)}{C_1}}$$ Eqn. (6.10)

The form of the resulting relationship between the normal velocity (v_n) and normal restitution coefficient (k_n) is shown in Fig. 6.6, related to an elastic k_n value of 1.0. The particular parameters used to construct the figure have been derived by trial and error to match approximately an experimental variation of k_n reported by Wu (1985). They are applicable to rocks with a mass of the order of 50 kg, impacting a rock surface with normal velocities of 5 to 15 m/sec. Variation in k_n of a form similar to that shown in Fig. 6.6 has been found experimentally by Azimi and Desvarreux (1977).

The dependence of the tangential restitution coefficient upon velocity has not yet been clarified by experiments. Limited experimental work reported by Wu (1985) indicates this coefficient to be nearly constant and of the order of 0.5 to 0.8.

6.9   Rockfall Movement Modes

As a result of gradual expenditure of energy, successive bounces of a falling rock fragment become progressively shorter. Eventually a condition of rolling results, where there is nearly continuous contact between the fragment and the path. Rolling is often the dominant mode of movement on long paths as illustrated by the Hedley example in Section 8.2.

Some of the computer models described in the literature include a rolling mode, characterized by a rolling friction coefficient f_r. The velocity of a rolling fragment on a path segment of a constant slope a is calculated as:

$$V = \sqrt{V_0^2 + 2gs \left(\sin \alpha - f_r \cos \alpha \right)}$$ Eqn. (6.11)

where v_0 is the initial velocity at the onset of rolling, and s is the rolling path distance.

The rolling friction model was used exclusively to derive runout paths of fragments in studies of talus building by Kirkby and Statham (1975), with good experimental results.

In models capable of simulating the bouncing mode, a criterion for transition from bouncing to rolling must be specified. This is often taken as a limiting absolute or normal velocity (e.g. Kobayashi and Kagawa, 1987). A different criterion is developed in the present study.

6.10   Current Status of Dynamic Modelling of Rockfall

The above overview indicates that research into dynamic modelling of rockfall has received considerable attention during the last decade. Probably the main reason for this is that dynamic models are capable of providing design parameters such as bounce height or velocity, which are useful for the structural design of defensive measures such as rockfall fences or ditches (e.g. Bhandari and Sharma, 1976; Piteau and Peckover, 1978; Ballivy et al., 1984; Chan et al., 1986).

The models differ widely in terms of their physical background and complexity. Based on their experience with the rockfall process, these authors are of the opinion that the most reliable means of modelling it, lie in using a relatively simple theoretical framework with the maximum flexibility and adaptability to empirical calibration. This was the underlying premise in the development of the model ROCKFALL described in the following chapter.

THURBER
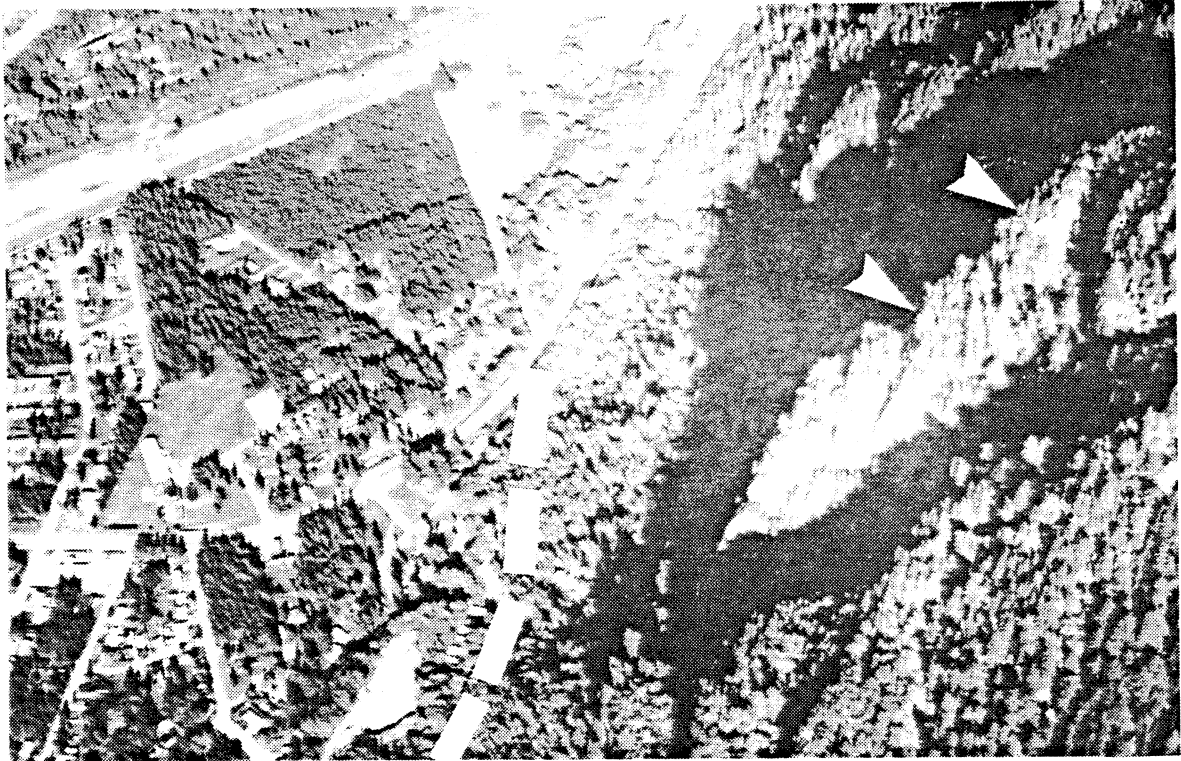
Figure 6.1. Oblique view of a community in southwestern British Columbia. Arrow indicates source cliffs. White dashed line is limit of rockfall deposits.

THURBER

Table 6.1

LOCATIONS OF PROFILES IN FIG. 6.2

---

  *1; Hedley

  *2; Similkameen A (Sweatlodge)

   3; Similkameen B (Rockslide)

   4; Similkameen C (Kame)

   5; Similkameen D (Winters Creek)

   6; Similkameen E (Campground)

   7; Similkameen F (Speedway)

  *8; Pukaist

  *9; Sunnybrae

 *10; Barnhartvale

  11; Silverhope A

  12; Silverhope B

  13; Silverhope D

  14; Silverhope C

 *15; Hope North

---

* Sites where fresh debris was found in the rockfall
   shadow area.

TALUS SLOPE APEX (FULCRUM)
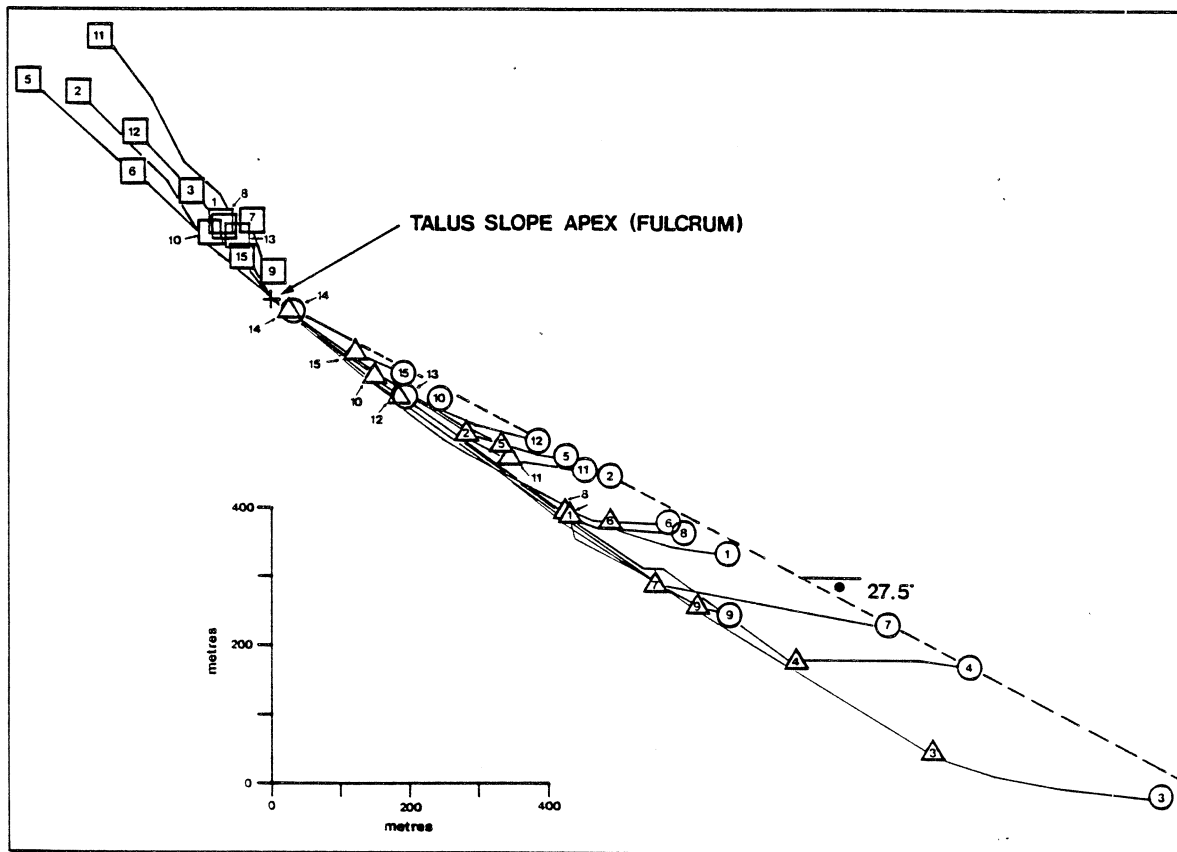
Figure 6.2. Profiles of fifteen surveyed rockfall paths from British Columbia. The profiles have been plotted with the talus apex as a common point. As in Figure 4.3 triangles designate the base of the talus slope and circles designate the distal margin of the rockfall shadow. The squares represent either known source areas or the crest of the source cliff.
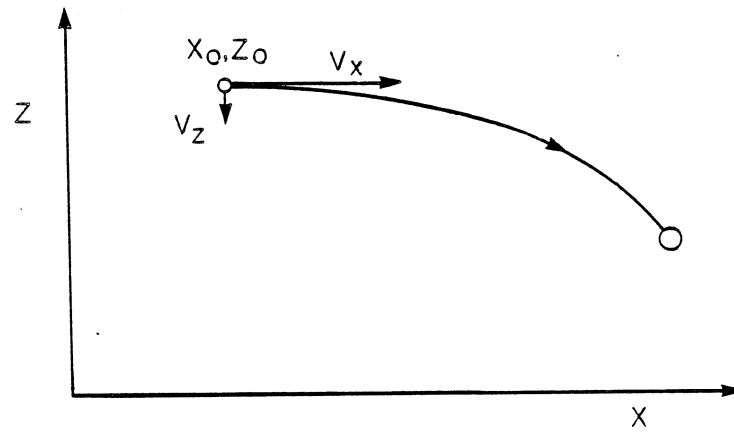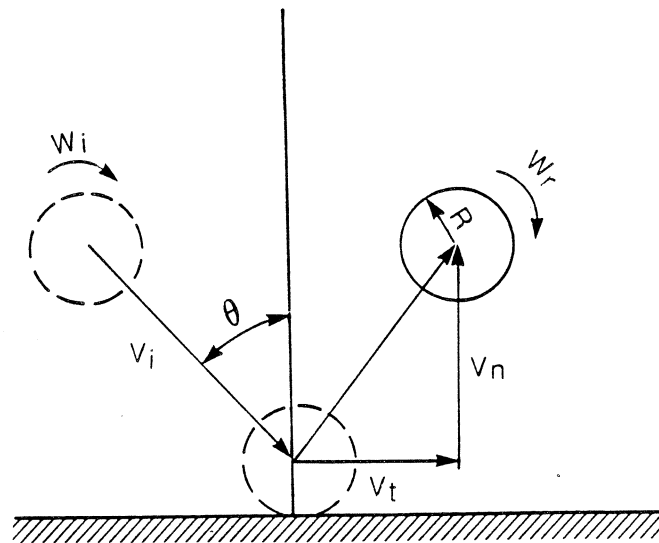
Figure 6.3 A: Ballistic parabola. B: Ideal impact of a spherical partical against plane surface
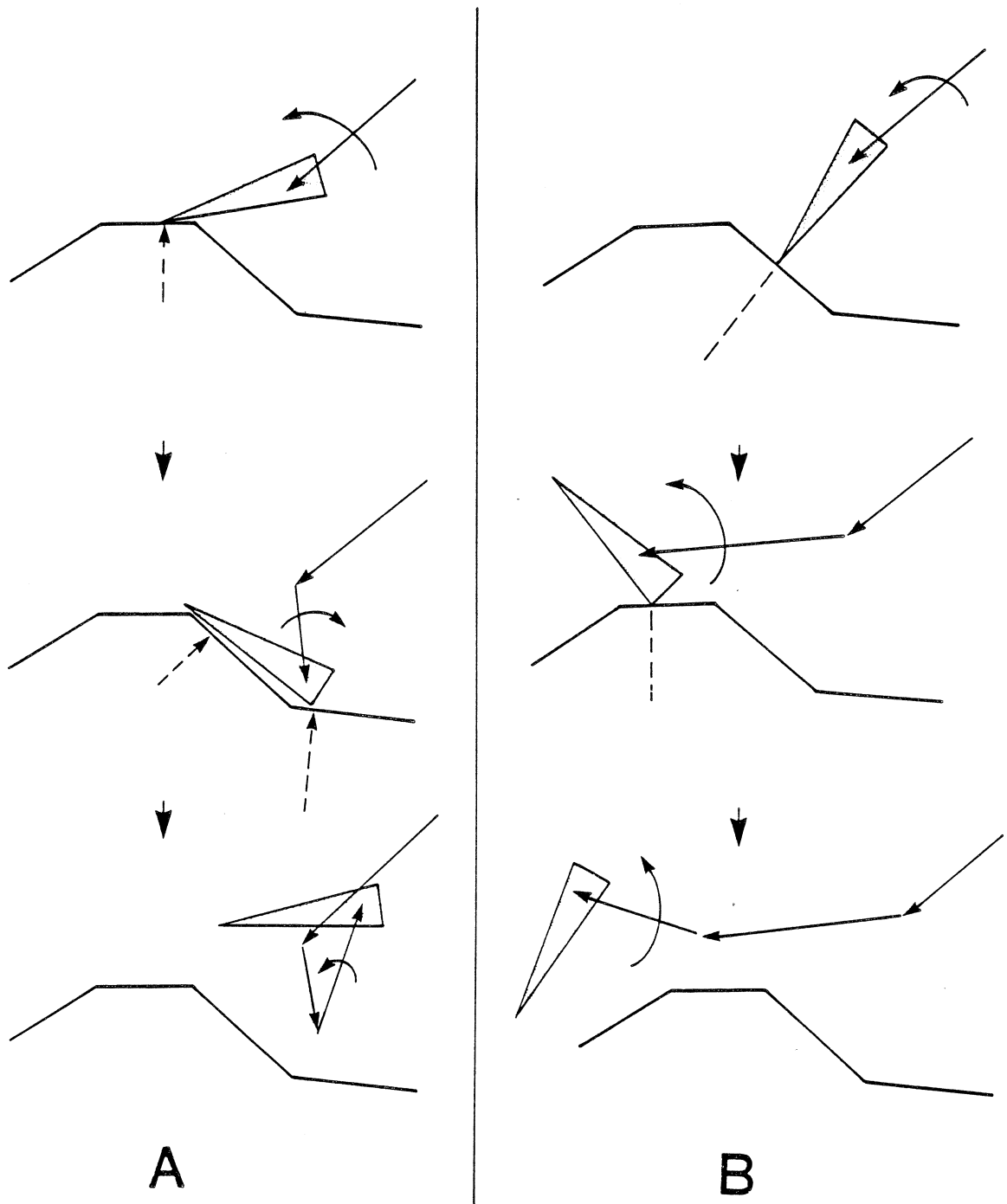
Figure 6.4. Two instances of irregular particle impact. Both cases involve the same particle with the same incident velocities only the relative rotation of Particle B is slightly more advanced at the moment of contact. Totally different response results.

$$K_n^e = \sqrt{\frac{C1}{C3}}$$

$$R = \frac{C2}{C1}$$

CONTACT FORCE

Fm

Fo

SLOPE C2

SLOPE C1

REBOUND SLOPE C3

0

CONTACT DEFORMATION
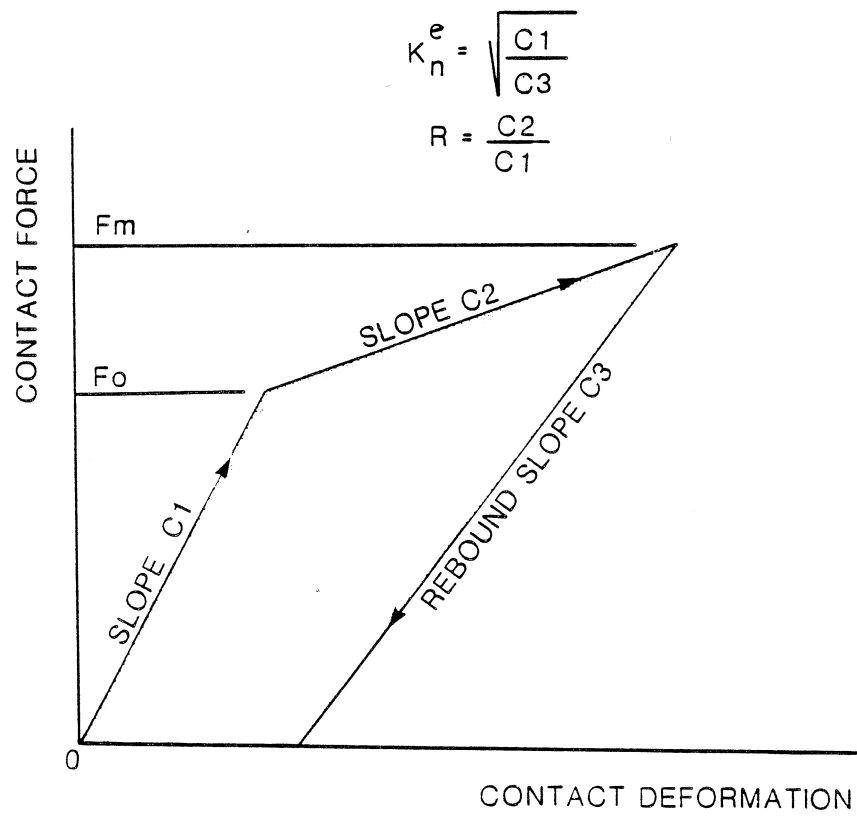
Figure 6.5. Contact deformation model developed by Falcetta (1985). See text for explanation.

THURBER
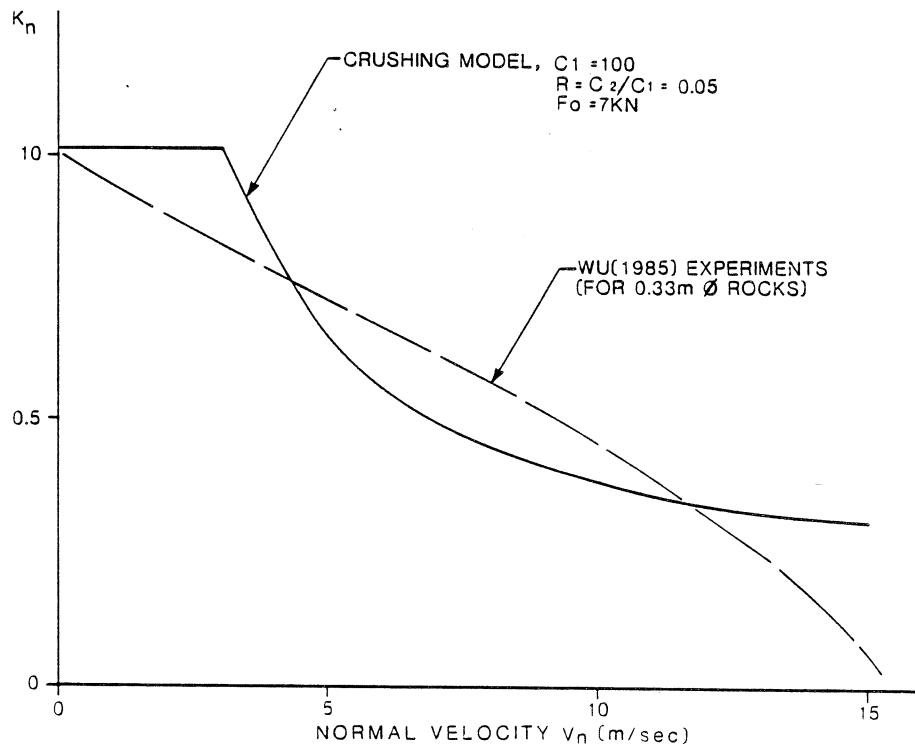
Figure 6.6. Form of the relationship between normal momentum (v_n) and the normal restitution coefficient (k_n) for the two cases represented by Table 7.1.

7. DEVELOPMENT AND EVALUATION OF AN ANALYTICAL MODEL

7.1 Objectives

The computer program (ROCKFALL) described in this chapter and in Appendix A is a multi-purpose dynamic model of rockfall, suitable for the following uses:

— Estimating maximum rockfall path lengths on various profiles.

— Statistical predictions of rockfall runout distributions, based on random assignment of input parameters.

— Plotting of single or multiple rockfall trajectories, suitable for planning the location and sizing of measures such as protective fences or ditches.

— Prediction of rockfall movement velocities, to calculate potential impact forces on structures.

Secondary objectives followed in the development of the model have been that it should be easy to use and that it should work on a microcomputer.

7.2 Solution Algorithm

The solution algorithm for ROCKFALL follows closely the general simplified model described in Section 6.7. The implementation is described as follows.

The rockfall path profile is described by a series of points connected by straight line segments. Each segment has a "surface type" associated with it. For example, the path shown in Fig. 7.1 consists of 8 segments with three different surface types separated by oblique marks. Surface 1 in this case is bare rock, Surface 2 talus and Surface 3 is soil populated by forest.

Each surface type is characterized by a normal (k_n) and tangential (k_t) restitution coefficient as defined in Equations 6.6 and 6.7 and a rolling friction coefficient defined in Equation 6.11.

Rock fragments are introduced onto the profile in two ways. The fragment may be assumed to begin rolling from a stationary position on the ground surface. It accelerates while rolling over the surface of the first segment and passes into an air trajectory by one of the mechanisms illustrated in Fig. 4.1.

While in the air, the fragment moves on a ballistic parabola. Air resistance is neglected.

7.3 Influence of Contact Crushing

ROCKFALL can be used with constant restitution coefficients specified by the user for each surface type. Such analyses can be regarded as representing "ideal" conditions, where each contact of the rock fragment with the slope surface meets optimal conditions. The constant restitution coefficients can be derived from back-analysis of maximum runout of known events, occurring under conditions similar to those prevailing on the slope being analyzed.

The assumption of constant restitution coefficients is reasonable only in cases where each impact involves approximately the same level of momentum normal to the contact surface. This is obviously not the case on paths such as that illustrated in Fig. 7.1 where the first impact on the talus surface follows a long free flight from the high cliff. According to full scale experiments by Broili (1974), observed with the help of cinematography, 75 to 86% of the kinetic energy gained in the initial fall is lost in the first impact. The subsequent impacts, involving lesser normal momenta, consume much less energy. It is for this reason that the bi-linear contact deformation

THURBER

model developed by Falcetta (1985) was used. The model is described in Fig. 6.5 and Equations 6.8 to 6.10.

Preliminary calibration of the model for large rocks was achieved using the results of Broili (1977), mentioned earlier. Fig. 7.2.a shows a model of three of the experiments reported by Broili (1977). The camera records indicated three modes of motion: a) the initial fall from a height of 210 m, b) a sequence of bounces and c) a long segment dominated by rolling movement. The three zones are simulated by the model in Fig. 7.2.a. According to Broili's observations, as reproduced in Fig. 7.2.b, the length of the zone of bouncing increased with decreasing volume of the rock fragment released. The phenomenon is plotted in Fig. 7.2.b over a range of 0.5 to 10 m³. By trial and error, we have been able to approximate the experimental relationship as shown by the dashed line in Fig. 7.2.b, based on the parameters given in the first column of Table 7.1.

For preliminary purposes only, in the absence of more detailed calibration, these parameters are considered applicable to impact of large rocks (1,000 to 20,000 kg mass) on talus surfaces, without heavy vegetation.

It is unlikely that the same parameters could apply for smaller rocks, bouncing on different surfaces. For small rocks contacting clean rock surfaces, we have considered the results of experiments carried out by Wu (1985). These experiments involved dropping of rocks 0.2 to 0.4 m in diameter from a height of 12 m on rock and wood surfaces of different inclinations. From a plot of restitution coefficients versus contact surface angle given by Wu (1985), the points indicated in Fig. 6.6 have been plotted. The model parameters providing a reasonably good fit to these results are given in the second column of Table 7.1.

It must be stressed that more detailed calibration based on controlled experiments is necessary.

7.4 Rolling Mode

The bouncing model does not simulate correctly the final stage of rockfall movement when bounces become negligibly short. It is therefore necessary to provide a transition at some point into a rolling mode, described by Equation 6.11.

Several different criteria for transition between the bouncing and rolling mode were tried, including a limiting length of bounce, limiting time and velocity. With all of these, there were problems with numerical instability of the model, as they allowed bounces of extremely short length or low amplitude. The most satisfactory results were finally reached with the criterion described in the following paragraphs.

ROCKFALL calculates the "energy head" of the fragment at every point during its descent, as indicated by the dotted line in Fig. 7.3. While in trajectory, the fragment has a constant energy "head" equal to:

$$E = z + \frac{V^2}{2g} \qquad \text{Eqn. (7.1)}$$

where V is the length of the velocity vector and z is the fragment elevation. After an impact, the velocity component normal to the path is reduced by a ratio k_n and the tangential by k_t. It can be shown that the resulting incremental loss of energy is:

$$\Delta E = \frac{V^2}{2g} \left[\left(\frac{k_t^2 + k_n^2 \tan^2 \theta}{1 + \tan^2 \theta} \right) - 1 \right] \qquad \text{Eqn. (7.2)}$$

where θ is the angle of incidence prior to the impact. Thus, the kinetic energy is reduced in each impact by a ratio ranging from k_t^2 for very flat trajectories, through $(k_t^2 + k_n^2)/2$ for $45°$ impacts to k_n^2 for steep trajectories approaching the perpendicular. The "energy line" resulting from plotting the relationship in Eqn. (7.1) appears as a series of steps, separated by horizontal lines the length of which equals the trajectory length ΔL. When the ratio $\Delta E/\Delta L$ is less than the tangent of the slope angle, the fragment accelerates continuously and the energy line rises above the path as shown in the upper part of Figure 7.3a. When the ratio becomes greater than the slope gradient, the fragment decelerates and the trajectories rapidly become shorter as shown in the lower part of the figure. Deposition of the fragment then occurs.

As shown in Figure 7.3b, in ROCKFALL, a transition into rolling mode is made when, during 3 consecutive bounces, the ratio $\Delta E/\Delta L$ is greater than the rolling friction coefficient, i.e. the rolling movement mode becomes more efficient than the bouncing mode. When there is a change in path slope, such as at the crest of small cliff, the fragment may temporarily move back into trajectory.

For long slope segments which have slope angles of 45 and below, ROCKFALL generally predicts rockfall fragment paths which are dominated by rolling movement. This is exemplified by the long travel paths simulated in the Hedley and Sunnybrae examples below, and it is in agreement with the empirical observations of Ritchie (1963). Under such circumstances, the variation and even the absolute value of the restitution coefficients, are of secondary importance compared to the magnitude of the chosen rolling friction coefficient.

7.5   Stochastic Solutions

ROCKFALL has the ability to choose the restitution coefficients in each individual impact at random from a specified range. In each impact, a random value of the normal coefficient is first chosen, using a random number generator. It is then reduced for the effects of crushing using the formulas described in Section 7.3, i.e. the crushing parameters are considered fixed, only the "elastic" restitution coefficients are random.

Random numbers are also used to "release" a number of rock fragments from a given geometric range.

Two example results are shown to illustrate potential uses of the stochastic analysis in ROCKFALL. Fig. 7.4 is a histogram of 100 landings of rocks released at random from 0 to 10 m height above the slope, over the release region indicated by the cross marks. Individual trajectories have not been plotted in this case, although they were shown on the computer screen. The top part of the figure shows a histogram compiling the distances travelled by the randomly moving rocks. Such an analysis could be used to estimate the probability of a certain point in the runout area being reached by releases from a given release zone.

The second example, shown in Fig. 7.5, has been compiled using the same method, but each individual trajectory has been plotted. The locus of the random trajectories outlines the profile areas and heights above the slope likely to be impacted and could be used to predict impact areas on structures or to position remedial measures such as fences, barriers or ditches.

7.6   Summary

The model developed in this study (ROCKFALL) is capable of simulating a wide range of rockfall behaviour and allows for practical uses. However, more thorough calibration is required.

The initial calibration effort indicated that, besides parameter variability associated with various surface types, differences due to the size and shape of the released fragments will need to be considered. Especially with regard to the crushing energy loss parameters, different sets of values will need to be used for large, medium and small rocks as it is unlikely that any simple

THURBER

crushing model can encompass the entire range of behaviour from crater-producing major impacts to minor bounces on a hard surface.

Another important conclusion not previously reported is the fact that long rockfall trajectories on moderate slopes tend to be dominated by the rolling behaviour. This is in agreement with the observations made in the field during this study and also with the full scale experimental observations made previously by Ritchie (1963), Broili (1977) and Kirkby and Statham (1975).

This observation explains the concept of a constant "rockfall shadow" angle as discussed in Section 6.3 and Figs. 4.3 and 6.2. The kinetic energy acquired by the fragment in the initial steep fall is largely lost in the first impact on the talus surface near the apex. Thus, regardless of the initial height of fall, each fragment begins rolling near the apex point at a moderate velocity and its final runout is approximated by projecting the slope of the energy line, i.e. the rolling friction gradient beyond the talus toe. The value 27.5° obtained from Fig. 6.2 would thus appear to be the lower limit of the rolling friction angle for large boulders moving over the finer talus.

Table 7.1

PRELIMINARY MODEL PARAMETERS

	Condition	
	Large Rocks (1,000-20,000 kg) on talus	Small Rocks (20-100 kg) on clean rock
Normal restitution coefficient* (no crushing)	0.7	0.9
Tangential restitution coefficient*	0.8	0.9
Yield contact force Fo (kN)**	50	10
Initial contact stiffness** C_1 - (kN/m)	100	100
Stiffness reduction ratio** $R = C_2/C_1$	0.05	0.05
Rolling friction coefficient	0.52	0.52

* For definition see Eqn. 6.6 and 6.7
** For definition see Fig. 6.5
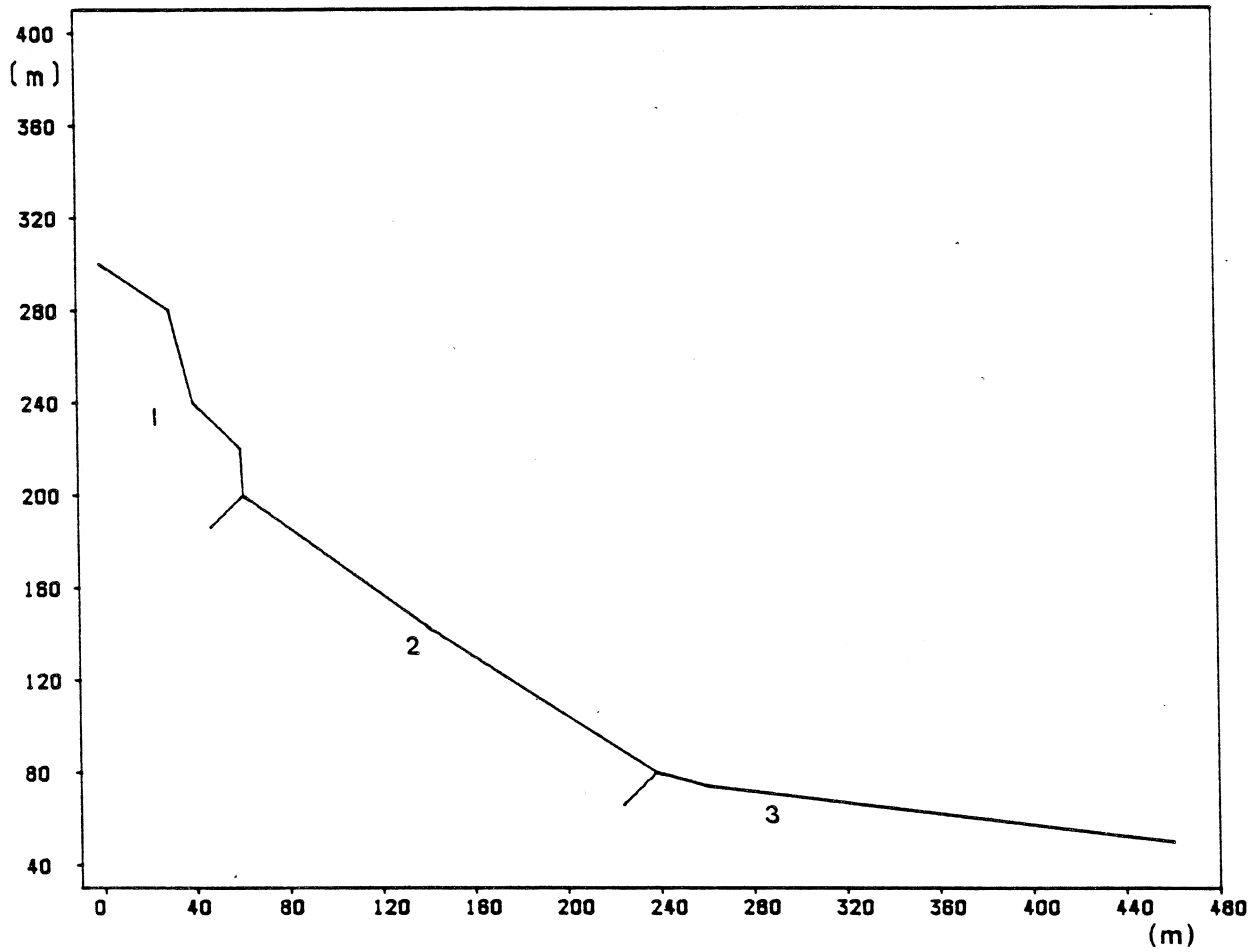
Figure 7.1. Typical slope profile used as input to the program ROCKFALL.

(m/sec):VELOCITY

```
==================================================================
ROCKFALL PATH > BROILLI <                    DATE 04-19-1988
==================================================================

SURFACE PROPERTIES

SURFACE          - KN -                - KT -        ROL.FRICTION
NO         MIN        MAX         MIN        MAX    COEFFICIENT
---------------------------------------------------------------
   1       0.70       0.70        0.80       0.80       0.80

CONTACT YIELD LIMIT           =   50
INITIAL CONTACT STIFFNESS     =   100
STIFFNESS REDUCTION RATIO     =   .05
```

(a)

(b)

Fragment Volume V(m³)

Experiments

Model
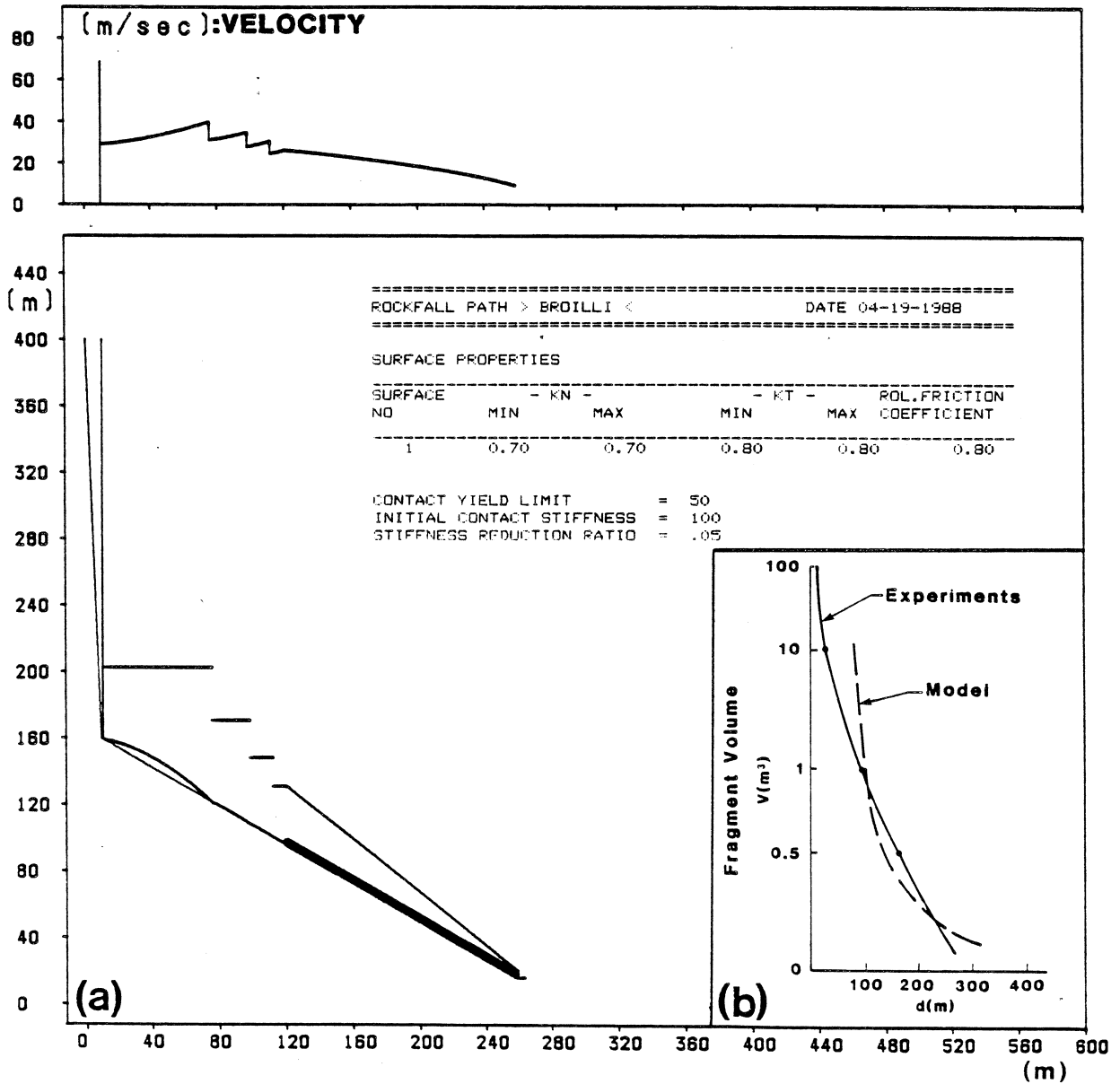
Figure 7.2. Simulation of full scale experiments carried out by Broili (1977). a. Typical ROCKFALL result, with a fragment volume of 0.5 m³. b. Comparison of experimental results of Broili and calculations using ROCKFALL, showing the distance to the point of onset of rolling as a function of fragment volume.
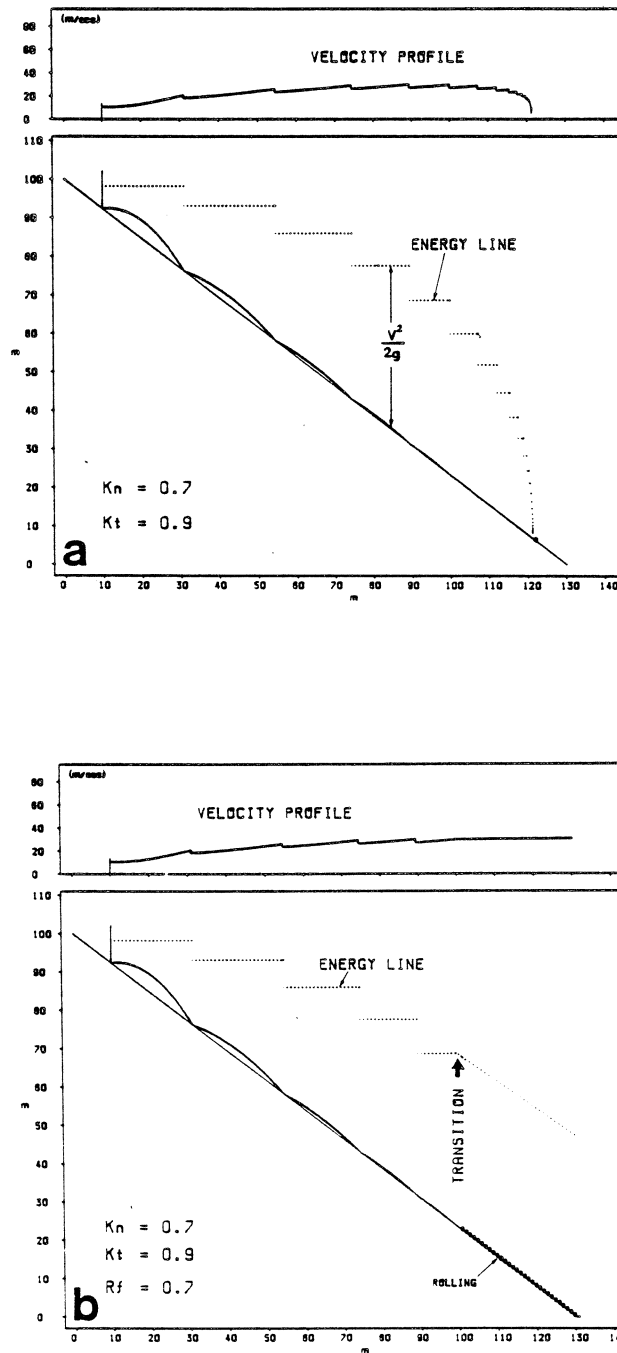
Figure 7.3. a. A fragment path simulated using constant restitution coefficients throughout its length. b. A fragment path simulated using constant restitution coefficients as in (a) but with a transition to the rolling mode. No deposition occurs on the slope. K_n = normal restitution coefficient, K_t = tangential restitution coefficient, R_f = rolling friction coefficient.

Figure 7.4. Example of stochastic analysis of rockfall runout using ROCKFALL.

Figure 7.5. Locus of trajectories obtained by ROCKFALL for 20 randomly moving fragments.

8. CASE HISTORIES OF TYPICAL ROCKFALL ACCIDENTS

8.1 Introduction

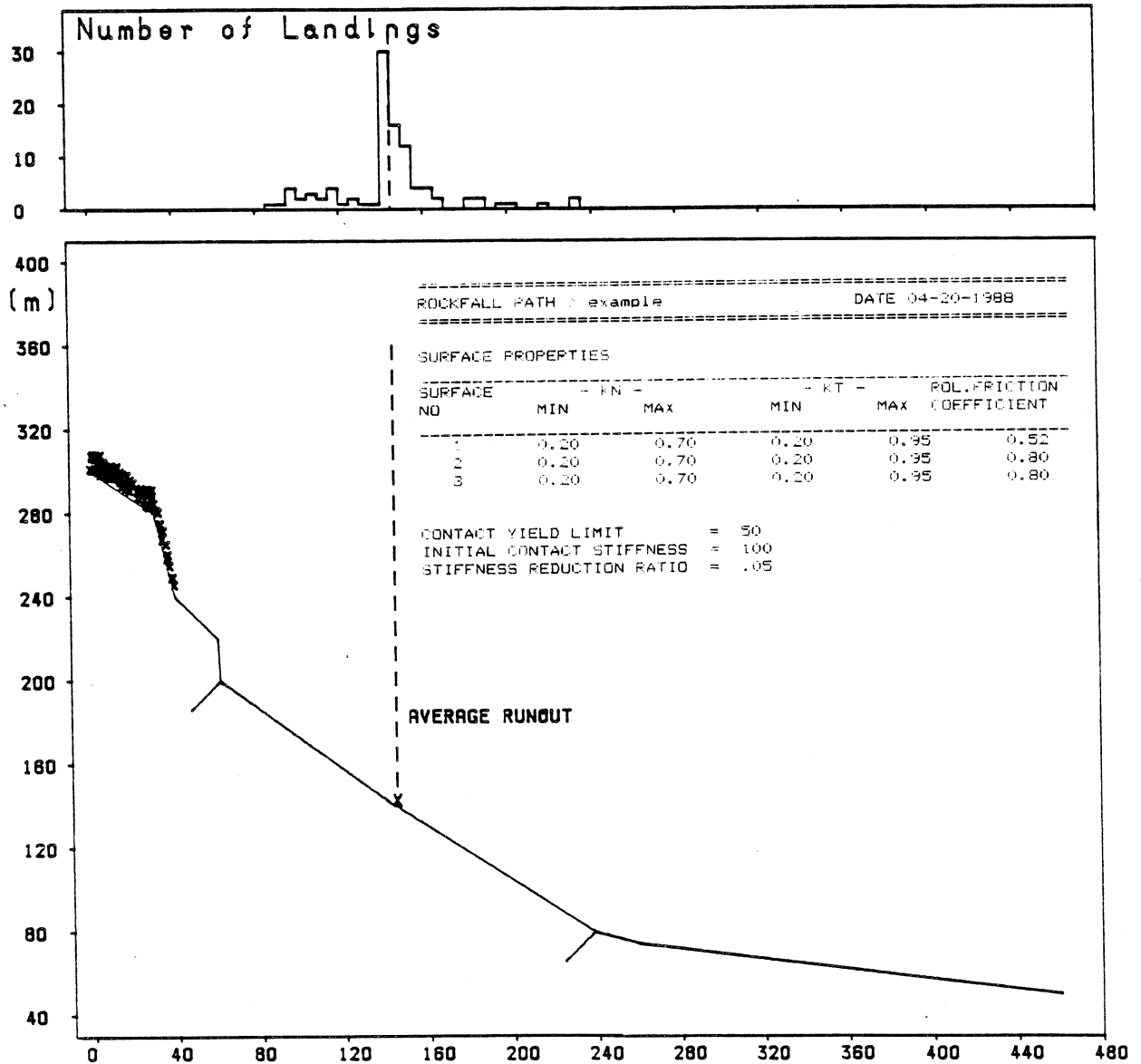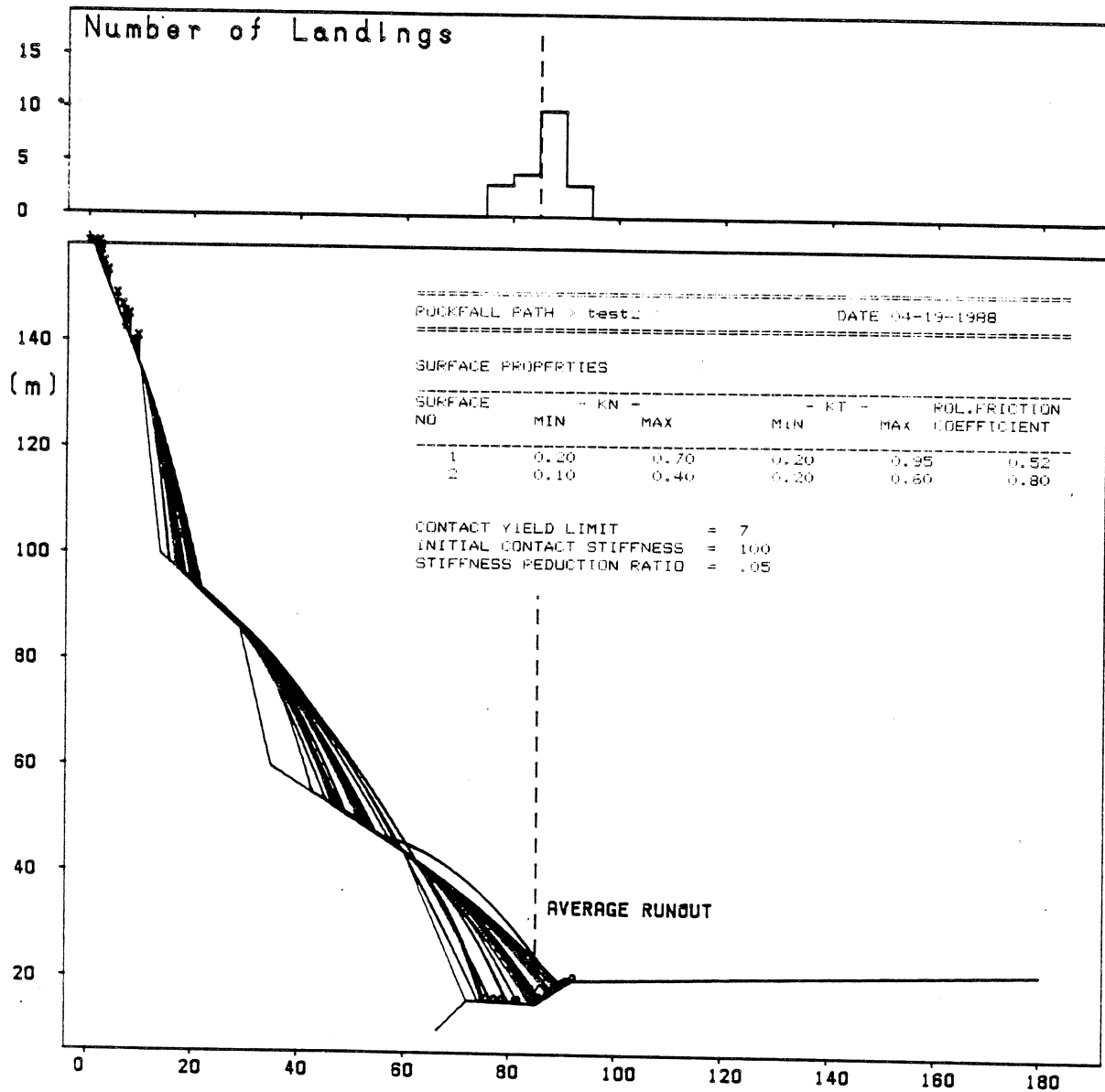Three case histories of rockfall accidents in British Columbia were investigated in detail (Fig. 8.1). The sites of three accidents (Sunnybrae, Hedley, and the Squamish Hwy.) were visited in September 1987 and data were collected on the geology of the detachment zone and the geometry of the path. Detailed theodolite surveys were also conducted on the path. At Hedley and Sunnybrae eyewitnesses were interviewed and the site on the Squamish Highway was visited with the Coroner of Squamish. In addition to these sites, a visit of rockfall-susceptible locations on the B.C. Rail line at Seton Lake (Fig. 8.1) was made in November, 1987.

8.2 Sunnybrae, B.C.; November 23, 1983

Sunnybrae is a small community in the British Columbia Interior (Fig. 8.1) located on the north shore of Shuswap Lake (Fig. 8.2) across from the town of Salmon Arm. The community lies at el. 350 m directly beneath the precipitous faces of Bastion Mountain which extends to el. 1300 m (Fig. 8.2) The cliffs are made up of metamorphosed limestone of the Sicamous Formation.

The steep, sparsely forested slopes extending from the foot of the cliffs down towards the lakefront are underlain by weak schistose bedrock units, thinly mantled by fine-grained talus derived from the same rock. The bedrock is exposed in numerous small cliffs and outcrops on the slope.

Only very few boulders can be observed in the wooded area surrounding Sunnybrae, except for the talus slope itself. It appears that the main product of weathering of the slope above is a relatively fine grained material.

Comparison of photographs of the precipitous faces of Bastion Mountain taken in 1905 and 1983 by Geological Survey of Canada field personnel indicate little change in the morphology of he faces and therefore limited rockfall activity in that time. But in 1959 a substantial rockfall from the main face of Bastion Mountain occurred suggesting that rockfall is a continuing, if infrequent, process in the vicinity of Sunnybrae.

At 01:50 hrs. on November 23, 1983, a wheelshaped boulder 6 x 6 x 2 m in dimension detached from an overhang near the base of the limestone cliffs, rolled and bounced down a path 790 m long, partly destroyed a house at the north end of Sunnybrae and killed two inhabitants (Fig. 8.3). The boulder demolished approximately one half of the house, leaving the western half relatively intact. A person sleeping in that part of the house escaped injury.. A second house was missed by a few centimetres. A description of the event was given by Miller (1983).

The release point of the boulder is shown in Fig. 8.2 and Fig. 8.4. It is in a vertical part of the cliff face some 25 m above its base. The rock is laminated, fine crystalline limestone, light to dark grey in color and very strong.

The boulder separated along an exfoliation joint dipping approximately 70° to the south (down the rockfall path). The upper edge of the fragment separated from the rock above along a curving near-horizontal joint, leaving an arch-like overhang over 2 m deep. The mechanism of detachment was similar to that in Fig. 3.1a. The exfoliation joint can be observed to continue upwards into the overhang. It appears partly open and slight groundwater flow issues from it, staining the face below (the rockfall boulder was reported by Miller, 1983 to have brown staining on one face). The eastern lateral boundary of the block was defined by a joint dipping approximately 50° to the west.

It is clear that the detachment of the boulder resulted in the creation of an overhang more exposed than that which existed before. The possibility cannot be ruled out that the event of

November 1983 was initial to a series of detachments from the same source area and with similar mechanics.

The travel path of the boulder was reconstructed by surveying the marks left along its path, most of which were still clearly discernible in 1987 (Fig. 8.5). The marks were of two types: impact craters, typically 4 x 1 m in plan and 0.3 to 0.5 m deep and elongated rolling marks, resembling a trench 2 m wide and 0.5 m deep, up to 30 m long. As shown in the profile in Fig. 8.5, the boulder moved predominantly by rolling throughout most of its descent. A long bounce occurred below the crest of the lower cliff, followed by several shorter bounces and abrupt changes in direction, due to topographic detail (see plan in Fig. 8.5). Small fragments broke off from the boulder at several places near the end of its path. These fragments were generally found far from the impact craters, indicating that they separated during rotation of the boulder.

A simulation of the rockfall path using the ROCKFALL computer program appears in Fig. 8.6. The boulder mass was assumed to be 150 tonnes so that most impacts were plastic. It is of interest to note that the length of the parabolic trajectory at the lower cliff in the simulation is very close to the length observed (cf. Fig. 8.5). Therefore, the velocity estimate shown in the upper part of the figure is realistic. The analysis indicates that the relative shortness of the path (travel angle 34.5°) is due to the plastic energy losses incurred in bouncing below the lower cliff. Had it continued rolling, the boulder may have travelled further. It is of concern that many homes are located beneath these cliffs within the zone defined by the empirical minimum shadow angle of 27.5° defined in Chapter 6.

8.3   Hedley, B.C.; January 17, 1939

Hedley is a small mining community located in the Similkameen Valley, 30 km southeast of Princeton, in the Interior of British Columbia. A rockfall struck the town at 01:00 hrs. on Burns Night, January 17, 1939. Part of the community was situated directly beneath the rock faces and the slopes of Stemwinder Mountain (Fig. 8.7).

The slopes north of the townsite are underlain by the Upper Triassic Nicola Group, consisting at this point of an interbedded, folded and sheared sequence of basalts and limestone.

The source of the 1939 rockfall is above the apex of a large talus cone consisting of relatively uniformly graded basalt fragments. Most of the talus surface consists of cubical fragments with median sizes of approximately 40 mm, ranging from 10 to 150 mm. The surface is quite mobile and susceptible to shallow sliding and consequently free of vegetation. Its profile is uniform at 37° as shown in Fig. 8.9.

The source area of the rockfall has been identified with the help of eyewitnesses. It is a large wedge scar similar to Fig. 3.3b but highly asymmetric (Fig. 8.8). One side of the wedge formed along a faulted contact plane between basalt in the footwall and recrystallized limestone in the hanging wall, dipping at a mean angle of 52°, a few degrees to the left of the sliding direction. The opposite side of the wedge consists of a series of near vertical cross joints striking almost perpendicular to the fault plane. This side of the wedge probably contained intact rock bridges, causing delayed and piecemeal retrogressive failure as described in Section 3.2.

The base of the wedge scar is level with the apex of the talus cone, so that there was no free fall component to the initial movement. Light coloured areas of relatively fresh rock at the upper end of the scar, some 50 m above the talus, indicate an initial volume of about 5,000 m³. A few large limestone boulders lie on the talus surface about 100 m below the apex. These boulders have a median size of approximately 0.7 m and a range of 1.5 m and are partly buried by the fine basaltic talus.

The limestone rock which formed the rockfall mass, as revealed in the cliff exposures, is laminated but strong and sparsely jointed, tending to break in large blocks. The underlying basalt is in contrast closely fractured.

No traces of the rockfall path were found on the talus, except for the few remnant boulders mentioned above.

The 1939 accident occurred in a newly built part of town known as the Ready Cash Subdivision, consisting of two streets parallel to the toe of the talus cone (Fig. 8.9). Several boulders reached the subdivision, approximately as reconstructed by arrows on Fig. 8.7. The boulders ranged from 1 to 2 m in size. Four houses were severely damaged (Fig. 8.10). A number of persons were awakened from their sleep by the walls of their bedrooms crushing under impact (Fig. 8.10). Fortunately, only two deaths occurred.

The profile of the longest rockfall path is shown in Fig. 8.11. The path was simulated with the computer program ROCKFALL, using impact and friction parameters identical to those used for the Sunnybrae example. The calculated reach distance agrees well with the actual experience.

The results of the computer simulation again confirm the predominant rolling mode of movement. The analysis could for practical purposes be replaced by one based on a frictional model.

The discontinuity patterns in the southeast face of Stemwinder Mountain indicate that similar places of detachment exist for future rockslope failures along the face. Although homes were moved from the runout area of the 1939 event (B.C. Order in Council 1576) several homes at the present Hedley townsite are located beneath rockslopes that are within the zone defined by the empirical minimum shadow angle of 27.5.

Meteorological data measured at Hedley were analyzed for the 1939 event but the data do not suggest an obvious meteorological trigger for the rockfall.

8.4 Squamish Highway, B.C.: January 16, 1982

The third case history investigated took place on the Squamish Highway (British Columbia Highway 99), 22 km north of Horseshoe Bay (Figs. 8.1, 8.12). On January 16, 1982 a rectangular boulder of metamorphosed tuff, approximately 0.7 x 1 x 2 m in size, detached from a narrow shelf on a natural slope above a highway cut (Fig. 8.13). Several short bounces occurred on bare rock. The boulder then traversed a steep snow covered slope and fell over the edge of the steep rock cut, to land directly on the roof of a stationary automobile which formed part of a line of vehicles stopped behind a highway obstruction. The passenger was killed instantly and the driver injured.

The analysis of the rockfall, summarized in Fig. 81.4 uses impact parameters typical of small fragments, as specified in Table 7.1. This is justified not so much by the size of the block, as the limited velocities developed in such a short path. A small initial drop is specified, to account for the velocity gained in toppling failure. As would be expected, the path is dominated by the bouncing mode and free flight.

The simulation indicates that the boulder struck the car with a velocity of approximately 28 m/s (100 km/hr.)

Observations at the site indicated that the boulder became detached from a face which was covered with clearly defined glacial striae and that the rockfall was the first from this particular segment of rockslope in the time since deglaciation.

Meteorological data recorded at Squamish was analyzed for this event. The data suggests that the rockfall was triggered by wet conditions associated with a sudden thaw.

THURBER

8.5   B.C. Railway, Seton Lake

Along the west shore of Seton Lake, B.C., approximately 240 km north of Vancouver (Fig. 8.1), the B.C. Rail line skirts the easterly slopes of the Chilcotin Range. The topographic relief is over 1,800 m vertical, with mean overall slope angles of the order of 30° and numerous high and steep cliff areas, beneath which the railway traverses talus cones and aprons (Fig. 8.15).

The slopes are formed of metamorphic rocks of the Palaeozoic Bridge River Group, including cherts, argillites and phyllites. Rock mass quality is highly variable in these rocks, characterized by resistant cliffs alternating with weak, highly fractured zones.

The railway track is subject to continuing rockfall, both from cut faces and from natural slopes high above the right-of-way. While the rockfall sources on cut slopes are being successfully controlled using scaling and stabilization, those above the track are inaccessible and there is no practical way of treating them.

A passenger was killed in this area in 1965 by a relatively small rock crashing through a window of a railway coach.

A typical rockfall site is shown in Fig. 8.16. The slope above this particular location has been subjected to dynamic analysis using the impact parameters corresponding to small rocks (Table 7.1). Figures 8.17 and 8.18 show the trajectories of 20 boulders each, originating at random locations on a steep talus slope with rock ledges above the railway. The only difference between the two figures is the range of fragment sizes assumed.

Fig. 8.17 shows trajectories predicted by ROCKFALL for rocks of the order of 0.1 x 0.1 x 0.1 m in dimension, weighing of the order of 3 kg each. These rocks move in high trajectories and show scattered landings over a wide area.

Fig. 8.18 on the other hand, shows trajectories corresponding to larger rocks, with typical dimensions of 0.5 x 0.5 x 0.5 m or 330 kg in weight. The rocks stay much closer to the ground (as observed by Ritchie, 1963) and generally run out in the vicinity of the tracks.

A ditch constructed adjacent to the track could be expected to control the larger fragments, but will be of limited effectiveness in controlling small rocks. This is presented as an example of the use of the rockfall computer model in locating and designing defensive works.

THURBER

1 = Sunnybrae
2 = Hedley
3 = Squamish Highway
4 = Seton Lake

ALBERTA

BRITISH COLUMBIA

Vancouver

100
Km
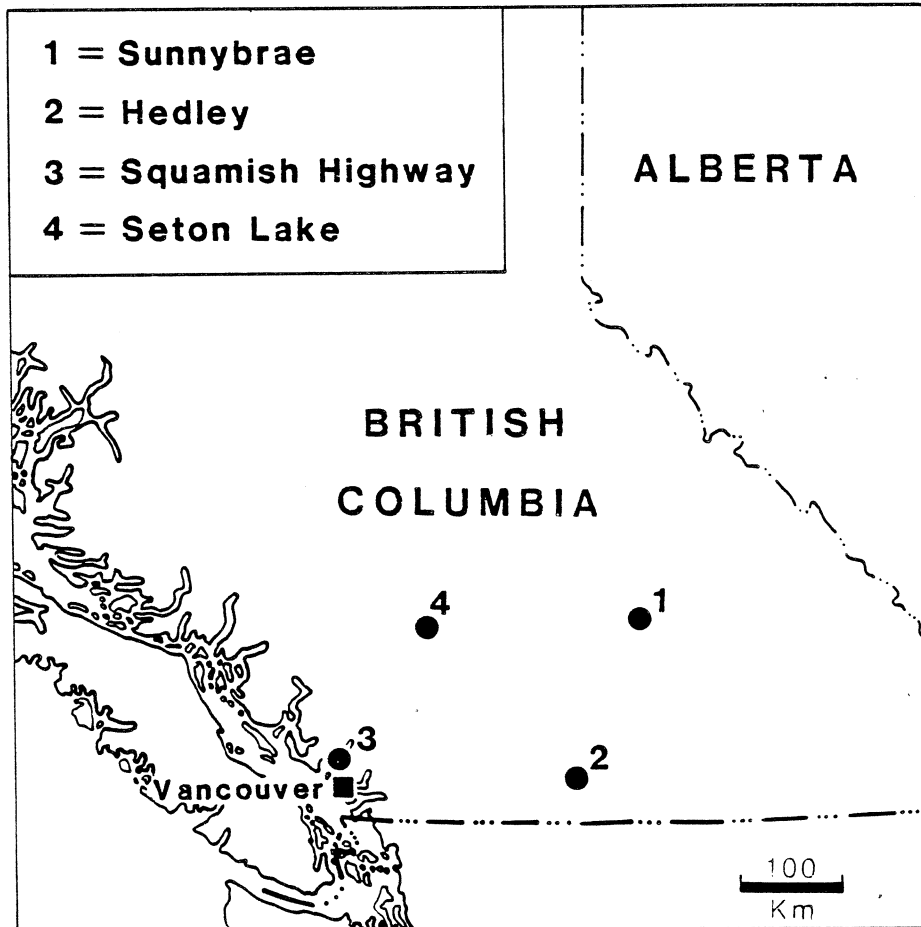
Figure 8.1. Location of case histories in southern British Columbia.

THURBER
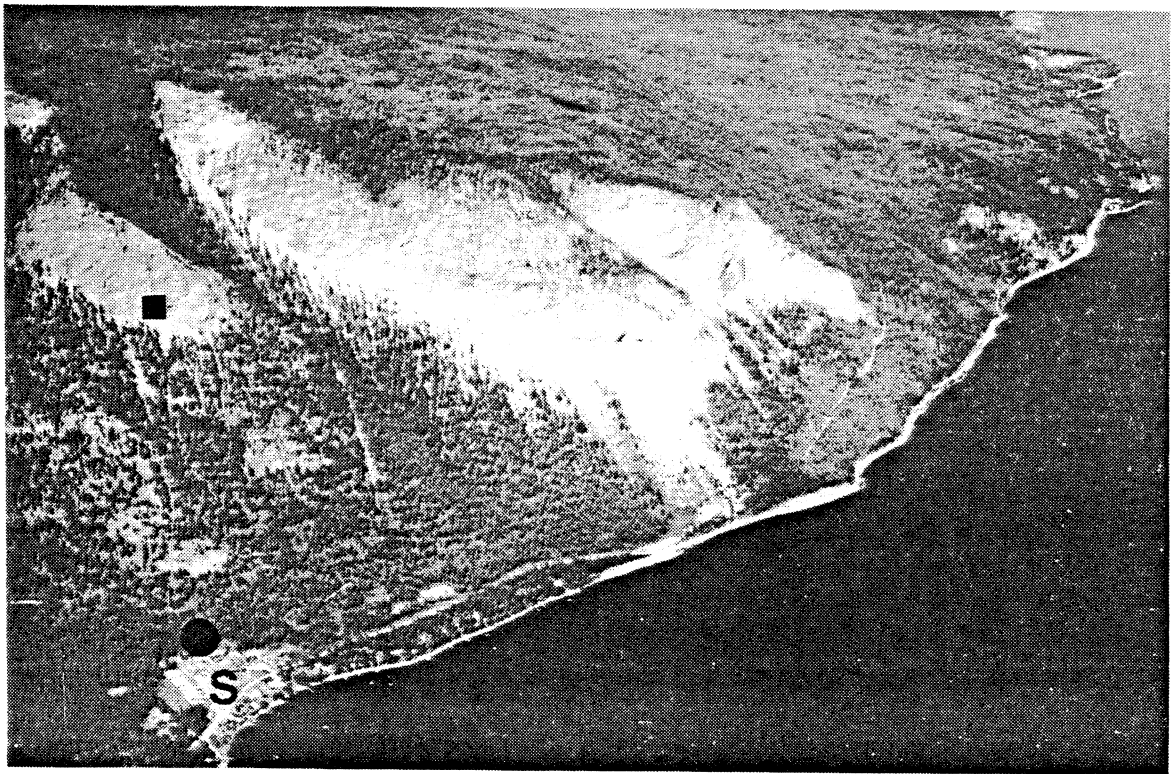
Figure 8.2. Oblique aerial view of Sunnybrae (S). Note the source cliffs for rockfall from Bastion Mountain. Black square is location of release point of 1983 rockfall. Black circle is location of damaged house in which two people were killed.

THURBER

Figure 8.3.   The 1983 Sunnybrae rockfall: (A) The damaged house in which two people were killed; (B) the boulder involved in the rockfall being buried where it came to rest.

THURBER
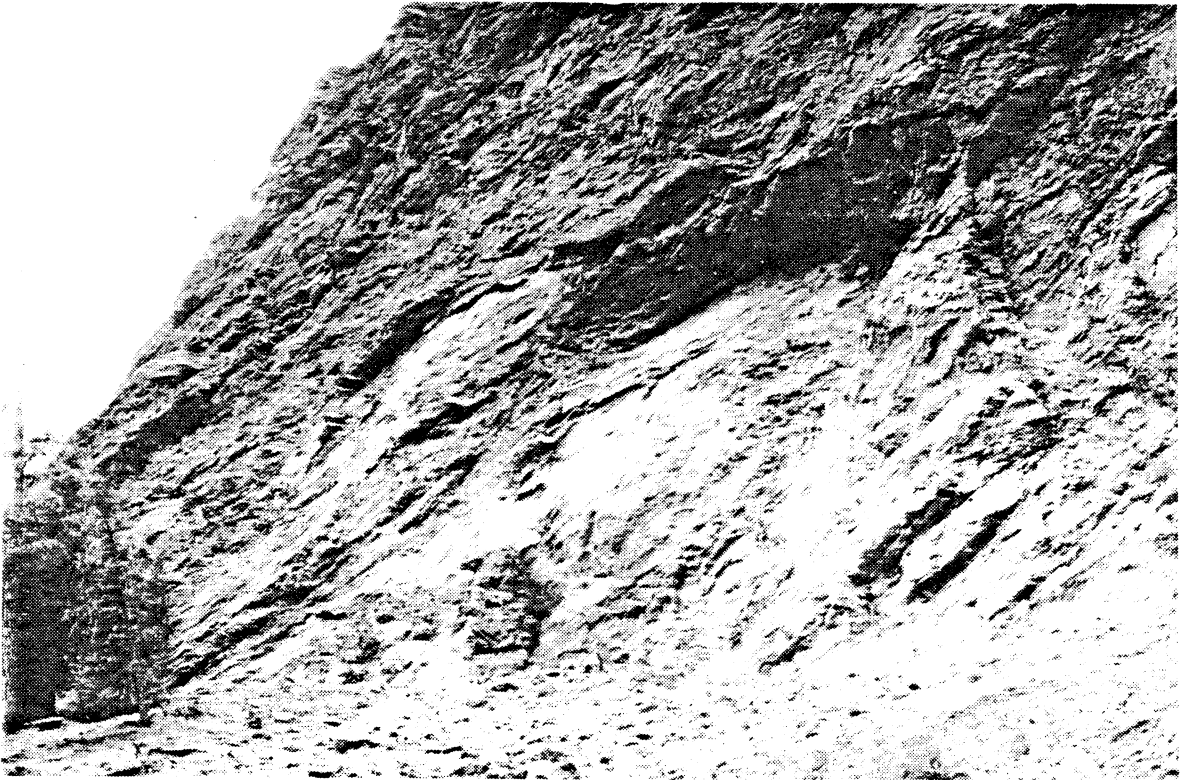
Figure 8.4. Release point of the 1983 Sunnybrae rockfall.

THURBER
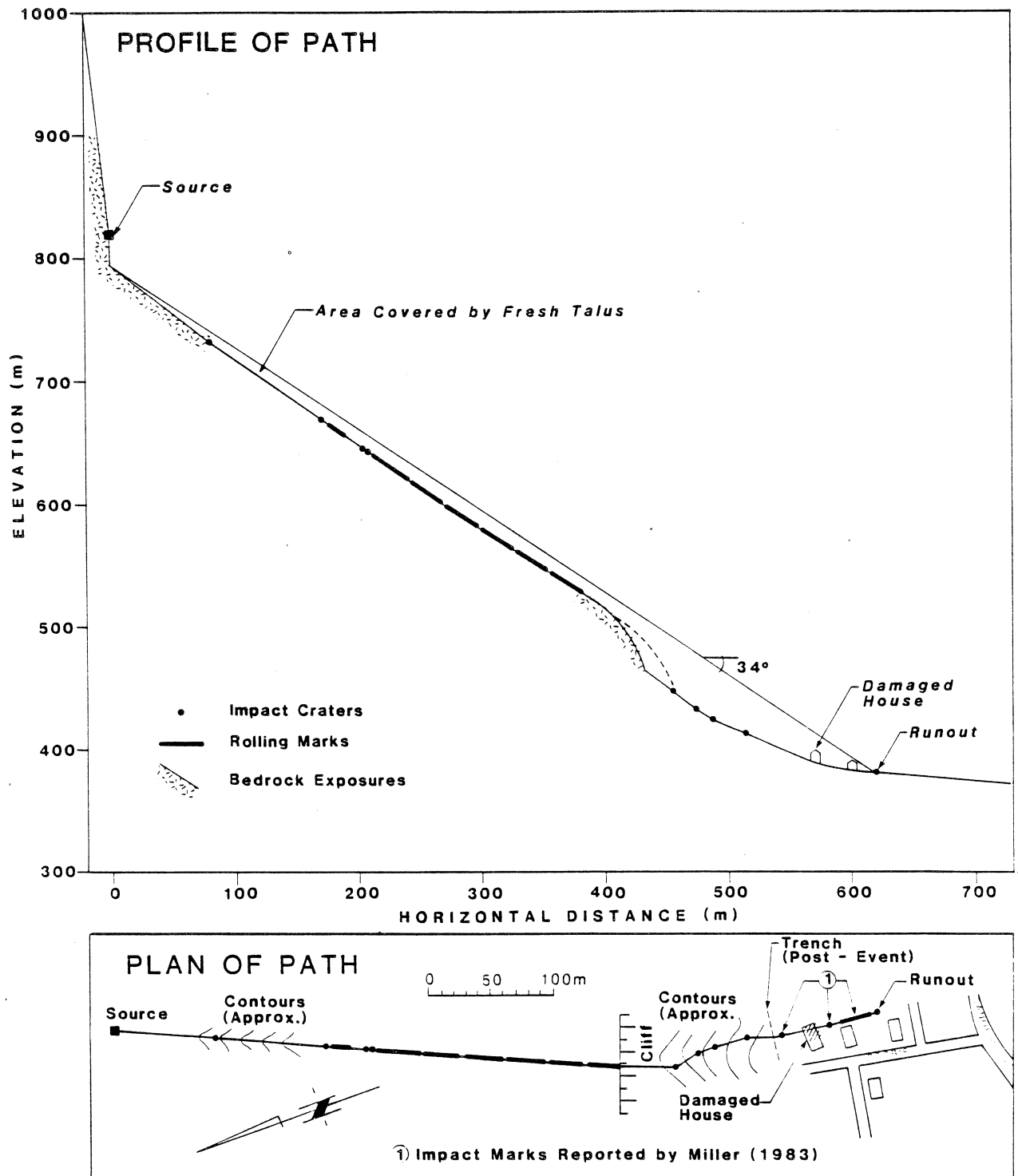
Figure 8.5. Path of the 1983 Sunnybrae rockfall in profile and plan.
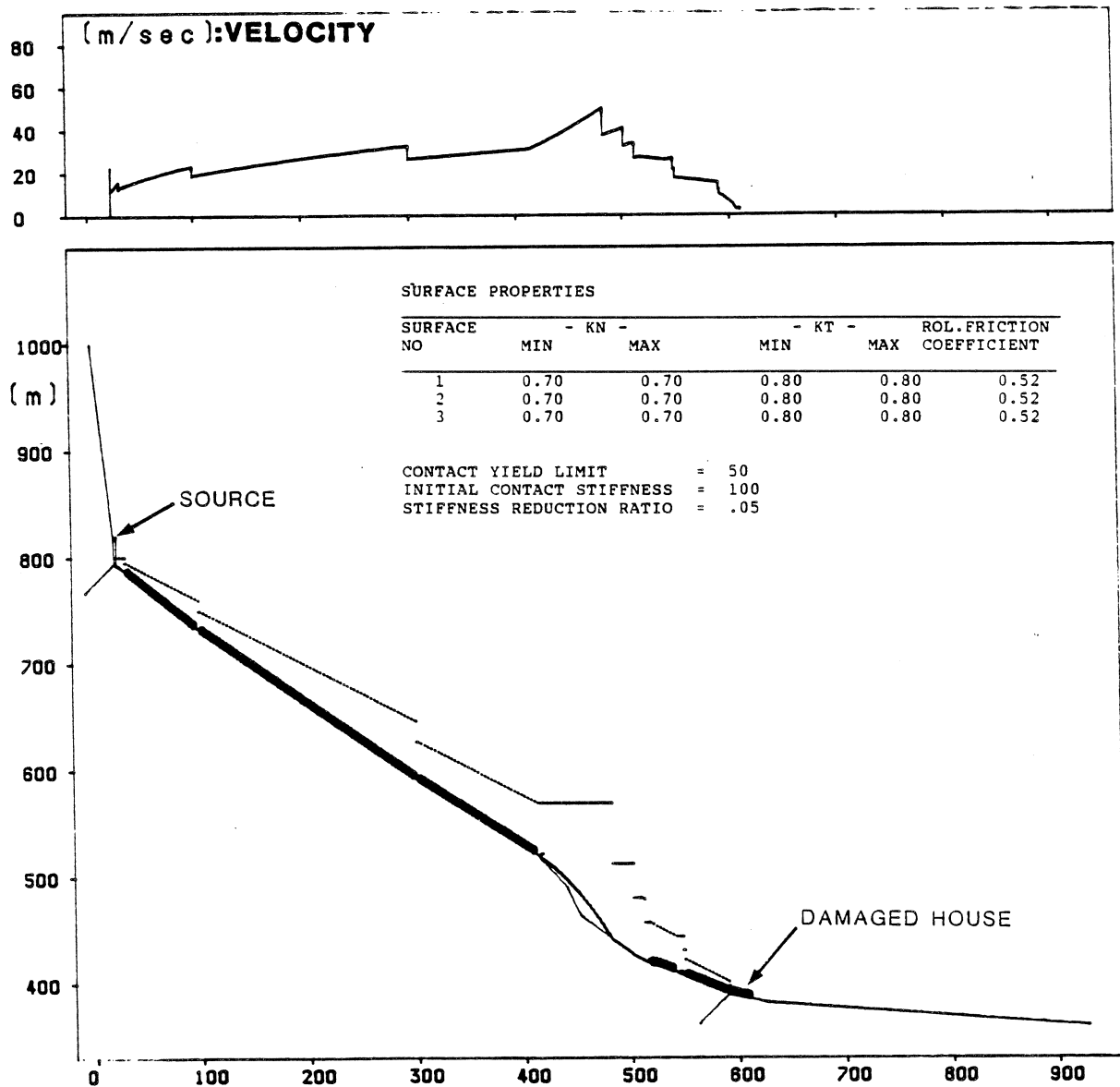
Figure 8.6. Simulation of the Sunnybrae rockfall path using the ROCKFALL computer program.
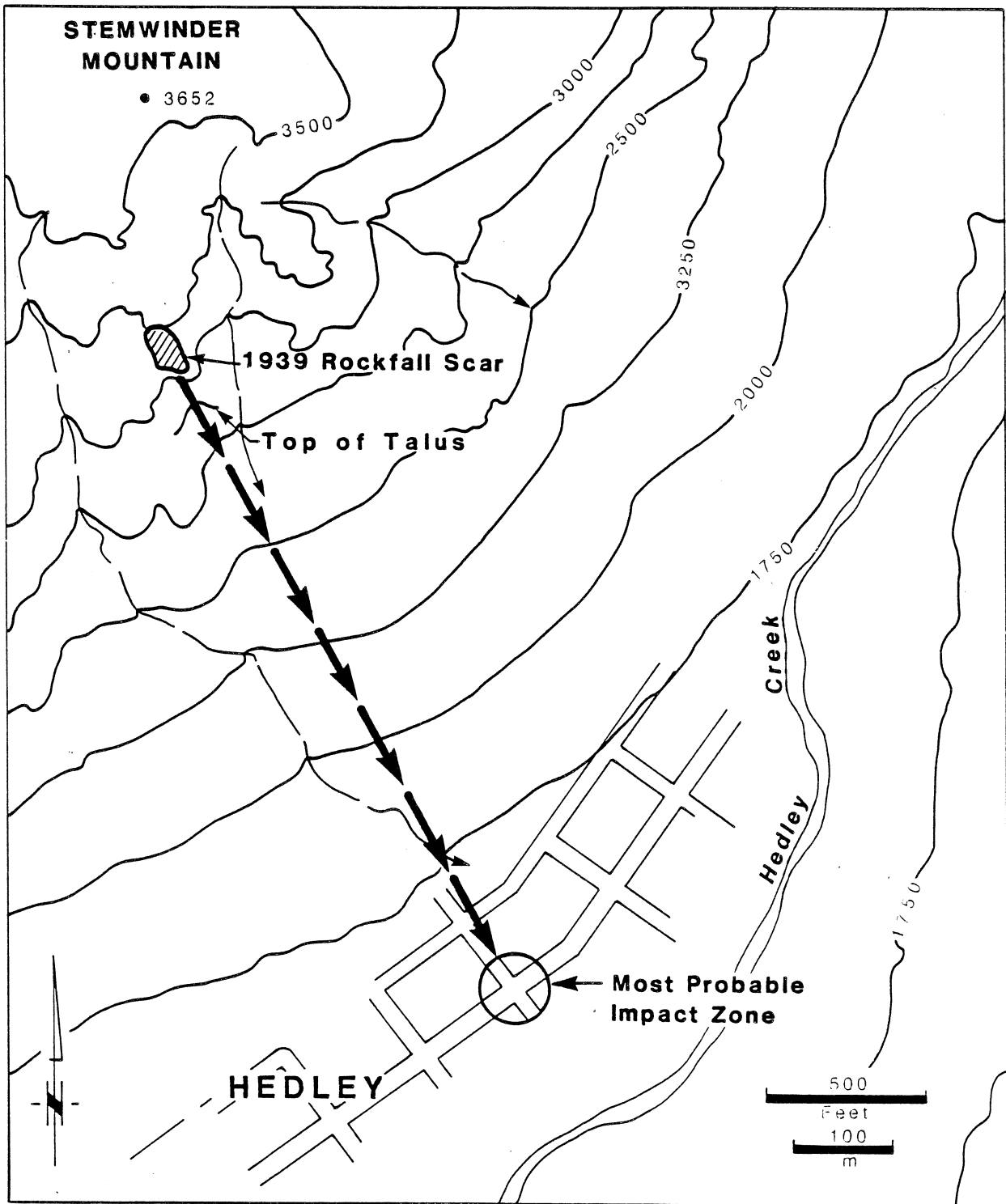
Figure 8.7. Map of Hedley showing location of 1939 rockfall release point and most probable impact zone.
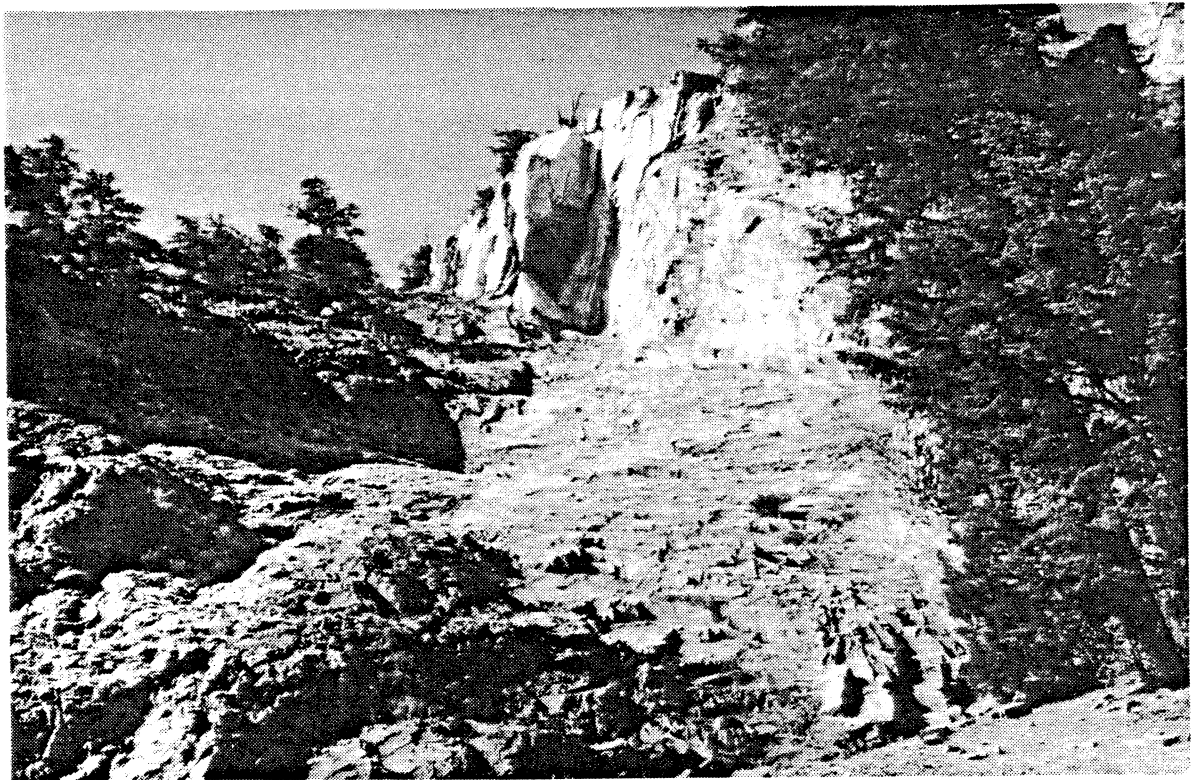
Figure 8.8. 1939 Hedley rockfall source area photographed in 1987.
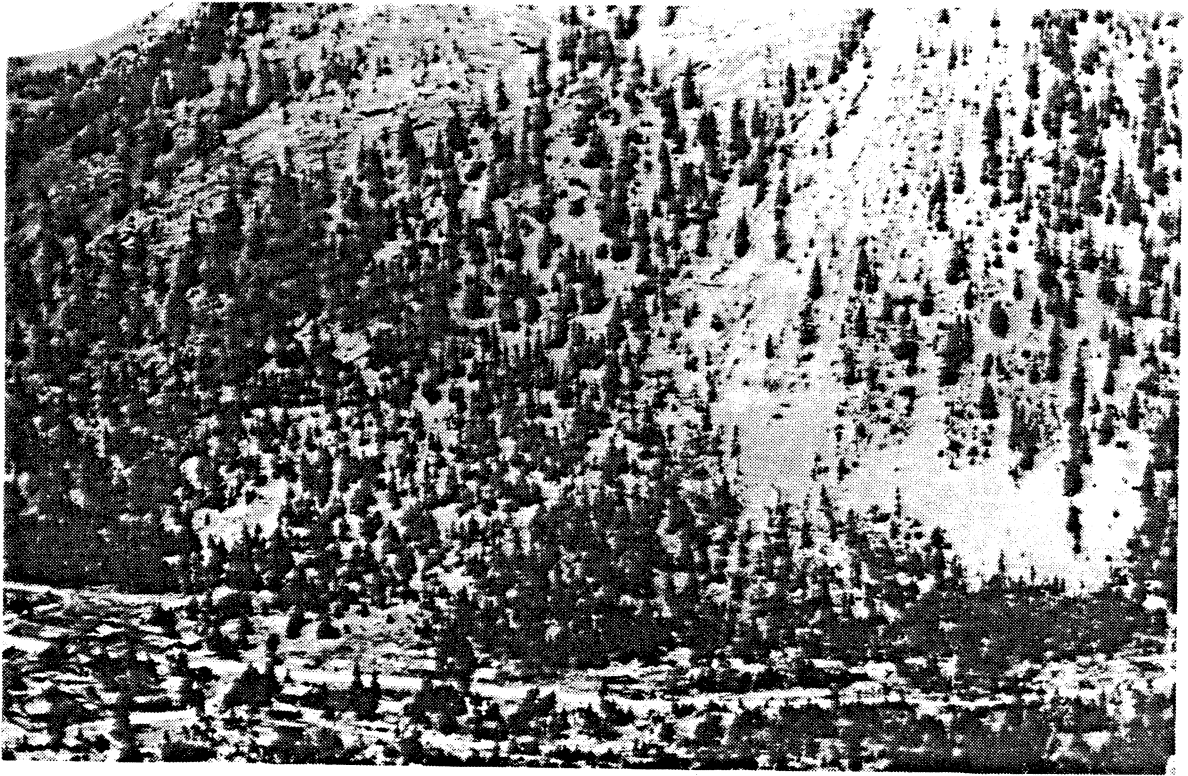
Figure 8.9. Area of Hedley affected by 1939 rockfall. Photograph taken in summer of 1939. Note location of houses close to the base of the talus slope within the rockfall shadow area.

THURBER
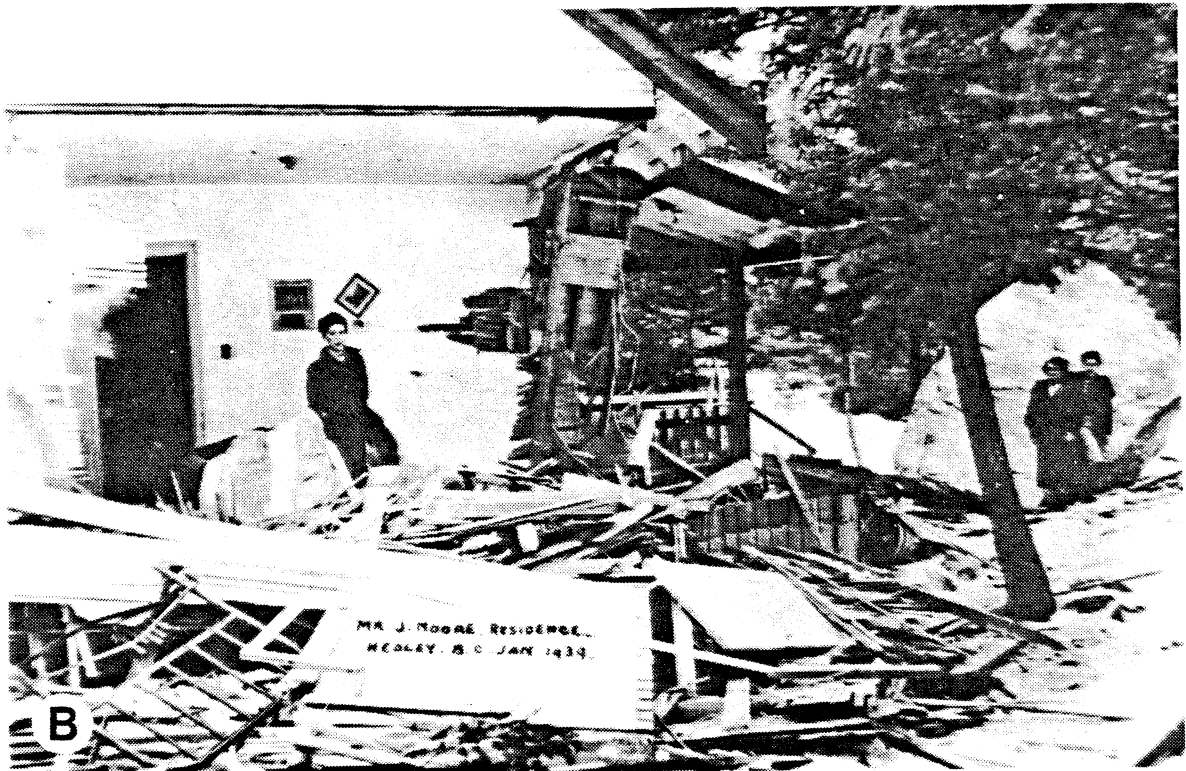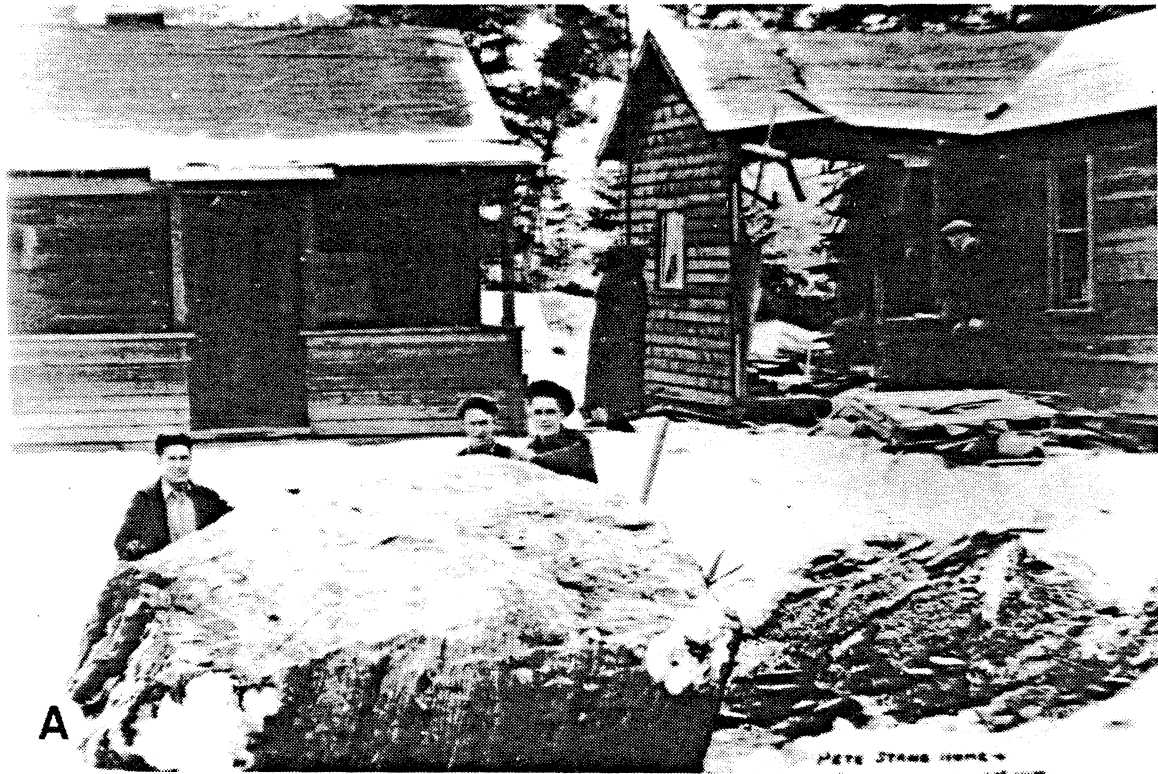
Figure 8.10. Archive photographs of damage caused by 1939 Hedley rockfall. A: Boulder which killed the two victims of the accident in the house behind. B: Damage to a room at the corner of the Moore residence where the two Moore children escaped injury.

THURBER
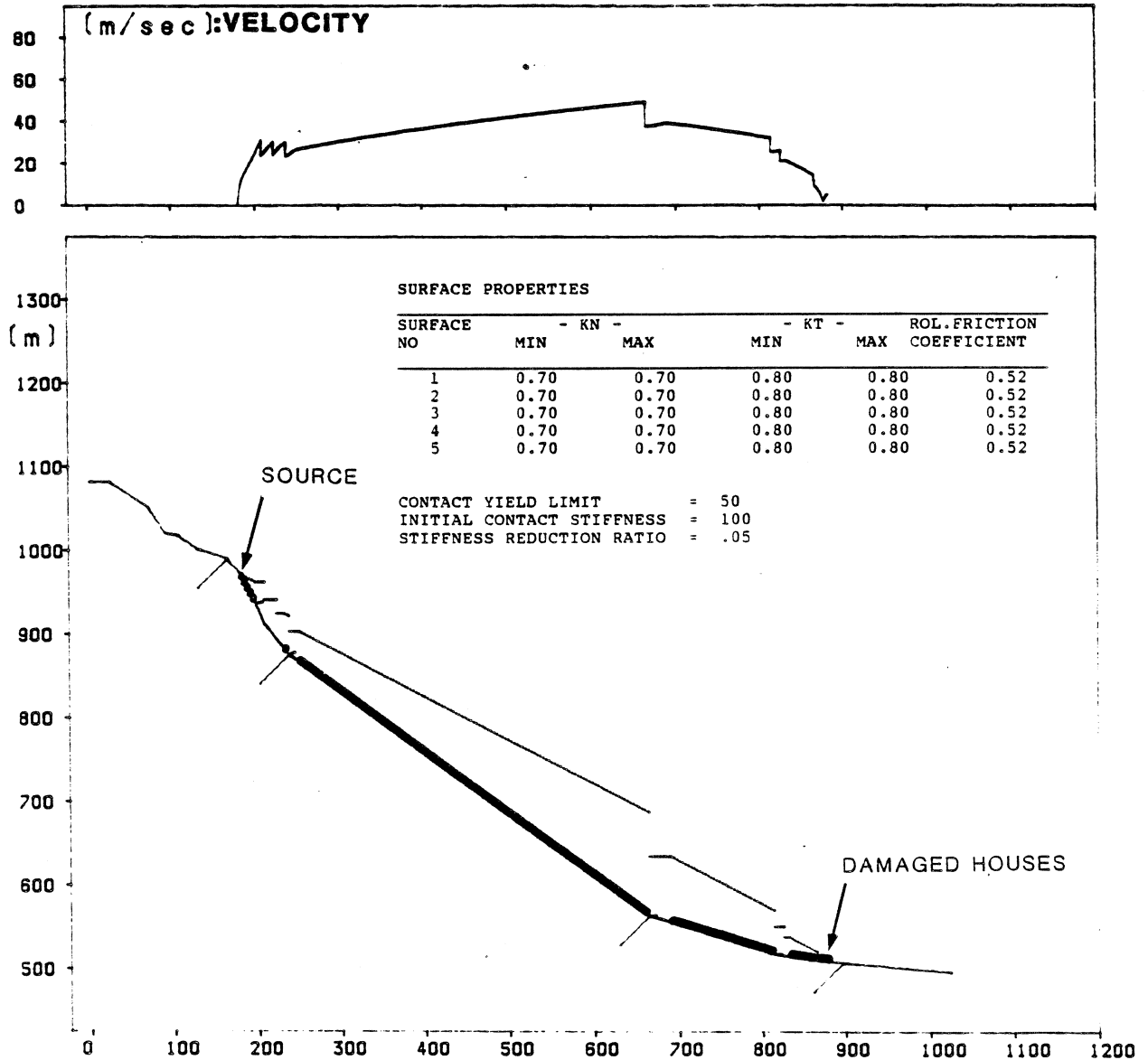
Figure 8.11. 1939 Hedley rockfall. ROCKFALL simulation of the longest rockfall path.
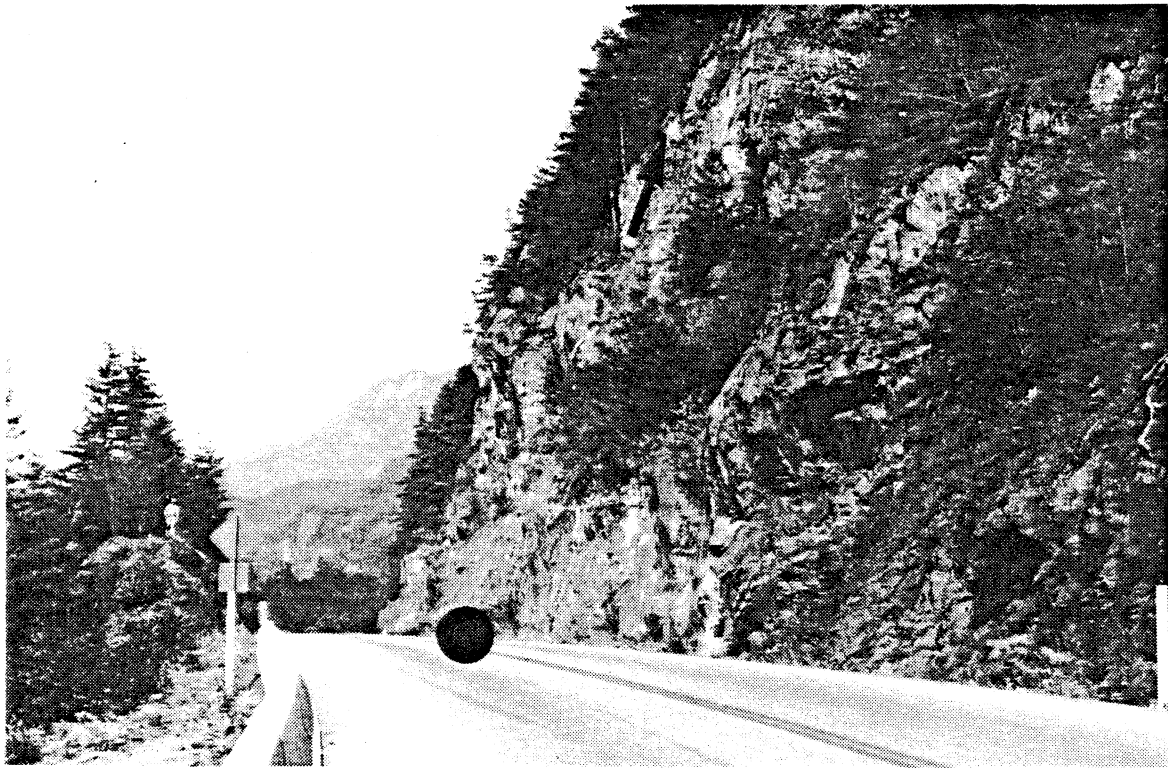
Figure 8.12. Squamish Highway, site of rockfall accident of January 16, 1982. Black circle is site of accident and source of rockfall is arrowed.

THURBER

Figure 8.13. 1982 Squamish Highway rockfall; photo shows source of the rockfall. The boulder stood on the shelf in the middle of the photo at the base of the pole before detachment.

THURBER

SURFACE PROPERTIES					
SURFACE NO	- KN - MIN	MAX	- KT - MIN	MAX	ROL.FRICTION COEFFICIENT
1	0.90	0.90	0.90	0.90	0.52
2	0.90	0.90	0.90	0.90	0.52
3	0.90	0.90	0.90	0.90	0.52

CONTACT YIELD LIMIT = 10
INITIAL CONTACT STIFFNESS = 100
STIFFNESS REDUCTION RATIO = .05
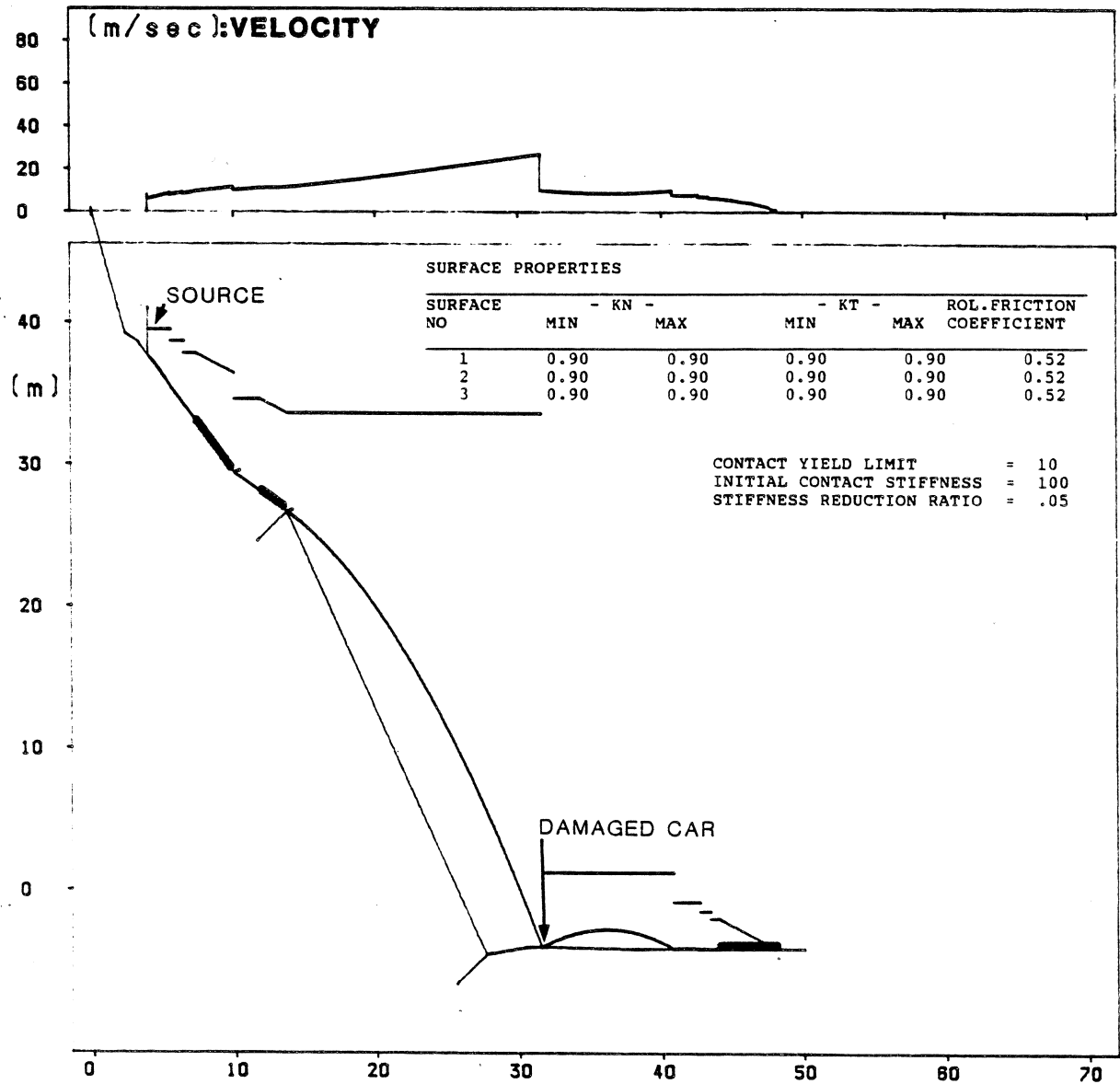
Figure 8.14. 1982 Squamish Highway rockfall; profile and computer analysis of the rockfall using ROCKFALL.

Figure 8.15. Seton Lake; site of fragment rockfall onto the BCR track.

THURBER
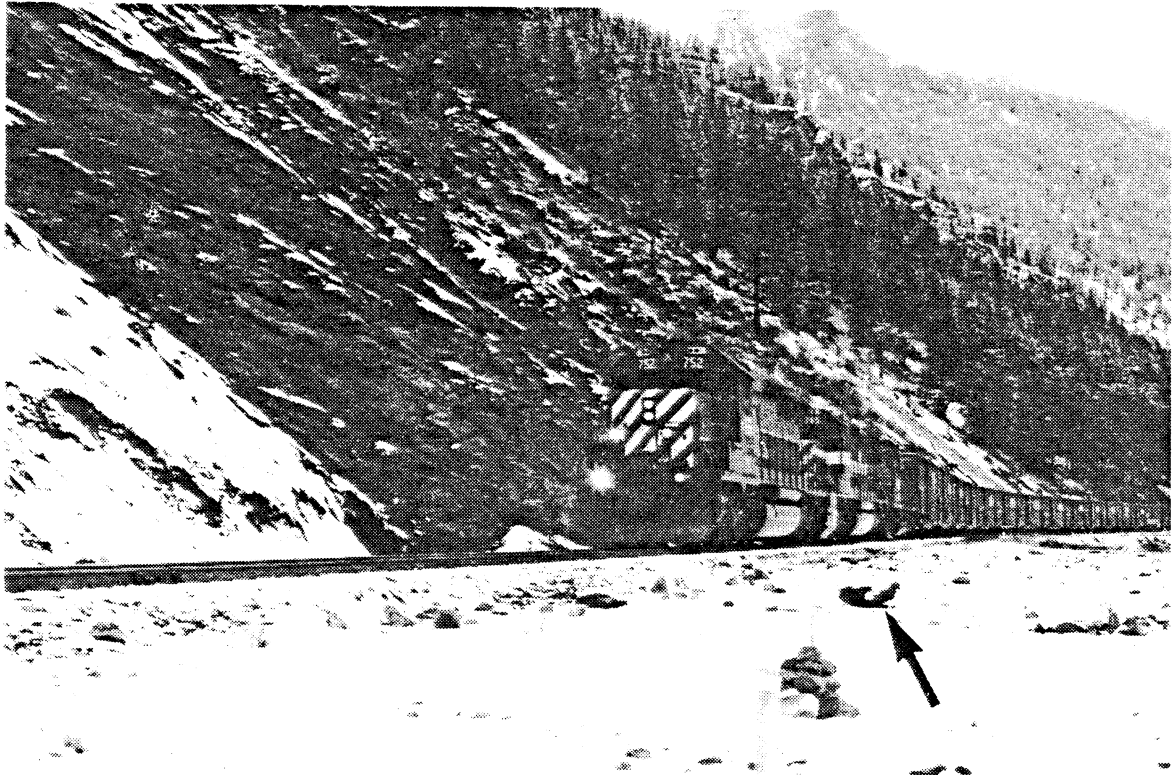
Figure 8.16. Seton Lake; a typical rockfall site. Rockfall fragment is arrowed.
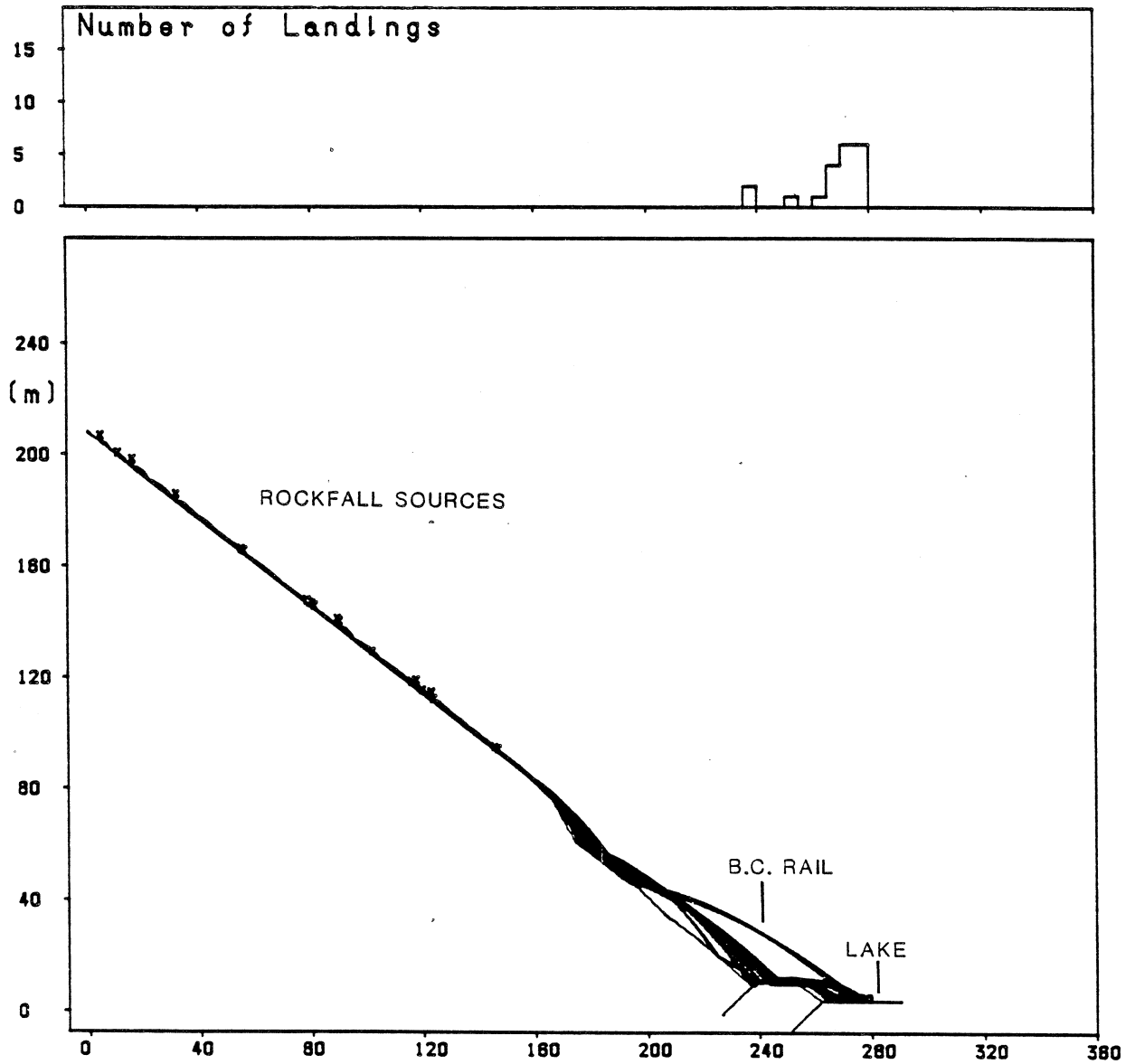
Figure 8.17. Seton Lake; twenty trajectories of boulders with characteristic dimensions of 0.1 x 0.1 x 0.1 m, simulated by ROCKFALL.
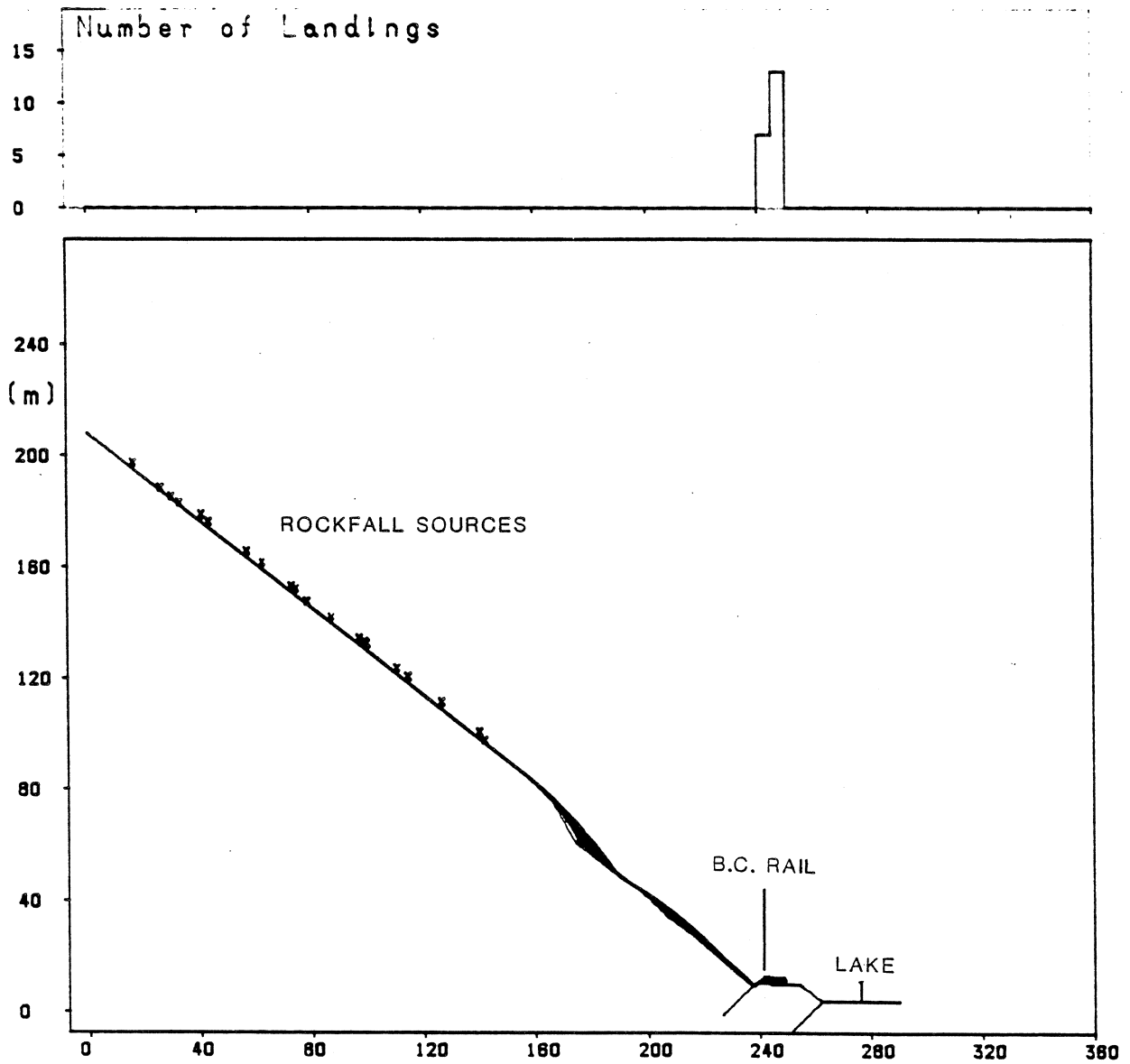
Figure 8.18. Seton Lake, twenty trajectories of boulders with charateristic dimensions of 0.5 x 0.5 x 0.5 m simulated by ROCKFALL.

9. SUMMARY OF CONCLUSIONS

9.1 Distribution and Significance of Rockfall Hazards

The present study shows that the major costs associated with rockfall are concentrated in the Cordillera, although there have been several notable rockfall accidents in Eastern Canada.

Loss of life due to rockfall accidents in settled areas and on transportation routes have been very small in Canada. This is probably due to the low population density.

Costs of rockfall in settlements are associated primarily with land alienation due to recognized rockfall hazard areas.

Costs of rockfall on transportation routes are considerable and result both from necessary remedial construction, accident cleanup and repair, and traffic delays. Combined costs of the order of $500 to $1,000 per km of railway track per year are indicated for the Cordilleran region.

The Pacific Salmon Fishery has sustained billions of dollars of damage as a result of a rockfall in the Fraser Canyon in 1914.

Apart from artificial rock cuts and certain special disturbed locations, rockfall activity is a relatively rare phenomenon, except on a very small scale. On average cliff faces, falls exceeding 1 m^3 in volume occur in the order of one in 100 years per 100 m of cliff length.

Rockfall impact probability is an extremely strong function of the distance from the source area, as indicated by Fig. 5.9. Within the rockfall "shadow" area, i.e. beyond the limits of talus, return periods of the order of 1,000 years relative to a house site are typical.

Rockfall probability can be strongly influenced by the occurrence of earthquakes.

## 9.2 Methods of Engineering Analysis and Prediction

Three alternative approaches towards mapping areas influenced by rockfall hazards have been outlined, including:

— An approach based on detailed assessment of geological evidence, especially existing rockfall deposits. This can be ambiguous in certain cases where rockfall deposits occur in conjunction with deposits created by other processes.

— The empirical method, based on observation of rockfall path profiles. It appears that a limiting vertical angle exists which in many cases limits the rockfall "shadow" zone. This is shown in Fig. 6.2. This approach is suitable for preliminary analyses.

— An analytical approach consisting of the formulation of a computer-based model of rockfall movement, including free flight, impact and rolling. This has received considerable attention from engineering geology researchers in many parts of the world over the last decade.

The available analytical models fall into two categories, rigorous and simplified, distinguished by the method of accounting for impact conditions. The authors present arguments in support of the simplified approach, which is better suited to empirical calibration.

A microcomputer-based simplified rockfall model (ROCKFALL) has been developed. Preliminary calibration of the input parameters has been done and trial analyses of actual case histories have been completed. With additional detailed calibration, the model will present a powerful tool for prediction of various aspects of rockfall movement and for evaluation of remedial designs in the vicinity of threatened settlements and transportation routes.

THURBER

10. REFERENCES

Åkerman, H.J.
1984:   Notes on talus morphology and processes in Spitsbergen. Geografiska Annaler, 66A: 267-284.

Aste, J.P., Cambou, B., and Falcetta, J.L.
1984:   Comportement des masses rocheuses instables. De la prévision à la prévention. Proceedings, 4th. International Symposium on Landslides, 1: 441-446.

Aste, J.P., Cambou, B., Clozel, P., and Falcetta, J.L.
1987:   Quantitative analysis of cliff stability. Proceedings, International Symposium on Engineering Geological Environment in Mountainous Areas, 1: 555-561.

Aulitzky, H.
1974:   Endangered Alpine regions and disaster prevention measures; Council of Europe, Nature and Environment Series, no. 6, 103 p.

Azimi, C. and Desvarreaux, P.
1977:   Calcul de chutes de blocs et vérification sur modèle réduit. Rapp. ADRGT.

Azimi, C., Desvarreaux, P., Giraud, A., and Martin-Cocher, J.
1982:   Méthode de calcul de la dynamique des chutes de blocs. Application à l'étude du versant de la montagne de La Pale (Vercors). Bulletin de liaison des laboratoires des ponts et chaussées, 122: 93-102.

Baillairgé, C.
1893:   The Quebec land slide of September 19, 1889. Transactions, Canadian Society of Civil Engineers, 7: 140-152.

Ballivy, G., Hardy, J., LeBuis, J., and Bergeron, R.
1984:   Techniques d'abattage d'une paroi rocheuse instable. Proceedings, 4th International Symposium on Landslides, Vol. 1, pp. 455-459.

Balk, R.
1939:   Disintegration of glaciated cliffs. Journal of Geomorphology, 2 :305-333.

Banks, D.C. and Strohm, W.E.
1974:   Calculations of rock-slide velocities. Proceedings, 3rd Congress, International Society of Rock Mechanics, 1B: 839-847.

Barton, N. and Choubey, V.
1977:   The shear strength of rock joints in theory and practice. Rock Mechanics, 10, pp. 1-54.

Battle, W.R.B.
1960:   Temperature observations in bergschrunds and their relationship to frost shattering. In Norwegian cirque glaciers. Edited by W.V. Lewis. Royal Geographical Society Research Series, 4: 5-10.

Bell, A.
1980:   Terrain mapping and regional slope stability evaluation in the Fraser Canyon, B.C. M.Sc. Thesis, University of British Columbia, 200 pp.

Benitez, M.A.H., Bollo, M.F., and Rodriguez, M.P.H.
1977:   Bodies falling down on different slopes - dynamic study. Proceedings, 9th International Conference on Soil Mechanics and Foundation Engineering, 2: 91-94.

Bjerrum, L. and Jorstad, F.
1968:   Stability of rock slopes in Norway. Norwegian Geotechnical Institute Publication No. 79, pp. 1-11.

THURBER

Bhandari, R.K. and Sharma, S.K.
1976:   Mechanics and controls of rockfalls. Journal of the Institution of Civil Engineers (India), 57: 14-24.

Brock, R.W.
1904:   The Lardeau mining district. Geological Survey of Canada, Summary Report XVAA, pp. 42-81.

Broili, L.
1974:   Ein Felssturz im grosversuch. Rock Mechanics, Supplement 3, pp. 69-78.
1977:   Relations between scree slope morphometry and dynamics of accumulation processes. ISMES Publication No. 90, pp. 11-23.

Bozzolo, D., Pamini, R., and Hutter, K.
1988:   Rockfall analysis - a mathematical model and its test with field data. In Landslides. Edited by C. Bonnard. Proceedings, 5th International Symposium on Landslides, 1: 555-560.

Butler, D.R.
1983: ·   Rockfall hazard inventory, Ram River, Mackenzie Mountains. Canadian Geographer, 27, pp. 175-178.

Camponuovo, G.F.
1977:   ISMES' experience on the model of S. Martino. ISMES Publication No. 90, pp. 25-38.

Carter, T.G., Yuen, C.M.K., and Pereira, R.N.
1984:   Analysis and remedial measures for stabilization of highway rock cuts in Newfoundland. Proceedings, 4th International Symposium on Landslides, 1: 461-468.

Chan, Y.C., Chan, C.F., and Au, S.W.C.
1986:   Design of a boulder fence in Hong Kong. Proceedings, Conference on rock engineering and excavation in an urban environment, Institute of Mining and Metallurgy, pp. 87-96.

Church, M., Stock, R.F., and Ryder, J.M.
1979:   Contemporary sedimentary environments on Baffin Island, N.W.T., Canada: Debris slope accumulations. Arctic and Alpine Research, 11: 371-402.

Clark, S.H.B, Foster, H.L., and Bartsch, S.R.
1972:   Growth of a talus cone in the Western Chugach Mountains, Alaska. Geological Society of America Bulletin, 83: 227-230.

Cundall, P.
1971:   A computer model for simulating progressive,large scale movements in blocky rock systems. International Society of Rock Mechanics Symposium on Rock Fracture, Nancy, Paper II-8.

Descoeudres, F. and Zimmerman, T.H.
1987:   Three-dimensional dynamic calculation of rockfalls. Proceedings, 6th International Congress on rock mechanics, 1: 337-342.

Dodds, R.K.
1966:   Rock movement along fractures during failure. Proceedings, 1st Congress International Society of Rock Mechanics, Lisbon, 2, pp. 133-137.

Douglas, G.R.
1980:   Magnitude frequency study of rockfall in Co. Antrim, N. Ireland. Earth Surface Processes, 5: 123-129.

Ecole Polytechnique Federale de Lausanne
1985:   Direction et utilisation des terrains instables. Rapport géneral, 250 pp.

THURBER

Eisbacher, G.H.
1979:   Cliff collapse and rock avalanches (sturzstroms) in the Mackenzie Mountains, northwestern Canada. Canadian Geotechnical Journal, 16: 309-334.

Eisbacher, G.H. and Clague, J.J.
1984:   Destructive mass movements in high mountains: hazard and management. Geological Survey of Canada, Paper 84-16.

Embleton, C. and King, C.A.
1975:   Periglacial geomorphology. Arnold, London, 203 pp.

Embleton, C. and Thornes, J.B., Editors
1979:   Process in Geomorphology. Edward Arnold, London. 436 p.

Evans, S.G.
1976:   Material-form relationships on talus slopes in southwestern British Columbia. Unpublished M.A. Thesis, University of British Columbia, Vancouver, B.C., 145 p.

Evans, S.G., Aitken, J.D., Wetmiller, R.J., and Horner, R.B.
1987:   A rock avalanche triggered by the October 1985 North Nahanni earthquake, District of Mackenzie, N.W.T. Canadian Journal of Earth Sciences, 24, pp. 176-184.

Falcetta, J.L.
1985:   Une nouveau modèle de calcul de trajectoires de blocs rocheaux. Revue Française de Géotechnique, 30: 11-17.

Fookes, P.G. and Sweeney, M.
1976:   Stabilization and control of local rock falls and degrading rock slopes. Quaterly Journal of Engineering Geology, 9: 37-55.

Gardner, J.S.
1970:   Rockfall: a geomorphic process in high mountain terrain. Albertan Geographer, 6: 15-20.

1980:   Frequency, magnitude, and spatial distribution of mountain rockfalls and rockslides in the Highwood Pass area, Alberta, Canada. In Thresholds in Geomorphology. Edited by D.R. Coates and J.D. Vitek. Allen and Unwin, London. pp. 267-295.

1983:   Rockfall frequency and distribution in the Highwood Pass area, Canadian Rocky Mountains. Zeitschrift für geomorphologie, 27: 311-324.

Goldsmith, W.
1960:   Impact: The Theory and Physical Behaviour of Colliding Solids. Edwards Arnold, London, p.

Goodman, R.E.
1980:   Introduction to rock mechanics. John Wiley, New York. 478 p.

Goodman, R.E. and Bray, J.W.
1976:   Toppling of rock slopes. Proceedings, Specialty Conference on Rock Engineering for Foundations and Slopes, American Society of Civil Engineers, 2: 201-234.

Govi, M.
1977:   Photo-interpretation and mapping of the landslide triggered by the Friuli earthquake (1976). Bulletin of the International Association of Engineering Geology, 15: 67-72.

Hadley, J.B.
1964:   Landslides and related phenomena accompanying the Hebgen Lake earthquake of August 17, 1959. United States Geological Survey Professional Paper 435: 107-138.

Harp, E.L., Tanaka, K., Sarmiento, J., and Keefer, D.K.
1984:   Landslides from the May 25-27, 1980, Mamoth Lakes, California, earthquake sequence. United States Geological Survey, Miscellaneous Investigations Series, Map I-1612.

Harper, T.R.
1975:   The transient groundwater pressure response to rainfall and the prediction of rock slope instability. International Journal of Rock Mechanics and Mining Science, 12: 175-179.

Heim, A.
1932:   Bergsturz und Menschenleben. Beiblatt zur Vierteljahrsschrift der Naturforschenden Gesellschaft in Zürich, 77: 1-217. (English translation by N.A. Skermer, Bitech Publishers, Vancouver, B.C.)

Hodgson, E.A.
1946:   British Columbia earthquake June 23, 1946. Journal of the Royal Astronomical Society of Canada, 40: 285-319.

Hoek, E. and Bray, J.W.
1977:   Rock slope engineering. 2nd edition. Institution of Mining and Metallurgy, London. 402 p.

Hungr, O.
1981:   Dynamics of rock avalanches and other types of slope movements. Ph.D. thesis, University of Alberta, Edmonton, Alta., 506 p.

Hungr, O and Evans, S.G.
1988:   Engineering evaluation of fragmental rockfall hazards. In Landslides. Edited by C. Bonnard. Proceedings, 5th. International Symposium on Landslide, Lansanne, 1: 685-690.

Hutchinson, J.N.
1972:   Field and laboratory studies of a fall in Upper Chalk cliffs at Joss Bay, Isle of Thanet. Proceedings, Roscoe Memorial Symposium, Cambridge, G.T. Fowlis, Henley-on-Thames, pp. 692-706.

Hutchinson, J.N.
1988:   Morphological and technical parameters of landslides in relation to geology and hydrogeology, state-of-the-art Report. In Landslides Edited by C. Bernard. Proceedings, 5th. International Symposium Landslides, Lansanne, 1: 3-35.

International Pacific Salmon Fisheries Commission
1980:   Hell's Gate Fishways. New Westminister, B.C., 8 pp.

Keefer, D.K.
1984:   Landslides caused by earthquakes. Geological Society of America Bulletin, 95: 406-421.

Keefer, D.K., Wilson, R.C., Harp, E.L., and Lips, E.W.
1985:   The Borah Peak, Idaho Earthquake of October 28, 1983-Landslide. Earthquake Spectra, 2: 91-125.

Kirby, M.J. and Statham, I.
1975:   Surface stone movement and scree formation. Journal of Geology, 83: 349-362.

Kobayashi, Y. and Kagawa, T.
1987:   The prediction of hazards from debris avalanches and rockfalls with the aid of computer simulations. Proceedings, International Symposium on Engineering Geological Environment in Mountainous Areas, Beijing, 1: 563-572.

Kotarba, A. and Stromquist, L.
1984:   Transport, sorting and deposition processes of alpine debris slope deposits in the Polish Tatra Mountains. Geografiska Annaler, 66A: 285-294.

Lied, K.
1977:   Rockfall problems in Norway. ISMES Publication 90, pp. 51-53.

Li, J-S and Whitman, R.V.
1986:   Earthquake induced displacements of sliding blocks. Journal of Geotechnical Engineering, 112: 44-59.

Lister, D.R.
1980:   Geotechnical studies and land subdivision in British Columbia. Proceedings, Specialty Conference on Slope Stability Problems in Urban Areas, Canadian Geotechnical Society, Toronto, Ont., 14 p.

Luckman, B.H.
1976:   Rockfalls and rockfall inventory data: some observations from Surprise Valley, Jasper National Park, Canada. Earth Surface Processes, 1: 287-298.
1988:   Debris accumulation patterns on talus slopes in Surprise Valley, Alberta. Géographie physique et Quaternaire, 42: 247-278.

Magni, E.R.
1984:   Rock cut stability along Ontario highways. Proceedings, 4th. International Symposium on Landslides, 1: 545-550.

Mathews, W.H.
1979:   Landslides of central Vancouver Island and the 1946 earthquake. Bulletin of the Seismological Society of America, 69, pp. 445-450.

Mathews, W.H. and McTaggart, K.C.
1978:   Hope rockslides, British Columbia, Canada. In Rockslides and avalanches. Vol. 1, Edited by B. Voight. Elsevier, Amsterdam, pp. 259-275.

McConnell, R.G. and Brock, R.W.
1904:   The great landslide at Frank, Alberta. Geological Survey of Canada. Annual Report 1902-1903, pt. 8, Appendix.

Miller, G.E.
1983:   Rockfall investigation, Bastion Mountain, Sunnybrae, B.C. Report, B.C. Ministry of Environment, 19 p.

Morgan, G.C.
1986:   Acceptability of natural hazards in transportation corridors. In Transportation Geotechnique, Vancouver Geotechnical Society.

Newmark, N.M.
1965:   Effects of earthquakes on dams and embankment. Geotechnique, 15: 139-160.

Peckover, F.L. and Kerr, J.W.G.
1977:   Treatment and maintenance of rock slopes on transportation routes. Canadian Geotechnical Journal, 14, pp. 487-507.

Piteau, D.R. and Clayton, R.
1977:   Discussion of paper "Computerized Design of rock slopes using interactive graphics for the input and output of geometrical data" by P.A. Cundall, M.D. Voegele and C. Fairhurst. Proceedings, 16th Symposium on Rock, Mechanics: 62-63.

Piteau, D.R. and Peckover, F.L.
1978:   Engineering of rock slopes. In Landslides, analysis and control. Edited by R.L. Schuster
            and R.J. Krizek. National Academy of Sciences, Transportation Research Board, Special
            Report 176, pp. 192-228.

Piteau, D.R. and Martin, D.C.
1982:   Mechanics of rock slope failure. 3rd International Conference on Stability in Surface
            Mining, Vancouver, B.C., pp. 113-170, AIMMPE, New York.

Rapp, A.
1960:   Recent development of mountain slopes in Kärkevagge and surroundings, northern
            Scandinavia. Geografiska Annaler, 42: 65-200.

Ritchie, A.M.
1963:   Evaluation of rockfall and its control. Highway Research Board Record, 17: 13-28.

Rochet, L.
1987a: Application des modèles numériques de propagation à l'étude des éboulements rocheux.
            Bulletin de liaison des laboratoires des ponts et chaussées, 150-151: 84-95.
1987b: Développement des modèles numériques dans l'analyse de la propagation de éboulements
            rocheux. Proceedings, 6th. International Congress on Rock Mechanics, 1: 479-484.

Rogers, G.C.
1988:   An assessment of the megathrust earthquake potential of the Cascadia subduction zone.
            Canadian Journal of Earth Sciences, 25: 844-852.

Schindler, C.M.
1987:   Unstable rock-masses in central Switzerland: geological documentation, precision
            surveying and observations, stabilization. Proceedings, International Symposium on
            Engineering Geological Environment in Mountainous Areas, Beijing, Vol. 1, pp. 457-463.

Schneider, J.
1942:   Der Felssturz am Gspaltenberg (Geneinde Flums) - Sommer 1941. Strasse und Verkehr, 1:
            1-13. (Available in English as Geological Survey of Canada Translation 3000).

Schumm, S.A. and Chorley, R.J.
1964:   The fall of Threatening Rock. American Journal of Science, 262: 1041-1054.

Schuster, R.L. and Fleming, R.W.
1986:   Economic losses and fatalities due to landslides. Bulletin of the Association of
            Engineering Geologists, 23: 11-28.

Statham, I.
1976:   A scree slope rockfall model. Earth Surface Processes 1: 43-62.

Statham, I. and Francis, S.C.
1986:   Influence of scree accumulation and weathering on the development of steep mountain
            slopes. In Hillslopes Processes. Edited by A.D. Abrahams. Allen and Unwin, London. pp.
            245-267.

Stethem, C.J. and Schaerer, P.A.
1979:   Avalanche accidents in Canada I. A selection of case histories of accidents, 1955 to 1976.
            National Research Council, Division of Building Research, DBR Paper 834, 114 p.
1980:   Avalanche accidents in Canada II. A selection of case histories of accidents, 1943 to 1978.
            National Research Council, Division of Building Research, DBR Paper 926, 75 p.

Spang, R.M.
1987:   Protection against rockfall - stepchild in the design of rock slopes. Proceedings, 6th.
            International Congress on Rock Mechanics, 1: 551-557.

Spang, R.M. and Rautenstrauch, R.W.
1988: Empirical and mathematical approaches to rockfall protection and their practical applications. In Landslides. Edited by C. Bonnard. Proceedings, 5th Symposium on Landslides, Lausanne, 2: 1237-1243.

Tamburi, A.J.
1974: Creep of single rocks on bedrock. Geological Society of America Bulletin, 85: 351-356.

Theodore, M.H.
1986: Review and case examples of rockfall protection measures in the mountain region of Canadian National Railway. In Transportation Geotechnique, Vancouver Geotechnical Society.

Varnes, D.J.
1978: Slope movement types and processes. In Landslides, analysis and control. Edited by R.L. Schuster and R.J. Krizek. National Academy of Sciences, Transportation Research Board, Special Report 176, pp. 11-33.

Voight, B. and Kennedy, B.A.
1979: Slope failure of 1967-1969, Chuquicamata mine, Chile. In Rockslides and Avalanches, 2. Edited by B. Voight. Elsevier, New York. pp. 595-632.

Washburn, A.L.
1973: Periglacial processes and environments. Arnold, London, 320 pp.

Wetmiller, R.J., Horner, R.B., Hasegawa, H.S., North, R.G., Lamontagne, M., Weichert, D.H., and Evans, S.G.
1988: An analysis of the 1985 Nahanni earthquakes. Bulletin of the Seismological Society of America, 78: 590-616.

Whalley, W.B.
1984: Rockfalls. In Slope Instability. Edited by D. Brunsden and D.B. Prior. John Wiley, New York. pp. 217-256.

Williams, A.T. and Davies, P.
1984: Cliff failure along the Glamorgan Heritage Coast, Wales, U.K. In Mouvements de terrains. Série documents du BGRM. No. 83, p. 109-119.

Witkind, J.J., Myers, W.B., Hadley, J.B., Hamilton, W., and Fraser, G.D.
1962: Geologic features of the earthquake at Hebgen Lake, Montana, Aug. 17, 1959. Bulletin of the Seismological Society of America, 52, pp. 163-180.

Worobey, G.A.
1972: An investigation of talus slope development in the Similkameen Valley, near Keremeos, British Columbia. Unpublished M.A. thesis, University of British Columbia, Vancouver, 170 p.

Wu, S-S.
1985: Rockfall evaluation by computer simulation. Transportation Research Record, 1031: 1-5.

Wyllie, D.C.
1980: Toppling rock slope failures, examples of analysis and stabilization. Rock Mechanics, 13, pp. 89-98.

Zvelebil, J.
1984: Failure of the sandstone rock slope in the Labe Canyon, Decin Highlands, Czeckoslovakia. Proceedings, 4th. International Symposium on Landslides, 1: 591-596.

Appendix

APPENDIX: ROCKFALL Computer Program: User's Manual

ROCKFALL

Dynamic analysis of fragmental rockfall trajectories using an IBM PC Compatable Microcomputer.

Copies of the program ROCKFALL
may be obtained on floppy disk from;

Dr. Oldrich Hungr, P. Eng.,
Thurber Consultants Ltd.,
Suite 200-1445 West Georgia Street,
Vancouver, British Columbia
V6G 2T3

THURBER

1. INTRODUCTION

    The program "ROCKFALL" implements a simplified (lumped-mass) model of fragmental rockfall trajectory simulation, described in Chapter 7.

2. STARTING THE PROGRAM

    The program is distributed in a compiled form on a single floppy disk, in a file called ROCKFALL.EXE. To start, simply enter "ROCKFALL" at the DOS prompt. The program title screen (Screen 1 attached) will appear. Select the graphics adapter installed in your computer.

    If you wish to use the program with a "Hercules" type graphics adapter, you must run the device driver "QBHERC.COM" prior to invoking ROCKFALL. The driver file is on the distribution disk.

3. GEOMETRY INPUT

    If there is no data file stored in the current directory, answer N to the question at the bottom of the screen. The program will prompt the input of the path geometry on Screens 2 and 3. These screens are self-explanatory, except the column "Surface" on Screen 3 refers to the code number of the surface type specified to apply in the last path segment. If the problem includes only one surface type, enter 1.0 in each segment. The example shown in Screen 3 has two surface types.

4. SURFACE PROPERTIES

    When the path has been specified, the two screens for input of surface properties appear (Screens 4 and 5). Each surface type may have different restitution coefficients and rolling friction coefficients. The momentum reduction parameters F0, C1 and R are common for all the surfaces and are explained in Section 6.8. If you wish to use constant restitution coefficients ("elastic" conditions), enter zero for the value of the contact yield limit force F0.

If a maximum and minimum value of each restitution coefficient is entered, the program will choose a random value from the given range in each impact. To specify fixed values, enter the same number for both maximum and minimum.

5. <u>ROCKFALL TRAJECTORY ANALYSIS</u>

When the material properties have been specified, the Main Menu appears (Screen 6). To analyze individual fragments rolling or falling from a specified starting point, choose Selection 1. The profile of the path appears, scaled automatically (Screen 7). Boulder mass needs to be specified only if crushing (plastic) impact parameters have been specified.

If an elevation is given which places the fragment above the ground surface, it will begin moving by free fall as shown on Screen 8. If an elevation is specified below ground surface (say 1.0 m), the fragment will be assumed to start on the ground surface at the given x-coordinate and to begin its movement by rolling.

If you specify 0 for elevation, this will terminate the analysis. Your choice will then be to end the session and print a summary of the properties and fragments analyzed to that point, or to return to the Main Menu and continue.

Selections 2 to 5 are similar to 1, except for using other output devices. Selection 5 plots a velocity profile of the last trajectory analyzed.

6. <u>STATISTICAL ANALYSIS</u>

The statistical solutions 6 and 7 require the input of a range of particle masses, starting x-coordinates and elevations above the path surface.

The actual mass and starting coordinates of each particle will be selected at random from the specified
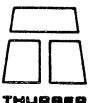
ranges. With Selection 6, only the starting point of
each particle will be plotted and a histogram of the
runout points (Fig. 8.16). With Selection 7, the
plotter will draw the actual trajectory of each
particle (see Fig. 8.15).

7. <u>EDITING</u>

The path geometry and properties can be changed by
Selections 8 to 10 or recorded in a file in the current
directory by Selection 11. Selection 12 will list all
data files (identified by an extension .ROC) and read
new data from disk.

ROCKFALL

VERSION 1.1   MARCH 1988

THURBER CONSULTANTS LTD.

Required hardware configuration:
        1. Printer in lpt1 (optional)
        2. DXY plotter in lpt2 (optional)

 Select applicable graphics adapter:
        CGA   - enter 2
        EGA   - enter 8
        VGA   - enter 12
        Hercules - enter 3   ? 3

IS THERE A FILE TO READ Y/N ?

                                    SCREEN 1

THURBER

PATH DESIGNATION test
NUMBER OF SLOPE SEGMENTS 6

IS THE ABOVE CORRECT ? Y/N

SCREEN 2

	X-COORD.	ELEVATION	SURFACE
0	0.0	32.0	1.0
1	6.0	25.0	1.0
2	10.0	14.0	1.0
3	18.0	4.0	1.0
4	24.0	4.0	2.0
5	26.0	5.0	2.0
6	46.0	7.0	2.0
7			
8			
9			
10			
11			
12			
13			
14			
15			
16			
17			
18			
19			
20			
21			

	X-COORD.	ELEVATION	SURFACE
22			
23			
24			
25			
26			
27			
28			
29			
30			
31			
32			
33			
34			
35			
36			
37			
38			
39			
40			
41			
42			
43			

THIS PAGE OK ? Y/N

SCREEN 3

THURBER

```
==========================================================================
ROCKFALL PATH > test <                         DATE 04-23-1988
==========================================================================
```

SURFACE PROPERTIES

SURFACE NO	- KN - MIN	MAX	- KT - MIN	MAX	ROL.FRICTION COEFFICIENT
1	0.70	0.70	0.90	0.90	0.52
2	0.50	0.50	0.80	0.80	0.60

THIS PAGE OK ? Y/N

SCREEN 4

```
ENTER CONTACT YIELD LIMIT FORCE, F0   50
ENTER INITIAL CONTACT STIFFNESS, C1   100
ENTER STIFFNESS REDUCTION RATIO, R     .05


IS THE ABOVE CORRECT ? Y/N ?
```

SCREEN 5

THURBER

a) INDIVIDUAL SOLUTIONS:

    Several Trajectories,All Output on Screen 1
    Show Trajectories on Screen, Summary on Printer 2
    Plot Last Trajectory on Plotter, Summary on Printer 3
    All Trajectories on Plotter, Summary on Printer 4
    Last Trajectory and its Velocity Profile on Plotter 5

b) STATISTICAL SOLUTIONS (Plotter Required):

    Runout Histogram for a Number of Boulders 6
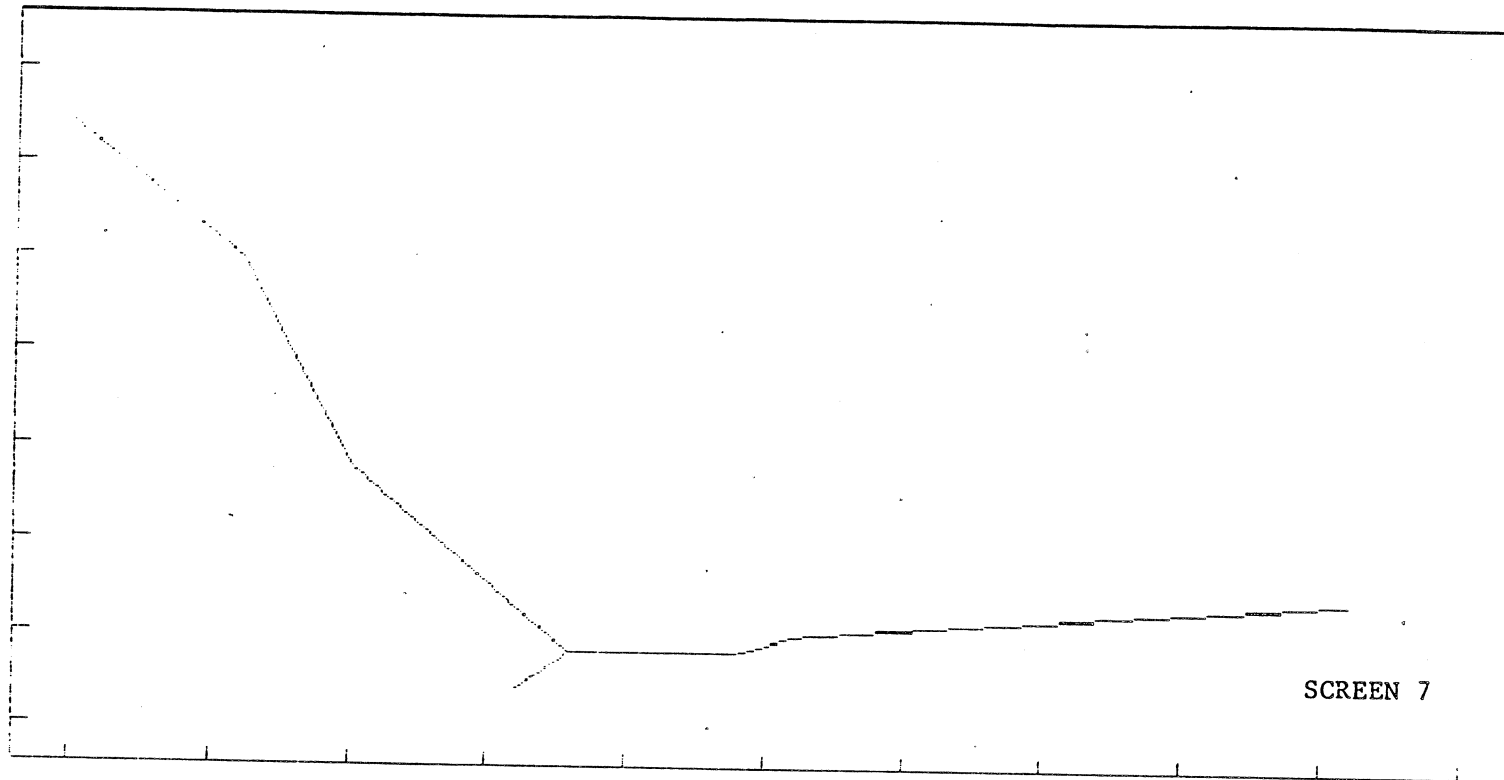   Runout Histogram, All Trajectories Plotted 7

c) UTILITIES:

    Change Path Geometry 8
    Change Material Properties 9
    Change Plot Coordinates 10
    Record Data on File 11
    Read a New File from Disk 12

ENTER SELECTION (OR 0 TO QUIT):
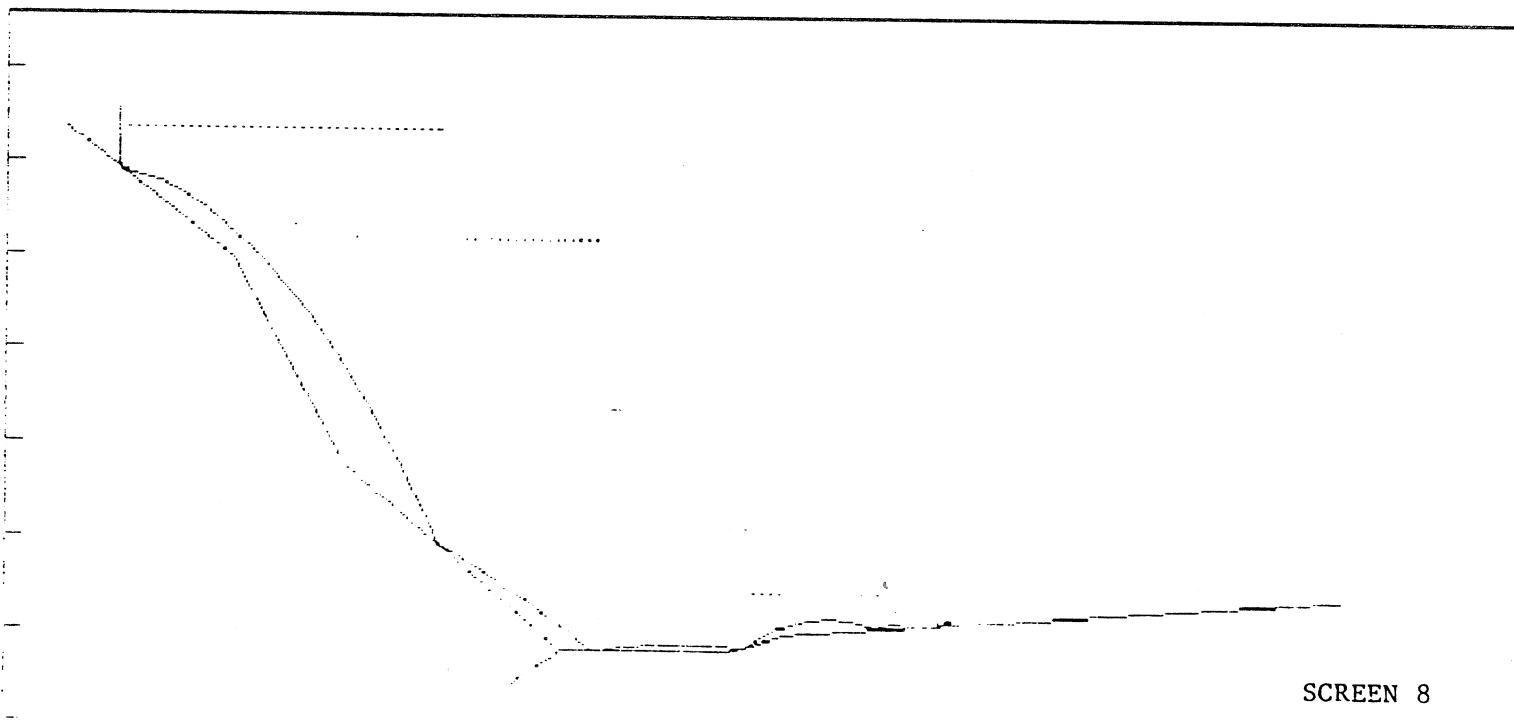
SCREEN 6

THURBER

SCREEN 7

ENTER NEW BOULDER MASS ? 1   ELEVATION ? 33   X-COORDINATE? 2

ONE DIVISION = 5 m

SCREEN 8

ENTER NEW BOULDER MASS ?

BOULDER NO. 2   ONE DIVISION 5 m